Universität Rostock

Traditio et Innovatio

Optimisation of Stem Cell based Approaches towards cardiac Regeneration

Dissertation

to obtain

the academic degree

doctor rerum naturalium (Dr. rer. nat.)

at the Faculty of Mathematics, Physics and Natural Science

University of Rostock

Submitted by

Frauke Thiele (née Hausburg), born on October 28, 1987 in Suhl,

Ettringen, 11.01.2019

https://doi.org/10.18453/rosdok_id00002896

Universität Rostock Traditio et Innovatio

Optimierung stammzellbasierter Ansätze für die kardiale Regeneration

Dissertation

zur

Erlangung des akademischen Grades

doctor rerum naturalium (Dr. rer. nat.)

der Mathematisch-Naturwissenschaftlichen Fakultät

der Universität Rostock

vorgelegt von

Frauke Thiele (geb. Hausburg), geb. am 28.10.1987 in Suhl,

Ettringen, 11.01.2019

Gutachter:

1. Gutachter:
   Prof. Dr. Robert David, Klinik und Poliklinik für Herzchirurgie Universitätsmedizin Rostock

2. Gutachter:
   Prof. Dr. Reinhard Schröder, Institut für Biowissenschaften, Universität Rostock

3. Gutachter:
   Prof. Dr. Stefan Brunner, Medizinische Klinik und Poliklinik 1 LMU München

Jahr der Einreichung: 2019

Jahr der Verteidigung: 2020

Die vorliegende Arbeit wurde in der Zeit von Juli 2012 bis September 2017 in den Forschungslaboratorien für kardialen Gewebe- und Organersatz (FKGO), am Referenz- und Translationszentrum für kardiale Stammzelltherapie (RTC), an der Klinik und Poliklinik für Herzchirurgie am Universitätsklinikum Rostock angefertigt.

Content

Summary

Aberrant behavior of resident cells triggered by genetic predisposition, environmental influences or personal life-style will increasingly cause illnesses. Among these, cardiovascular diseases (CVD) are the leading cause of death in the western world already at present. Hence, the advancement of new therapeutic options for adequate and comprehensive support for every patient will be a major challenge for physicians and scientists over the next few years and decades.

The human heart possesses only negligible myocardial regeneration capacity after a myocardial infarction (MI), thus, it cannot compensate the massive cell loss of 0.5 – 1 billion cardiomyocytes. Endogenous functional repair and regeneration is not possible. The transplantation of hearts represents the last resort, but the supply of suitable donor organs does by large margins not meet the demand.

Accordingly, the field of regenerative medicine comprises cell transplantation of either adult autologous or allogenic stem cells as well as innovative strategies based on cell fate alteration of proper cell types to restore myocardial tissue. However, circulating progenitor cells are more suitable for re-vascularization than re-muscularization. Initial clinical studies using transplanted adult stem cells such as mesenchymal (MSCs) and haematotoetic (HSCs) stem cells led only to marginal improvement of the left ventricular ejection fraction.

Therefore, solid basic research in order to decipher key cellular and molecular mechanisms of heart development is urgently required. For this reason, the present thesis investigated the possibility of non-viral manipulations of several cell types, including adult and embryonic stem cells as well as somatic fibroblasts.

One approach addresses the question whether one cardiac transcription factor (TF) is sufficient to generate a functional and purely ventricular cardiomyocyte subtype. It could be demonstrated that forced exogenous overexpression of Nkx2.5 with an adjusted differentiation protocol gives rise to spontaneously beating cells with several characteristics of immature, predominantly ventricular cardiomyocytes (cardiac marker expression on protein and RNA level) originating from murine embryonic stem cells (ESCs). However, the obtained single cells still present a heterogeneous

population, with variations in cell shape, beating frequencies and their response to ion channel modulators.

Furthermore, two alternative approaches for modulation of cell fate are presented which allow to avoid DNA as well as viral introduction of TFs. Further progress in cell modification besides conventional methods is an urgent demand for clinical translation. Delivery of modified mRNA and miRNA are safe strategies circumventing drawbacks such DNA integration into the host genome and possible mutagenesis and tumorigenicity.

It was demonstrated that synthetic mRNA equipped with a methylated cap, modified nucleosides (as 5-methylcytidine-5'-triphosphate (5mC) and pseudouridine-5'-triphosphate (Ψ)) and a poly-A-tail of 100 adenosine residues led to a fast and efficient translation of EGFP in several cell types, including fibroblasts of various origins and human bone-marrow derived mesenchymal stem cells (MSCs), compared to mRNA without nucleoside modifications. The focus of this work aimed at the establishment a PCR-based protocol to generate highly reproducibly modified mRNA. Additionally, first experiments using modified MyoD have demonstrated the functionality of mRNA in combination with an adjusted protocol to initiate an effective cell fate alteration of murine fibroblasts towards skeletal myoblasts. The concept also has been transferred to a cardiomyocytic programming approach with murine ESCs via overexpression of Nkx2.5 encoding mRNA.

Avoiding exogenous TF overexpression is the second alternative technology investigated in the present thesis. Small non-coding RNA molecules (microRNAs) play a crucial role as post-transcriptional modulators and offer numerous possibilities to affect cell fate. However, the safe and efficient transfection using human bone-marrow derived $CD133^+$ SCs was the paramount aim in this study. $CD133^+$ SCs give rise to cells of the haematopoietic, endothelial and myogenic lineages and are potential candidates for cell transplantation therapies already transplanted in several clinical trials. To improve their outcome in cell transplantations, a non-viral magnet-bead based polymer delivery system to introduce miRNA was established. This method permitted an efficient uptake of miRNA with simultaneously minimal toxic effects and no influence on the hematopoietic characteristics. Specific magnetic targeting via the superparamagnetic core of the delivery system was demonstrated in *in vitro* experiments. This offers the opportunity to guide

the cells to the site of interest in further *in vivo* scenarios, which may prevent the massive wash out after transplantation and consequently, may lead to an improved cardiovascular regeneration.

Zusammenfassung

Heutzutage und voraussichtlich zunehmend in der Zukunft ist aberrantes Verhalten von körpereigenen Zellen, verursacht durch genetische Prädisposition, Umwelteinflüsse und persönliche Verhaltensweisen, eine Ursache für eine Vielzahl verschiedener Krankheiten. Unter diesen stellen kardiovaskuläre Krankheiten (CVD) die Haupttodesursache in der westlichen Welt dar. Daher ist die Entwicklung neuer Therapiemöglichkeiten für eine adäquate und umfassende Versorgung jedes Patienten eine der größten Herausforderung für Ärzte und Wissenschaftler in den nächsten Jahren und Jahrzehnten.

Das menschliche Herz weist nur ein geringes Regenerationspotenzial nach einem Myokardinfarkt (MI) auf, welches nicht den massiven Zellverlust von 0,5 – 1 Mrd. Kardiomyozyten kompensieren kann. Eine natürliche Regeneration ist daher nicht möglich. Für die letzte Rettung, eine Herztransplantation, stehen nicht in ausreichendem Maße Spenderherzen zur Verfügung - zudem bedingt sie eine dauerhafte Immunsuppression.

Das Feld der Regenerativen Medizin umfasst sowohl Zelltransplantation von adulten autologen und allogenen Stammzellen als auch neue innovative Strategien basierend auf der Veränderung von bestehenden geeigneten Zellen um das Herzgewebe wiederherzustellen. Jedoch haben Studien gezeigt, dass zirkulierende Vorläuferzellen zwar eine Revaskularisierung unterstützen, jedoch keine Remuskularsierung. Des Weiteren zeigen erste klinische Studien einer autologen Zelltransplantationen von mesenchymalen (MSCs) und hämatopoetischen (HSCs) Stammzellen lediglich eine marginale Verbesserung der Auswurffraktion des linken Ventrikels.

Daher ist eine solide Grundlagenforschung zum Verständnis der zu Grunde liegenden zellulären und molekularen Prozesse dringend erforderlich. Aus diesem Grund werden in dieser Arbeit verschiedene Manipulationen an adulten und embryonalen Stammzellen sowie somatischen Fibroblasten vorgestellt.

In einem Ansatzbeschäftigt sich die vorliegende Arbeit mit der Fragestellung, ob ein kardialer Transkriptionsfaktor (TF) ausreichend ist, um eine funktionsfähige und reine ventrikuläre kardiale Subpopulation zu erzeugen. Es konnte gezeigt werden, dass ausgehend von murinen embryonalen Stammzellen (ESCs) nach exogener Überexpression von Nkx2.5 und anschließender angepasster Differenzierung, spontan schlagende Zellen generiert werden können.

Diese weisen typische Merkmale von unreifen, überwiegend ventrikulären Kardiomyozyten auf, wie auf Protein- sowie RNA-Ebene gezeigt werden konnte. Jedoch stellen die erhaltenen Einzelzellen nach wie vor eine noch heterogene Population dar, mit Variationen in Zellform, Schlagfrequenz und ihrer Reaktion auf verschiedene Ionenkanalmodulatoren.

Des Weiteren wurden zwei alternative Modifikationsmöglichkeiten vorgestellt. Mit diesen kann eine Modulation des Zellschicksals ermöglicht werden ohne eine Integration der TF mittels DNA oder viralen Vektoren. Dieser Schritt ist notwendig um Zellmodifikationen attraktiver für eine klinische Anwendung zu gestalten. Die Einbringung von modifizierter mRNA (mmRNA) und microRNA sind sichere Vorgehensweisen bei denen Nachteile wie ungewünschte systemische Verteilung, DNA Integration in das Wirtsgenom sowie mögliche Mutagenese und Tumorbildung vermieden werden.

Es konnte gezeigt werden, dass synthetische mmRNA versehen mit einer methylierten „5`-Kappe“ (*„5`-cap“*), modifizierten Nukleosiden (5-Methylcytidin-5’-Triphosphat (5mC) und Pseudouridin-5’-Triphosphat (Ψ)), und einem poly-A-Schwanz bestehend aus 100 Adenosinnukleotiden zu einer schnelleren und effizienteren Translation von EGFP in verschiedenen Zelltypen, im Vergleich zu mRNA ohne Nukleosidmodifikation, führt. Zu den untersuchten Zellen zählen Fibroblasten (von verschiedenen Spezies) sowie humane mesenchymale Stammzellen aus dem Knochenmark. Ein Hauptaugenmerk dieser Arbeit liegt auf der Etablierung eines PCR-basierten Protokolls zur Sicherstellung einer hoch reproduzierbaren Generierung synthetischer mmRNA. Darüber hinaus werden in ersten *proof-of-principle* Experimenten die Möglichkeiten einer effektiven Änderung des Zellschicksals mittels mmRNA Integration und angepassten Differenzierungsprotokollen aufgezeigt. Hierzu wurde zunächst in einem Funktionalitätsnachweis präsentiert, dass eine Umprogrammierung muriner Fibroblasten durch eine mehrmalige Applikation von MyoD mRNA in Richtung skelettaler Myoblasten möglich ist. Anschließend wurde dieses Konzept auf eine kardiomyozytäre Programmierung von murinen ES Zellen mittels Nkx2.5 mRNA übertragen.

Das zweite alternative Konzept dieser Arbeit beruht auf der Vermeidung einer exogenen Überexpression von TFs. Kurze nicht-kodierende RNA Moleküle (sogenannte microRNAs) spielen eine entscheidende Rolle als post-transkriptionale Modulatoren und weisen somit eine Vielzahl von Möglichkeiten zur Beeinflussung des Zellschicksals auf. Jedoch war das vorrangige

Ziel dieser Arbeit zunächst eine sichere und effiziente Transfektion humaner $CD133^+$ SCs aus dem Knochenmark, welche bereits in klinischen Studien zur Herzregeneration eingesetzt werden. $CD133^+$ SCs differenzieren in hämatopoetische, endotheliale und myogene Zellen und sind potenzielle Kandidaten für eine Stammzelltransplantation. Um den positiven Effekt einer Zelltransplantation zu erhöhen wurde ein nicht-virales magnetisches Polymer-basiertes Transfektionssystem zur Einschleusung von microRNA etabliert. Diese Methode erlaubt eine effektive Aufnahme von microRNA bei gleichzeitig geringer Toxizität und ohne Einfluss auf die hämatopoetischen Merkmale. Des Weiteren konnte auf Grund des superparamagnetischen Kerns des genutzten Transfektionssystems ein gezieltes magnetisches Targeting in *in-vitro* Experimenten veranschaulicht werden. Dies eröffnet die Möglichkeit, beliebige Zellen gesteuert an eine bestimmte Stellen in *in-vivo* Experimenten zu führen und somit das massive Auswaschen von transplantierten Zellen zu vermindern. In Folge dessen kann eine kardiovaskuläre Regeneration verbessert werden.

1. Introduction

In the near future, both the western world and developing countries will be confronted with an aging society and its negative health consequences. The emergence of age-related disorders and diseases of affluence pose challenges for physicians and scientists urgent need for new options to treat the disease. Unusual behavior of resident cells is the cause of numerous serious diseases in animals and humans such as cancer, neurodegenerative (e.g. Alzheimer's or Parkinson's disease) or cardiovascular (ischemic heart disease and stroke) disorders and diabetes mellitus. Adult organs, such as the human heart, possess only limited self-renewal capacity and therefore lack the potential to restore the original function themselves [1, 2]. The increasing demand for new treatment options conforms to the needs and limits of former medical applications. Regenerative medicine opens up new strategies for cell based replacement therapies as well as disease modelling and drug development [3–5].

Basic research with respect to molecular and cell biological investigation during the last years underlines the importance for understanding developmental biology and disease origins. Previous studies were often criticized due to ethical concerns regarding human embryonic stem cells and hampered by limited availability of human adult stem cells. However, recent research based on the knowledge gained from programming strategies using mature somatic cells, either reprogramming to a pluripotent state (iPSC) or direct conversion from one somatic cell to a new somatic cell type.

Modification of suitable cell material should be considered with respect to a functional improvement of inherent cell properties together with efficient conversion into desired cell types. Therefore, several concepts were explored using lineage specific transcription factors (TFs), modified mRNA, microRNA and small molecules. The application of virus- and DNA-free strategies is always preferable and increases the opportunities for clinical translation. The main focus should be the generation of fully functional cells with characteristics as close as possible to their natural counterparts. Yet, previous approaches were hampered by the immature properties of the derived cell types [6].

1.1. Cardiovascular diseases/Cardiac disorders

Cardiovascular diseases are the leading causes of death worldwide. In 2015 8.8 million people died of ischemic heart disease and 6.2 million from stroke which is often associated with the

former. Combined, both types of illness result in a total of ~31.3 % of deaths worldwide (WHO, 2015). Most common reasons for an myocardial infarction (MI) are hypertension and narrowing of the coronary arteries in consequence of arteriosclerosis [7]. This leads to an occlusion of coronary vessels and hereafter to an undersupply of oxygen of the affected tissue [8] and thereby resulting in cell death [9]. The course of cardiomyocyte cell death is varied and not precisely defined [9], as both death by apoptosis [10, 11], death by necrosis [10, 12–14] and death in association with autophagy [15–17] have been described. As a result, 25 % of the human left ventricle (0.5 – 1 billion cardiomyocytes) can be destroyed by a myocardial infarction within few hours [18, 19].

Following the injury, a cascade of numerous biochemical and mechanical processes is stimulated, which, in consequence, leads to reduction of cardiac functions [20–26]. Initial stages are: wall thinning, collagen degradation and ventricular dilatation [24]. Occurring fibrosis leads to myocardial scar formation, which causees wall stiffening and thereby leads to reduced systolic function due [25]. Furthermore, the large cell loss affected electrical conduction triggered by faulty electrical coupling within the heart [20, 25].

The human heart possesses only a minor turnover rate of 1 % at the age of 25 which decreases to 0.45 % at the age of 75 [1]. Hence, during an average age of 75 years, less than 50 % of the human cardiomyocytes can be replaced. Moreover, the number of cardiomyocytes in the left ventricle increases 3,4-fold only from the first year of life until the age of 20 showing more cardiomyocyte cycling and division in young humans [2]. The affected tissue cannot accomplish functional repair and remodeling through this negligible myocardial regeneration capacity after a MI. Resident cell populations like cardiac progenitor cells (CPCs) or preexisting cardiomyocytes which undergo dedifferentiation represent possible sources for heart regeneration after injury [2, 27, 28]. Corroborating this, it was recently discovered that populations of progenitor cells can display uneven behavior and even different marker expressions [19] but nevertheless are able to differentiate into cardiomyocytes. This includes isolated cells from: i) adult rat heart expressing c-kit^{+}/Sca-1^{-} [29, 30], ii) two-day-old rat pups expressing isl1^{+}/c-kit^{-}/Sca-1^{-} [31, 32], iii) adult mouse heart expressing Sca-1^{+}/c-kit^{-} [33] and iv) adult mouse heart expressing the ATP-binding cassette sub-family G member 2 (Abcg2 or CDw338) [34]. Furthermore, homing of cells from different origins could improve ventricular function [18], in particular endogenous circulating extra-cardiac progenitors [19, 35–39]. However, extra-cardiac progenitors after sex-mismatched

heart transplantation give rise to a marginal part of 0.04 % to cardiomyocyte, whereas endothelial cells were the common cell chimerism, averaging 24 % in endomyocardial biopsies from seven patients [35]. This implies that circulating progenitor cells are more suitable for revascularization than remuscularization [18].

For this purpose, it is of considerable importance to develop new strategies to support cardiomyocyte regeneration, with regard to clinical applications in the future. Current research aims at cell transplantation of either autologous or allogenic stem cells or terminally differentiated cells from various origins, as well as stimulation of endogenous cell populations and direct reprogramming.

1.2. Cardiac development

The heart is the first organ formed during early stages of embryonic development, as it is responsible for nutrient and oxygen supply as well as removal of waste. The complex system of the mammalian four-chambered heart formation requires the generation of diverse muscle and nonmuscle cell-types, including cardiomyocytes of left and right atria as well as left and right ventricles, conduction system, pacemaker, vascular smooth muscles, endo- and epicardial cells [40–43] (Figure 1, Figure 2). Poorly understood consequences of false embryonic development are congenital heart defects (CHD) present at birth, due to malformation of heart structure. CHD is the most common defect at birth worldwide with a prevalence between 0.58 – 0.9 % [44, 45]. Some molecular genetic mechanisms are associated with various degrees of illness [46–48], like dysregulation of the transcription factors of the forkhead family [49], Nkx2.5 [50–59] or Gata4 [57, 60–63], which lead for instance to atrioventricular block, atrial septal defects or pulmonary stenosis.

The cell fate is determined by spatiotemporally stringent molecular regulations. Myocardial cells are derived from Bry^+ mesoderm progenitors of the primitive streak during gastrulation [64–66]. Cardiovascular fate-determinants are both the bHLH transcription factor MesP1 [67–72] and vascular endothelial growth factor receptor 2 (VEGFR2 or Flk1) [68, 69, 73] which mark early cardiovascular progenitor cells. At an early stage of mouse embryogenesis (E 7.5), a $Nkx2.5^+/Hcn4^+$ cell population of the first heart field (FHF) forms the cardiac crescent [74–81]. Meanwhile, an $Isl1^+$ cell population is added to the linear heart tube at later developmental stages

[82–86]. The so called second heart field (SHF) is derived from the pharyngeal mesoderm and is in medial and posterior position with respect to the FHF [31, 87, 88].

The first heart field progenitor cells give rise to myocardium of the left ventricle and a minor part of the right ventricle, the right and left atria and most cell complexes of the conduction system (CS), such as the atrioventricular (AV) node and the ventricular CS [41, 82]. Multipotent progenitor cells of the SHF generate the myocardium of the right and left atria, the right ventricle and the outflow tract, as well as vascular smooth muscles and the endocardium of the heart [73, 87, 89]. It was recently reported that apart from this, avian pacemaker cells in the sino-atrial (SA) node arise from a so-called tertiary heart field (THF) [90]. Furthermore, epicardial progenitor cells form cardiac fibroblasts, vascular smooth muscle cells and atrial and venous endothelial cells [41, 91–93]. In addition, procardiogenic factors from the surrounding endoderm and mesoderm play a decisive role during different stages of heart development. In particular, this includes signaling pathways of bone morphogenetic proteins [94–96], nodal and fibroblast growth factors [97–99] as well as canonical and non-canonical Wnt/JNK [100–104].

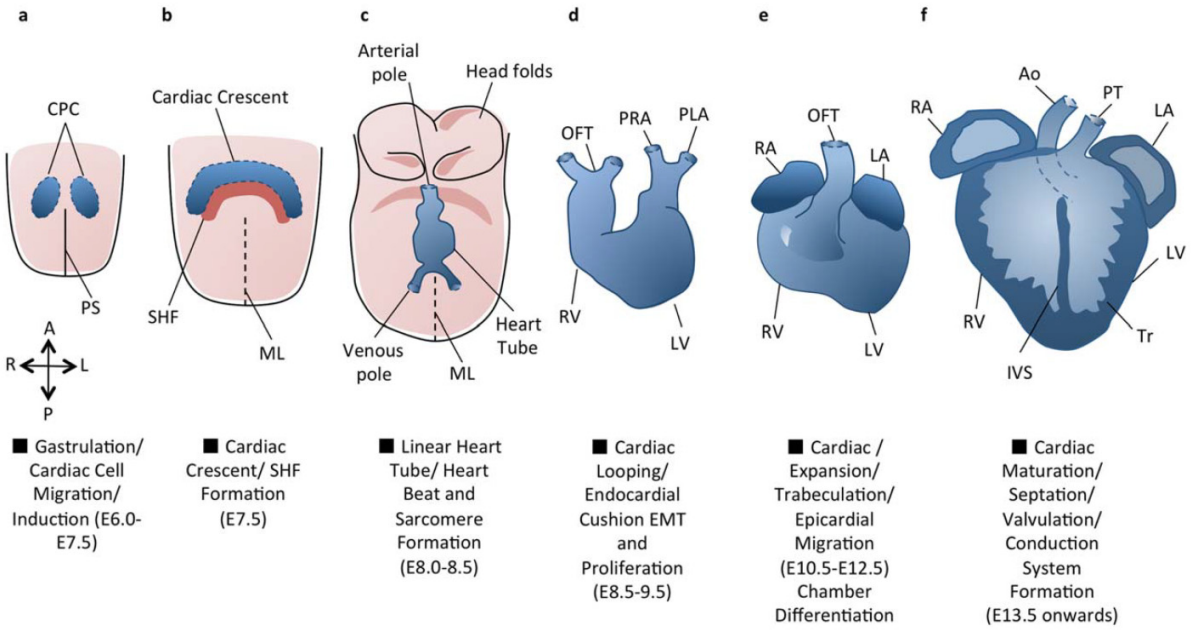

Figure 1: Overview of murine cardiac development

Schematic representation of murine cardiac development starting with (a) cardiac progenitor cells (CPC) on both sides of the primitive streak (PS) which (b) migrate towards the midline forming the cardiac crescent. At the same time, the formation of the second heart field begins. (c) At E8.0-8.5 linear heart tube formation occurs initially along the midline (ML) and afterwards (d) underwent a dextral looping forming the order of left and right ventricle (LV and RV). (e) Subsequent subdivision and (f) cardiac

maturation lead to the mammalian four chambered heart. Adapted from (Buckingham et al., 2005). A: Anterior, Ao: Aorta, CPC: Cardiac Precursor Cells, IVS: Interventricular septum, L: Left, LA: Left Atrium, LV: Left Ventricle, ML: Midline, OFT: Outflow Tract, P: Posterior, PHF: Primary Heart Field, PLA: Primitive Left Atrium, PRA: Primitive Right Atrium, PS: Primitive Streak, PT: Pulmonary Trunk, R: Right, RA: Right Atrium, RV: Right Ventricle, SHF: Secondary Heart Field, Tr: Trabeculae. [105]

Heart development is controlled by the interaction of the aforementioned cardiac transcription factors and consequently, Gata, Mef, Hand, Tbx, Nkx and members of other families are highly conserved across species [106, 107]. Homologues of Nkx2.5 and Mef2 are present in the contracting pharynx of the nematode *Caernorhabditis elegans* [108]. Tinman and pannier as the homologues of Nkx2.5 and Gata4 in the common fruit fly *Drosophila melanogaster* play an important role in the development of the tubular heart [109–111]. Expression of Nkx2.5 and Gata family members promotes the myocardial development and the expression of downstream cardiac genes in zebrafish and *Xenopus* embryos [112–115].

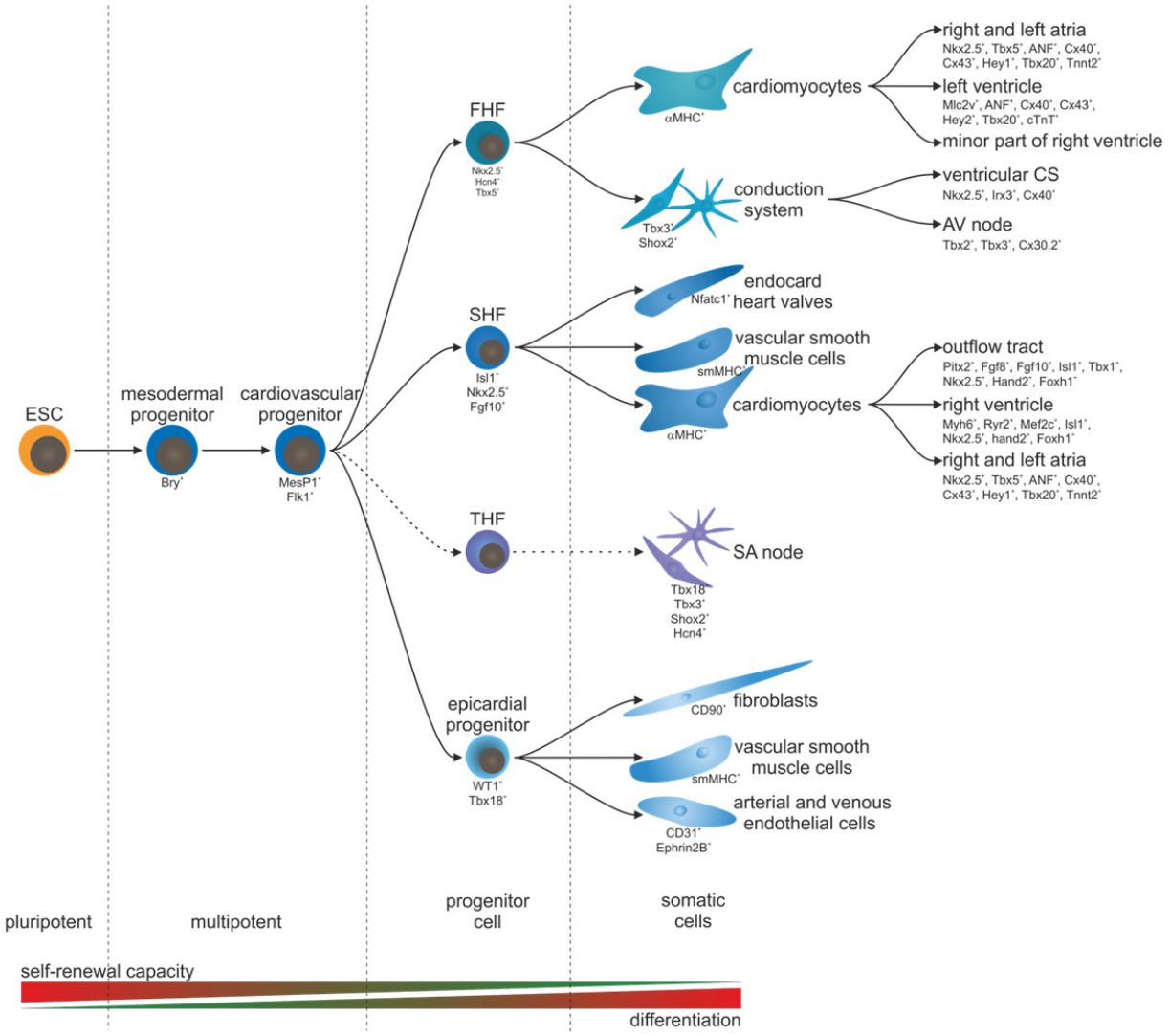

Figure 2: Commonly used concept of transcription factors regulating cardiovascular cell differentiation during development based on current models.

A multipotent mesodermal Bry^+ progenitor cell population forms the so far known beginning of the cardiovascular lineage. An specification is marked by early cardiovascular TFs MesP1 and Flk1 which gives rise to four subpopulations: i) the first heart field (FHF) – cells differentiate into cardiomyocytes of the right and left atria, the left ventricle and the minor part of the right ventricle, and the conduction system (CS), including ventricular CS and atrioventricular (AV) node, ii) the second heart field (SHF) – cells gives rise to cardiomyocytes of the right and left atria, the right ventricle and the outflow tract, vascular smooth muscle cells and the endocard of the heart, iii) the avian tertiary heart field (THF) – cells differentiate into pacemaker cells of the sinoatrial (SA) node and iv) a epicardium-derived progenitor cell population (EPDCs) which generate fibroblasts, vascular smooth muscles cells as well as arterial and venous endothelial cells. [116]

1.3. Reprogramming strategies for cardiovascular lineages

Development of new and elaboration of existing cardiomyocytic programming strategies becomes increasingly important to compensate the insufficient self-renewal capacity of the human heart to enable replacement of damaged tissue after injury. Various strategies permit progress in disease modelling and drug development, as knowledge of heart development provides first indications. The concepts for cell replacement streategies are highly diversified and range from basic research in the field of manipulative strategies of embryonic and adult stem cells as well as somatic cells up to application of autologous and allogenic transplants of various cell types (Figure 3) [117, 118].

However, attention will focus more and more on the issue of patient specific therapeutic approaches responding to individual prerequisites and needs as well as alternatives to allogenic heart transplantation. The inherent regenerative ability e.g. after MI should be effectively exploited through supporting preexisting CPC and CM by application of valuable factors.

The foremost priority of programming strategies should be the generation of cells as close as possible to their natural counterparts. To enable a technology transfer from bench to bedside, procedures should be xeno-, serum-, feeder- and DNA-free. The approaches described below suggest prospective options to overcome hurdles associated with purity, yield and safety of physiologically functional CM subtypes.

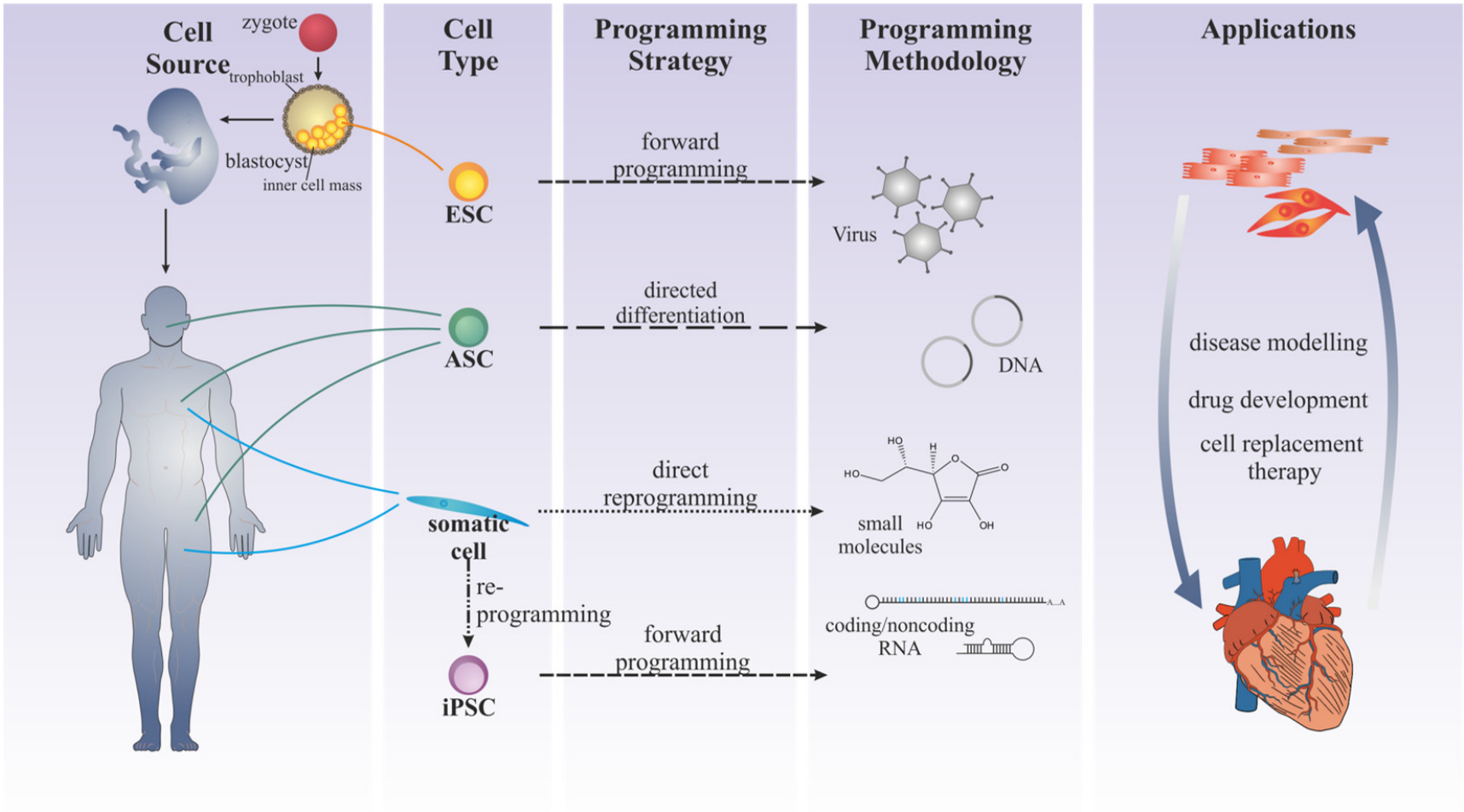

Figure 3: Common cell (re)-programming strategies in the cardiovascular field

Three promising approaches were developed for cardiovascular lineage development: i) forward differentiation of embryonic (ESC) or induced pluripotent stem cells (iPSC), ii) directed differentiation of adult stem cells (ASC) and iii) direct reprogramming of one somatic cell type into another somatic cell type of the same germ layer or even across germ layers. The underlying techniques and protocols could be distinguished in terms of their programming methodologies, such as viral or non-viral introduction of either cardiac specific transcription factors (TF) as DNA and mRNA or DNA-free approaches using different non-coding RNAs or small molecules cocktails to affect several signaling pathways. Generated cardiomyocyte-like subtypes could be used for disease modelling, drug development or cell replacement therapies. [117,118]

1.3.1. Forward differentiation of pluripotent stem cells

1.3.1.1. Cardiac differentiation of embryonic stem cells

In order to study key cellular and molecular programs of early heart development, pluripotent cells are a more suitable cell source. The first murine ESCs were isolated in 1981 by two independent groups [119, 120] and it has taken 17 years until one group successfully obtained the first human ESCs from the inner cell mass of a blastocyst [121]. Primed mESCs and hESCs share many common features [122–124]: i) expression of conserved pluripotency markers Oct4, Sox2 and Nanog [125, 126], ii) unlimited proliferation *in vitro* due to their solid self-renewal capacity [126, 127], and iii) multilineage differentiation potential to form all embryonic germ layers (endoderm, mesoderm and ectoderm) and their derivatives [128, 129].

hESCs bear serious disadvantages for research as well as clinical trials. The use of hESCs is mainly hampered by ethical issues concerning their generation and cloning, which lead to restricted availability. The countries in Europe act differently regarding ethical concerns of human embryonic stem cells (http://hpscreg.eu/). Malta, Luxembourg and Ireland for example have currently no legislation on this subject. In contrast, in Lithuania, Poland, Germany, Slovakia, Austria and Italy, hESC research or cloning are mostly prohibited or subject to stringent legislations. Additionally, immunological concerns arise with regard to their estimated immune-privileged status. Numerous publications have proven that undifferentiated murine ESCs cause significant immune rejection [130–132], which needs to be under consideration in further hESC studies.

Naïve mESCs require leukemia inhibitory factors (LIF) [133, 134] to maintain their pluripotency through activation of the signal transducer and activator of transcription (STAT3) as well as regulation of signaling proteins such as the extracellular signal-regulated kinase (ERKs) [135–137]. Moreover, co-culture with mitotically inactivated primary mouse embryonic fibroblasts or fibroblast-derived cell lines is needed [138]. The secreted extracellular matrix promote the self-renewal capacity and suppress differentiation, which could be used as conditioned medium as well [139].

Since the first study of spontaneous differentiation [140], murine ESCs have become a valid basis for *in vitro* modelling and manipulation of cardiac development. So far, existing protocols consist mainly of two main concepts: i) forced exogenous overexpression of lineage specific TFs [141–

144] and ii) cardiac stimulation through specific culture conditions by adding proteins or small molecules, like ascorbic acid or resveratrol [145–149].

The forced exogenous overexpression of lineage specific TF allows targeted differentiation towards particular cardiac phenotypes. Shox2 overexpression affects regulators of Wnt signaling, hereby enriching a pacemaker subpopulation [150]. Studies revealed that the presence of Nkx2.5 is essential for a proper differentiation toward a ventricular-like phenotype [144, 151] and that MesP1 results in early intermediate cells [68, 69]. However, neither of these approaches is sufficient to generate mature and pure ventricular cardiomyocyte subtypes, which could induce arrhythmias if transplanted as heterogeneous population [152]. Therefore, further purification towards a homogenous cell population will be an indispensable prerequisite. Improvements were achieved using the nodal cell inducer Tbx3 (T-box transcription factor 3) plus an additional Myh6-promotor-based antibiotic selection step [153–155]. The so-called iSABs (induced sinoatrial bodies) are over >80 % pure physiologically and pharmacologically functional pacemaker cells with a comparable beating frequency to normal murine SA nodal cells.

1.3.1.2. Cardiac differentiation of induced pluripotent stem cells

Besides ESCs, the relatively new and exciting class of pluripotent stem cells, the so-called "induced pluripotent stem cells" (iPSCs), could give deeper insights into developmental biology and personalized drug screening, avoiding ethical concerns of human ESCs. In 2006, Takahashi *et al.* published the reprogramming of mouse fibroblasts via the introduction of the four Yamanaka-factors: octamer-binding transcription factor 3/4 (*Oct3/4*; O), sex determining region Y-box 2 (*Sox2*; S), Krueppel-like factor 4 (*Klf4*, K) and *c-Myc* (M) [156]. For their outstanding work, the Nobel Prize in Physiology or Medicine was awarded in 2012 to Sir John B. Gurdon and Shinya Yamanaka "for the discovery that mature cells can be reprogrammed to become pluripotent" (http://www.nobelprize.org/nobel_prizes/medicine/laureates/2012/). Until now, numerous publications successfully generate iPSCs using different methods: i) retro-, lenti- and adenoviral [156–159], ii) protein [160, 161], iii) modified mRNA [162–166], iv) miRNA [167] or v) small molecules [168, 169]. So far, the full mechanism behind iPSC generation is still unclear and the number of articles is marginal. The most widely accepted model involves a stepwise process [170, 171] for the generation of different pluripotent cell types such as iPSCs and F-class cells [172–176]. Concerns regarding their mutagenicity and tumorigeneses are still valid. Ethical issues and responsible use of cloning using iPSC technology should not be

underestimated as current research demonstrates the possibility to generate fertile progenies using murine iPSCs with a success rate of 3.5 % [177].

The indirect reprogramming requires the initial iPSC generation step, followed by a specific cardiogenic differentiation. The most beneficial approaches are based on time- and dose-dependent application of cardiogenic modulators, such as activators or inhibitors of Wnt/β-catenin or TGFβ signaling [178–180]. Initial attempts were inefficient and time-consuming, with a success rate for obtianing spontaneously beating cells of approximately 1-10 % [181, 181, 182]. Generally, the cells did not exhibit full myocyte morphology and sarcomeric structure [183]. In addition, iPSC-derived CMs represent a heterogeneous population of nodal-, atrial-, and ventricular-like phenotypes, as obvious from electrophysiological studies [181]. The transplanted cells displayed low survival post-implantation, poor control and high tumorigenicity [184, 185].

1.3.2. Directed differentiation of adult stem cells

Initial approaches using ASCs for regenerative medicine were performed in 1957 by E. Donnall Thomas by means of bone-marrow transplantation between identical twins. These laid the foundation for the Nobel Prize in Physiology or Medicine in 1990 which was awarded to E. Donnall Thomas together with Joseph E. Murray “for their discoveries concerning organ and cell transplantation in the treatment of human disease” (http://www.nobelprize.org/nobel_prizes/medicine/laureates/1990/). Nowadays, adult stem cell transplantations are approved in clinical trials regarding cardiovascular disorders and appear to be one concept for future clinical use [186–188]. Nevertheless, they are still subject of controversial discussions regarding their only modest therapeutic outcome [187], the massive cell death observed after transplantation and the low rate of cell retention [189–192].

Directed differentiation of ASCs may afford more promising results of these multipotent cells. Various ASC sources are used so far, such as bone marrow-derived mesenchymal stem cells (BM-MSCs) [193–200], adipose-derived stem cells (ADSCs) [201–206], dental follicular stem cells (DFSC) [207], cardiac resident stem cells [208], hematopoietic stem cells (HSCs) [209] and endothelial progenitors [210]. Using various exogenous manipulation strategies, ASCs can potentially be differentiated towards CM-like cells. A cardiogenic differentiation *in vitro* or *in vivo* is favored by either i) co-culture with isolated cardiomyocytes [209], ii) treatment with methylation inhibitors, such as 5-azacytidine and histone deacetylase inhibitors, such as

trichostatin A [195, 201, 210], iii) respective forced exogenous expression of TFs, such as Nkx2.5 and Gata4 [194] or iv) co-transplantation of various aforementioned cell types [211]. However, recently published articles have implied that reliable cardiac marker expression occurs on the basis of cell fusion with recipient cardiac cells and to a lesser extent by differentiation, demonstrated in *in vivo* experiments [212, 213]. In particular, the generation of fully mature cells and cells of a specific cardiac subtype was not yet successful.

1.3.3. Direct reprogramming of somatic cells

An alternative approach avoiding an intermediate pluripotent state is called direct reprogramming or direct conversion. It is based on the direct cell fate alteration from terminally differentiated somatic cells or lineage progenitors to a mature cell type of interest of the same germ layer or even across germ layers. In order to achieve this, systematic intervention related to specific genetic cell properties has to be performed. In the majority of cases, lineage-specific factors, proteins, microRNAs and small molecules were used to affect respective signaling pathways and subsequently hierarchical structures of cell behavior.

The first successful step was taken in 1987 when Weintraub's group reported that one single key transcription factor, MyoD, is sufficient to convert murine fibroblasts into skeletal muscle cells [214]. Subsequently, numerous publications were issued covering direct conversion of various cell types, using one or more transcription factors, in particular to cardiomyocytes [40, 215, 216, 216–219]. Patient-specific lineage-conversion holds an enormous potential to gain better understanding of molecular biological impacts on pathogenesis, e.g. disease-related point mutations and single nucleoside polymorphisms [220]. Individual patient-specific conversion promises many advantages for clinical application: i) lowering the risk of tumorigenesis and inflammation after cell transplantation, ii) avoiding the need for transplantation by the opportunity of directly converting resident cells and iii) ethically acceptable. Despite these advantages, the generation of large numbers of functional healthy cells is an unmet goal. Hence, considerable further efforts will be necessary to develop a valid and clinically relevant therapeutic option.

Researchers made extensive efforts to overcome problems of availability and monitoring by focusing on transdifferentiation of a particular resident cell type, cardiac fibroblasts (CFs). CFs are highly abundant in the human adult heart. Likewise, CFs ensure the desired properties due to

their heterogeneity and plasticity as well as their resistance to the hypoxic environment of the post-infarct myocardium [23, 221, 222].

To date, no single key-regulator, such as MyoD, is known to efficiently convert the cell fate of mature somatic cells to cardiomyocytes. Current attempts are knowledge-based applications to directly or indirectly influence early cardiomyocyte differentiation.

An induced direct switch of cell fate in the most cases requires the forced overexpression of lineage specific TFs, supported by cardiogenic culture conditions or *in vivo* applications. The most commonly used TF combination to induce cardiomyocyte (iCM)-like cells from various fibroblast origins contains *Gata4* (transcription factor Gata4), *Mef2c* (Myocyte-specific enhancer factor 2c) and *Tbx5* (T-box transcription factor Tbx5) (GMT) [223–227]. Each of these single factors plays an important role during early heart development [107, 228–230] promoting cardiomyocyte differentiation [231–233]. However, the achieved expression of marker genes varies widely among laboratories, leading to 30 % $cTnT^+$ (cardiac troponin T) [223], 10-15 % iCM [225], 3 % αMHC^+ (alpha myosin heavy chain) [226] or 20 % αMHC^+ [227]. Chen *et al.* suggested that overexpression of GMT in tail tip fibroblasts and in cardiac fibroblasts is inefficient, as the generated cells displayed a weak similarity to mature cardiomyocytes on molecular and electrophysiological levels (0 % αMHC^+, 0 % $Nkx2.5^+$, 35 % $cTnT^+$) [224]. Recently published data demonstrated the influence of the protein expression levels of GMT in a certain ratio [234]. Higher protein levels of Mef2c together with lower levels of Gata4 and Tbx5 enhanced the reprogramming efficiency and quality of iCM. Additional combination alternatives are Gata4, Mef2c, Tbx5 and Hand2 (GMTH) [235, 236] or GMTH + Akt1 which among others enhanced polynucleation and thus evoked a more mature cardiac phenotype of iCMs [237]. The efficiency can be positively influenced by grafting of cells *in vivo* [225, 235], indicating a considerable role of the microenvironment in the heart. Another combination strategy is based on key cardiac TFs *MesP1* with v-ets erythroblastosis virus E26 oncogene homolog 2 (*ETS2*) with addition of ActivinA and BMP2 [238] to influence signaling pathways during cardiogenesis. This protocol leads to an immature phenotype of cardiomyocytes expressing the core cardiac factors Nkx2.5, Isl1, Tbx20, the mesodermal signaling molecules BMP2, TDGF1 as well as muscle markers Myl2, Myh6.

Aside from forced overexpression of TF, transient genetic manipulations have been developed in different laboratories: i) introducing modified mRNA (see below: 1.4.1) or ii) microRNA (see below: 1.4.2) and iii) small molecules. Wang and colleagues efficiently converted fibroblasts merely using one TF, *Oct4*, along with a defined small-molecule cocktail [239]. The small-molecule cocktail contains an ALK4/5/7 inhibitor (SB431542), GSK3 inhibitor (CHIR99021), LSD1/KDM1 inhibitor (parnate) and an adenylyl cyclase activator (forskolin) to induce the reprogramming efficiency, including modulators of epigenetic enzymes, signaling pathways, metabolism and transcription. In these proof-of-principle experiments, spontaneously contracting cardiomyocytes with a ventricular-like phenotype were generated. Another improvement was achieved due to inhibition of pro-fibrotic signaling, for instance using small molecules affecting RhoA-ROCK or TGF-β pathways [240].

All of these experiments yielded only immature cardiomyocytes within an inhomogeneous population lacking structural and electrophysiological characteristics of adult cardiomyocytes. It is consequently of great interest to fully understand the mechanisms underlying reprogramming strategies to enhance purity, safety and efficiency.

1.4. Non-viral and DNA-free modifications

Classical strategies for gene and cell therapies were based on virus-mediated delivery of DNA due to their high efficiency. However, the use of retroviral or lentiviral systems is associated with high safety concerns, including undesirable systemic spread, DNA integration into the host genome, causing insertional mutagenesis and tumorigenicity as well as uncontrolled expression through incorrect promotor selection. For this purpose, among others, non-viral lipid- and polymer based delivery systems are currently under examination [241–243].

Circumventing the aforementioned drawbacks, modified mRNA or microRNA offer new opportunities for clinically relevant applications. The major advantages are their operation site in the cytoplasm, avoiding the necessity of nuclear translocation, as well as their fast and controllable application, which making them a favored tool for slowly proliferating cells such as adult stem cells.

1.4.1. Modified mRNA

Recent progress in the field of modified mRNA (mmRNA) eradicated existing doubts regarding efficiency, stability and immunogenicity [244, 245]. Initial attempts in developmental biology

were made with unmodified mRNA in embryos of lower vertebrates such as fish and frog [246, 247] as well as rodent embryos [248]. At that time, usage of unmodified mRNA was neither appropriate for mammalian cell cultures nor as therapeutic method in human beings. The technology was hampered by the instability and susceptibility to degradation as well as inefficient translation and immunostimulatory effects and was therefore rarely used for introduction of foreign genetic information [249, 250].

The use of mRNAs encoding for functional proteins has indicated progress for innovative methods. For example, manipulation of autologous dendritic cells yields plenty of benefits for cancer immunotherapy and therapeutic vaccination [251–255]. Furthermore, mRNAs encoding therapeutic proteins such as EPO or SP-B have proven to be of great relevance for clinical use [256, 257]. On the one hand, mRNA-mediated programming of fibroblasts to iPSCs is more efficient with up to 4.4 % iPSCs and on the other hand, cells generated by this technique demonstrate a global transcriptional signature more closely resembling that of hESCs than retrovirally programmed iPSCs [162–166].

Initial steps have been enabled by the discovery and subsequent utilization of SP6 and T7 RNA polymerases derived from the bacteriophage genome [258, 259]. In recent years, several laboratories made considerable efforts to improve mRNA properties, usually implemented by mimicking mature eukaryotic mRNA. Synthetic mRNA was equipped with either cis- or trans-acting factors, comprising: i) a methylated 5’ cap-structure analog (3′-O-Me-m7G(ppp)G or phosphate-modified analogues), ii) a 5’ untranslated region (5’ UTR) containing e.g. a Kozak consensus sequence, iii) modified nucleosides such as 5-methylcytidine-5’-triphosphate (5mC) or pseudouridine-5’-triphosphate (Ψ), iv) a 3’ untranslated region (3’ UTR) containing stable non-coding sequences of e.g. 3’ UTR of the human globin, and v) a poly-A-tail of 100 – 250 adenosine residues.

The use of cap analogs leads to ribosome recruitment and translation [260, 261], mRNA splicing [262], stabilization [263–265] and translational repression via microRNA [266, 267]. The translation is initiated by diverse nucleoside sequences around the initiation codon AUG [268–270] in the 5’ UTR. Usually, the innate immune system is activated through pathogenic mRNA leading to inflammatory response and apoptosis. This can be prevented by incorporation of modified nucleosides such as 5mC or Ψ [256, 271–273] as well as other modulations to reduce

the stimulation of Toll-like receptors (TLR) [271], protein kinase PKR [274] and retino acid-inducible protein I (RIG-I) [275]. The composition of modification has to be optimized in pilot experiments for each cell type under investigation to achieve the best protein expression combined with long term cell viability [276, 277]. In addition, modifications of the 3' UTR due to avoid AU-rich sequences or usage of histone stem loops are necessary to prevent removal of the poly-A-tail [278–280]. The stability of the poly-A-tail itself depends on the number of adenosine residues [281]. Along with the cap, the poly-A-tail is necessary for an efficient translation as well as for protection from degradation [282, 283].

In addition, the innate immune response can be reduced by stringent purification procedures using high performance liquid chromatography (HPLC) to eliminate short double stranded RNA [284]. Additional risks may be excluded by standardization of the mRNA production process. Relevant GMP-qualified mRNA was used in recent clinical trials [285, 286].

In vivo intramyocardial applications of synthetic modified mRNA have been shown to be a feasible application method after MI. Human vascular endothelial growth factor-A (VEGF-A) improves heart function and long-term survival of treated mice due to mobilization and differentiation of resident endogenous heart progenitors ($WT1^+$ EPDCs) [287]. Application of Insulin-like growth factor-1 (IGF-1) promotes cardiomyocyte survival and delay of cell apoptosis under hypoxic conditions [288]. Another study confirmed the use of mmRNA in small and large animal models [289]. A robust protein expression was observed 6 h after direct myocardial injection and was detectable for up to 2 weeks with only limited biodistribution (< 10 % in lung, liver and spleen). This rapid and transient expression indicates that the technology is reliable and controllable for a variety of cardiovascular applications.

1.4.2. microRNA

Another promising approach for genetic manipulation consists of the introduction of small non-coding RNA molecules (abbreviation: microRNA, miR), thereby omitting exogenous TF overexpression.

MicroRNAs are a new category of regulatory mediators during development and maintenance [290–292]. They fulfil their purpose as posttranscriptional repressors of mRNAs by complementary binding to the 3' UTR of the target mRNA [293–297]. Mature microRNAs are evolutionarily conserved 21-25 nucleoside long non-protein-coding RNAs [296]. The microRNA

database miRBase continuously publishes data obtained by deep sequencing technologiesand currently contains 28645 entries of hairpin precursor miRNAs, expressing 35828 mature miRNA products, in 223 species (http://www.mirbase.org/, June 2017, release 21) [298]. It should be emphasized that only a modest change in mRNA expression (20 – 50 %) on transcription level can be achieved by microRNA repression [299, 300], which was proven by the limited repression (<2-fold) on protein level [301, 302]. However, a single microRNA has up to hundreds of target mRNAs [300] demonstrating the global range of microRNA interaction.

To date, seven so-called „cardiomiRs“ have been identified, which are highly relevant for cardiomyogenesis [303, 304]; microRNA-1, -30a-e, -133, -181a, -195, 208a/b, -499 [292]. As an example, microRNA-1 interacts with several myogenic TFs like SRF (serum response factor), Mef2c, MyoD and Nkx2.5 as repressor and cooperator in a regulatory loop [305–307]. Regulation can be mediated by inhibition of the notch signaling pathway due to direct repression of Dll1 [308] and its downstream effector Hes1 [198]. This, in turn, will lead to the expression of Gata4, Nkx2.5 and Myogenin. Loss-of-function experiments in *drosophila melanogaster* have led to embryonic mortality in the larval stages, and in equal manner, miR-1-mutants manifest severe defects in sarcomeric gene expression [309, 310].

Initial attempts, using four cardiomiRs (miR-1, -133, -208 and -499) in addition with a chemical Janus kinase inhibitor achieved the switch of cell fate towards a cardiomyogenic phenotype with 28 % αMHC^{+} cells *in vitro* using mouse cardiac fibroblasts as starting material and an improved cardiac function *in vivo* [311, 312]. Another forward reprogramming strategy is based on cardiomyocyte progenitor cells, overexpression of miR-1 and miR-499 enhanced differentiation into cardiomyocytes via repression of histone deacetylase 4 or Sox6 [313]. The results have been confirmed, showing that the improved cardiac performance after miR-499 application occurred through repression of Sox6 and Rod1 [314].

Furthermore, microRNAs may help to overcome several obstacles arising due to MI and particularly stem cell transplantations; e.g. modest efficiency, apoptosis, inflammation and low retention of transplanted cells [187, 189–192]. As recently published, numerous microRNAs possess a potentially anti-apoptotic effect and may enhance cell survival; e.g. microRNA-30b [315], -19a [316], -181c [317], -17 [318], -22 [319] -21, -146a, -155 [320]. Moreover, microRNA-21 has a beneficial effect on inflammatory injured myocardium [321, 322].

Overall, microRNAs possess regulatory complexity due to their impact on several processes, including cell proliferation, differentiation, apoptosis and tumorigenesis [323].

2. Aim of this work

The investigation of advanced therapeutic options for the treatment of injured tissue after MI is currently of great interest and will be a main research focus over the next few years. Therefore, this thesis aimed to contribute to the knowledge on a basic research level in the field of regenerative medicine to promote ideas of remuscularization.

The dissertation focused on one hand on the evaluation of forward programming into specific cardiac subtypes using murine ESCs. The forced exogenous overexpression of the cardiac transcription factor Nkx2.5 should provide insights whether one factor is sufficient to generate fully mature and functional ventricular cells. To this end, a cardiac differentiation protocol was adjusted to the demands needed, including selection of an appropriate cell clone, culture conditions and antibiotic selection time point. The obtained spontaneously beating single cells were examined on the protein as well as RNA level in order to determine evidence for quality and maturity. Furthermore, the achieved cells were analyzed with respect to their potential to respond to ion channel modulators to verify the functional behavior compared to murine neonatal cardiomyocytes.

The second focal point was set on strategies avoiding DNA and viral introduction. It has become apparent that the use of several RNA molecules such as mRNA and microRNA is a promising approaches of cell fate alteration. Therefore, a PCR-based protocol for the generation of highly reproducible mmRNA was developed. The best modification candidate was applied to several cell types, using EGFP mmRNA. Initial experiments verified the direct conversion of one somatic cell type to another somatic cell type using modified MyoD mRNA and forward programming of murine ESCs using modified Nkx2.5 mRNA. Another possibility to improve already existing stem cell therapies of bone-marrow derived $CD133^+$ SCs is an additional genetic manipulation using microRNA. Therefore, we aimed to establish a superparamagnetic polymer-based non-viral delivery system. With this concept, an efficient and gentle uptake of microRNA could be ensured, with negligible impact on $CD133^+$ haematopotic SC potential. One huge advantage using this novel delivery system is the specific magnetic targeting possibility to guide the cells of interest to the side of interest, thereby may enhancing the regenerative potential of $CD133^+$ SCs due to reducing a massive wash out after transplantation.

3. Materials and Methods

3.1. Materials

For a detailed list of laboratory materials and devices please refer to appendix (V).

3.2. Cell culture

3.2.1. Murine embryonic stem cells

W4 murine embryonic stem cells (mESCs) [324] were cultured in DMEM supplemented with 15 % FBS Superior (Biochrom AG, Germany), 1 % Cell Shield® (Minerva Biolabs GmbH, Germany), 100 µM non-essential amino acids, 1000 U/mL leukemia inhibitory factor (Phoenix Europe GmbH, Germany) and 100 µM β-mercaptoethanol (Sigma-Aldrich GmbH, Germany) at 37 °C, 5 % CO_2 and 20 % O_2.

Prior differentiation mESCs were co-cultured for at least seven days on inactivated murine embryonic fibroblasts SNL 76/7 (STO cell line). Three days before differentiation mESCs were replaced from SNL feeder due to enzymatic split with collagenase IV (1 mg/mL) and accutase (400-600 units/mL) as previously described [154].Generated clones were subsequently cultured under antibiotic selection (Table 1).

Table 1: mESC clone culture under antibiotic selection

Clone	Antibiotic	Stock solution	Working solution
W4			
W4 αMHC #15	Hygromycin	100 mg/mL	250 µg/mL
W4 αMHC #15 Nkx2.5 #A-T	Hygromycin Blasticidin	100 mg/mL 10 mg/mL	250 µg/mL 10 µg/mL

3.2.2. Differentiation of mESCs

Differentiation of mESCs was performed in cardiogenic differentiation medium, containing IBM (Biochrom AG, Germany) supplemented with 10 % FBS Superior, 1 % Cell Shield®, 100 µM non-essential amino acids, 450 µm 1-thioglycerol (Sigma-Aldrich GmbH, Germany) and 213 µg/mL ascorbic acid (Sigma-Aldrich GmbH, Germany). Differentiation was initiated by hanging-drop culture for two days at 37 °C, 5 % CO_2 and 20 % O_2. For this purpose 400 cells per drop were plated on the cover of a square petri dish. Afterwards, formed embryoid bodies (EBs)

were cultured for four days in suspension culture, whereby they were regularly shaked. The following characterization of the cells were carried out under two different concentrations of oxygen, 1 % O_2 and 20 % O_2 from day seven of differentiation.

In order to assure a qualitative statement of spontaneously beating areas per EB (Figure 7), a defined number of EBs were plated on gelatine coated well plates and subsequently counted for 14 days.

To ensure the optimal time point for the antibiotic selection step (Figure 8), a defined number of EBs were plated on gelatine coated well plates and either treated with 2 µg/mL puromycin on day 7, 9, 11, 13 or 15 of differentiation. Single cells were obtain through dissociation four days after puromycin treatment with collagenase IV and accutase and counted 12 days later.

Molecular- and cell biological analysis as well as determination of beating frequencies were performed on day 25 of differentiation on single cell level.

3.2.3. Fibroblasts

Monkey kidney fibroblasts COS7 as well as murine embryonic C3H10T1/2 (Clone 8, ATCC, USA) were cultured in DMEM (Biochrom AG, Germany) supplemented with 10 % FBS (Pan Biotech GmbH, Germany), 100 µM non-essential amino acids (Biochrom AG, Germany) and 1 % penicillin/streptomycin (PAA Laboratories GmbH, Germany) at 37 °C, 5 % CO_2 and 20 % O_2. Mouse embryonic C3H10T1/2 cells were used in passages 13-15. BJ human foreskin fibroblasts (Stemgent, USA) were cultured in EMEM (Biochrom AG, Germany) supplemented with 10 % FBS, 100 µm non-essential amino acids and 1 % penicillin/streptomycin at 37 °C, 5 % CO_2 and 20 % O_2. BJ human fibroblasts were used in passages 15-25.

3.2.4. Human mesenchymal stem cells

Mesenchymal stem cells (hMSCs) were obtained from bone marrow (BM) aspirates of patients during coronary artery bypass grafting as previously described [325]. All donors gave their written consent to use their bone marrow for research proposes according to the Declaration of Helsinki. At first, density gradient centrifugation was performed to isolated mononuclear cells (MNCs). For plastic adherence selection cells were cultivated in Mesenchymal Stem Cell Growth Medium (MSCGM™, Lonza, MD, USA) containing 1 % penicillin/streptomycin (PAA) at 37 °C, 5 % CO_2 and 20 % O_2. hMSCs were used in passages 2-4.

3.2.5. Human hematopoetic stem cells

$CD133^+$ hematopoetic stem cells (HSC) were purified from freshly isolated MNCs (see 3.2.4). Cells were magnetically enriched using human MACS CD133 MicroBeads (Miltenyi Biotec GmbH, Germany) following the manufacturer's instructions. The subsequent experiments were performed using cell samples with a minimal viability and purity of 80 % (determined by adapted ISHAGE guidelines (3.4.1.2). $CD133^+$ HSCs were cultured for the establishment of miRNA/PEI/MNP transfection system in DMEM supplemented with 2 % FBS and 1 % penicillin/streptomycin (PAA) and in StemSpan™ H3000(STEMCELL™ Technologies, Canada) supplemented with StemSpan™ CC100 (STEMCELL™ Technologies) as optimized culture medium at 37 °C, 5 % CO_2 and 20 % O_2.

3.3. Molecular biological investigation

3.3.1. RNA isolation

The isolation of total RNA from mESC clones was performed using NucleoSpin® RNA isolation kit (Macherey-Nagel, Germany) and from cardiogenic derived single cells at day 25 of differentiation using NucleoSpin® RNA isolation kit XS (Macherey-Nagel, Germany) following the manufacturer's instructions. Purity and concentration was analyzed with NanoDrop 1000 Spectrophotometer (Thermo Fisher Scientific Inc., USA). Samples were stored at -80 °C until further processing.

3.3.2. Reverse transcription

The synthesis of first strand cDNA from aforementioned total-RNA was transcribed using the RevertAid H Minus First Strand cDNA Synthesis Kit (Thermo Fisher Scientific Inc., USA) following the manufacturer's instructions. The reverse transcription was performed applying the $Oligo(dT)_{18}$ primer. The reaction was conducted using the MJ Mini™ thermal cycler (Bio-Rad Laboratories GmbH, Germany). Samples were stored at -20 °C until further processing.

3.3.3. Quantitative real-time polymerase chain reaction

Quantitative real-time polymerase chain reactions (qPCR) were carried out through TaqMan™ PCR-technology. A sequence-specific oligonucleotide (TaqMan® Gene Expression Assay; Table 11) bound with the fluorophore 6-carboxyfluorescein (FAM) at the 5'end and a quencher at the 3' end is used to determine the direct proportionality of released fluorescence detection and amount of DNA. A qPCR reaction consists of TaqMan® Universal PCR Master Mix (Thermo Fisher

Scientific Inc., USA), respective TaqMan® Gene Expression Assay, UltraPure™ DNase/Rnase-Free Distilled Water (Thermo Fisher Scientific Inc., USA) and 10 ng respective cDNA and were performed using the StepOnePlus™ Real-Time PCR System (Applied Biosystems, Germany) with the following program (StepOne™ Software Version 2, Applied Biosystems, Germany): start at 50 °C for 2 min, initial denaturation at 95 °C for 10 min, denaturation at 95 °C for 15 s and annealing/elongation at 60 °C for 1 min with 40 cycles. Analysis and evaluation of gene expression profiles were performed using the ΔΔCt method for relative quantifications. For this, mean values of target genes were normalized to the mean values of the housekeeping genes mHprt and mPolr2a and relative considered to a respective control probe.

3.4. Cell biological investigation

3.4.1. Flow cytometry

All subsequent flow cytometry analysis were performed using BD FACS LSRII flow cytometer (BD Biosciences, Germany) with BD FACSDiva Software 6.1.2 (BD Biosciences, Germany).

3.4.1.1. Analysis of EGFP expression

Flow cytometry analysis of EGFP mmRNA transfected cells were carried out 4 h, 12 h, 24 h, 48 h and 72 h after transfection. Therefore, supernatant and cells were collected and fixed with 4 % formaldehyde. To examine viability, cells were stained with Near-IR LIVE/DEAD Fixable Dead Cell Stain Kit (Molecular Probes, USA). EGFP expression, viability and mean fluorescence were analysed for every cell type under investigation.

3.4.1.2. Analysis of CD133 surface marker pattern

The evaluation of CD133 surface marker and cell viability was performed with the Boolean gating strategy adapted on the ISHAGE guidelines for $CD34^+$ cell analysis [326]. Therefore, cell samples were analysed 0 h and 18 h after isolation (see 3.2.5) using following antibodies: CD34-FITC (clone: AC136), CD133/2-PE (clone: 293C3), isotype control mouse IgG 2b-PE (all aforementioned: Miltenyi Biotec GmbH, Germany), CD45-APC-H7 (clone: 2D1) and 7-AAD (both BD Biosciences, Germany). Unspecific binding was reduced using FcR blocking reagent (Miltenyi Biotec GmbH, Germany). Following incubation (10 min, 4 °C), samples were measured immediately.

3.4.1.3. Analysis of miRNA uptake efficiency

Flow cytometry analysis of $CD133^+$ HSC transfected with Cy3™-labelled miRNA was carried out 18 h after transfection. Therefore, supernatant and cells were collected and fixed with 4% formaldehyde. To examine viability, cells were stained with Near-IR LIVE/DEAD Fixable Dead Cell Stain Kit (MolecularProbes, USA). miRNA uptake (proven by Cy3™ detection), viability and mean fluorescence were analysed.

3.4.2. Immunohistochemistry

Unless otherwise specified, all subsequent immunohistochemistry images were performed using ELYRA PS.1 LSM 780 confocal microscope (Carl Zeiss, Germany) and ZEN2011 software (Carl Zeiss, Germany).

3.4.2.1. Visualization of pluripotent expression pattern of mESCs

W4 generated mESC clones were seeded on cover slips and fixed after 48 h with 4% formaldehyde and incubated afterwards with 50 mM ammonium chlorid. Cells were permeabilized with 0.2 % Triton X-100 and blocked with 1 % BSA (in PBS). All antibodies were incubated in blocking solution containing 0.01 % saponin (Sigma-Aldrich GmbH, Germany) in 1 % BSA, primary antibodies for 1 h at RT and secondary antibodies for 40 min at RT. Antibody staining was performed one after another to avoid cross reactivities. The following antibodies were used for mESC clones, primary antibodies: Nkx.2.5 (Santa Cruz Biotechnology Inc., USA; 1:100), Oct4 (Abcam, UK; 1:200), Sox2 (Abcam, UK; 1:200), and secondary antibodies: Alexa Fluor® 568 donkey anti-goat (Life Technologies, USA, 1:300) and Alexa Fluor® 568 donkey anti-rabbit (Life Technologies, USA, 1:300). Additionally, the cells were counterstained with Phalloidin-FITC (1:500). Samples were mounted with Fluoroshield™ with DAPI (Sigma-Aldrich, Germany) for nuclei staining.

3.4.2.2. Visualization of cardiogenic-derived single cells

Cardiogenic-derived single cells were treated in an analogous manner (3.4.2.1). The following antibodies were used for single cells, primary: Cx43 (Santa Cruz Biotechnology, Inc., USA, 1:100), cTnnT (Abcam, UK; 1:100), HCN4 (Alomone labs, Israel; 1:100), Myh6 (Abcam, UK; 1:100), Myh7 (Sigma-Aldrich GmbH, Germany; 1:500), α-actinin (Abcam, UK; 1:100), secondary antibodies: Alexa Fluor® 568 donkey anti-goat (Life Technologies, USA; 1:300), Alexa Fluor® 647 donkey anti-mouse (Life Technologies, USA, 1:300), Alexa Fluor® 488 donkey anti-rabbit (Life Technologies, USA; 1:300) and Alexa Fluor® 568 donkey anti-

rabbit(Life Technologies, USA; 1:300). Samples were mounted with Fluoroshield™ with DAPI for nuclei staining. Images were performed using the superresolution technology structured illumination microscopy (SIM). Therefore, sample images were recorded with the 100x alpha 1.46 Plan Apochromat® (Carl Zeiss) objective with oil immersion. Z-stacks were recorded in SIM mode with a 16 bit depth at 5 angles, with averaging 4; 23 µm grid was applied for 405 laser line, 34 µm – 488, 42 µm – 561, 51 µm – 633. The obtained SI raw datasets were computationally reconstructed by ZEN software and presented at alignment of Maximum projections.

3.4.2.3. Visualization of EGFP expression

Immunostaining of EGFP mmRNA transfected COS7, C3H10T1/2, BJ, hMSCs and mESC clones was performed 24 h after transfection with a FITC conjugated anti-GFP antibody (Abcam, UK; 1:100) according to the manufacturer's protocol. Fluorescence was detected with Axiovert 40 CFL (Carl Zeiss, Germany).

3.4.2.4. Visualization of mRNA-derived myoblast-like cells

mmRNA-derived myoblast-like cells (3.7.2.2) were seeded on cover slips and fixed after 24 h with 4 % formaldehyde. Cells were permeabilized with 0.1 % Triton X-100 and blocked with blocking solution (PBS with 0.2 % gelatine, 10 % FBS). The following antibodies were incubated at RT in blocking solution: primary antibody MyHC (Abcam, UK; 1:200) and secondary antibody, Alexa Fluor 647 goat anti-mouse IgG (Life Technologies, USA, 1:500). Additionally, the cells were counterstained with Phalloidin-FITC to visualize Actin-positive cells (1:1000; Enzo Life Science, Inc., USA) and DAPI (1:2000, Invitrogen, USA) for nuclei staining. Samples were mounted Fluoroshield™ with DAPI.

3.4.2.5. Intracellular visualization of miRNA-PEI-MNP complexes

To visualize the intracellular distribution of miRNA-PEI-MNP complexes (optimal conditions: 20 pmol miRNA; N/P ratio: 7.5; 3 µg/ml MNPs) 5 x 10^4 $CD133^+$ SCs were fixed after 18 h with 4 % formaldehyde. Cells were spun down on cover slips and mounted with Fluroshield™ with DAPI on microscope slides. $CD133^+$ SCs used for laser scanning confocal microscopy (tile-scan with 1062.33 x 1062.33 µm and z-stack with 7 µm depth using 40x oil immersion) were transfected with Cy3™ dye-labeled Pre-miR Negative Control #1 (Ambion, USA) and unlabeled PEI as well as MNPs. For SIM imaging, $CD133^+$ SCs were transfected with complexes consisting of: Pre-miR™ miRNA Precursor Molecules – Negative Control #1 (Ambion, USA)

labelled with Cy5™ dye (Mirus Bio LLC, USA), PEI stained with FluoReporter® Oregon Green® 488 (Molecular Probes, USA) and MNPs stained using Atto 565 dye conjugated to biotin (1:1000 *w*/*w*; ATTO-TEC GmbH, Germany). Recently published paper, describes the precise procedure in detail [327, 328].

3.4.3. CFU assay of CD133$^+$ HSC

The Colony-Forming Unit (CFU) assay was performed using MethoCult™ H4434 Classic (STEMCELL™ Technologies, Germany) following the manufacturer's instructions. For this, CD133$^+$ HSCs were transfected with complexes consisting of: Pre-miR™ Precursor Molecules – Negative Control #1, non-labelled PEI and non-labelled MNPs. 1 x 10^3 cells were seeded per 35 mm dish 18 h after transfection and colonies were evaluated 14 d after incubation at 37 °C, 5 % CO_2 and 20 % O_2.

3.5. Live cell imaging

Life cell imaging was preformed using ELYRA PS.1 LSM 780 confocal microscope and ZEN2011 software. Cells were incubated during observation at 37 °C.

3.5.1. Analysis of beating frequencies

The spontaneous beating frequency of cardiogenic-derived single cells was analyzed at day 25 of differentiation. For this, cells were plated after dissociation on gelatine coated 24 well plates and kept in differentiation culture until observation. The recording was performed using 10-fold optical magnification and 20 images per second. After recording, mean region of interest (mROI) was specified and the varying light intensity at the mROI determined. The displayed peaks equates to a beat of the cell.

3.5.2. Physiological investigation

Using aforementioned method for the determination of spontaneous beating frequencies (3.5.1), cell characteristics were examined under different physiological conditions. However, only spontaneous beating single cells could be analyzed in terms of their physiological behavior. Single cells without own spontaneous beating were not implied in the analysis.

Cardiogenic-derived single cells were evaluated under administration of the following reagents: Noradrenaline (1 µM), Acetylcholine (10 µM), Mibefradil (10 µM), Verapamil (10 µM), Tetrodotoxin (10 µM) and potassium rich extracellular fluid (20 mM). First, beating frequency was determined as baseline (t0). Second recording comprised a period of 2 minutes to include 2

time points: 10 s after application (t1) and 1 min after application (t2) of the respective reagent. The closing record was performed 5 min after application (t3). Findings represent the differences between the respective time point after application to the baseline beating frequency.

3.5.3. Calcium transient

In order to visualize a calcium transient in generated CM-like single cells, cells were incubated for 60 min at RT using X-Rhod-1 (4 µm; Thermo Fisher Scientific Inc). Afterwards, cells were washed two times with pre-warmed PBS and analyzed in fresh pre-warmed differentiation medium.

3.5.4. Visualization of magnetic targeting with miRNA/PEI/MNPcomplexes

To visualize the magnetic cell targeting capacity of miRNA/PEI/MNP complexes (optimal conditions: 20 pmol miRNA; N/P ratio: 7.5; 3 and 5 µg/ml MNPs) $CD133^+$ HSCs were transferred and reseeded on a 12 well plate 18 h after transfection. Unbound complexes were washed out and a magnetic field was applied locally using a magnetic plate (OZ Biosience, France; field strength 70 – 250 mT and 50 – 130 t/m, respectively [329]). After a further 24 h at 37 °C, 5 % CO_2 and 20 % O_2 cell number was documented and counted subsequent with ImageJ 1.48 (NIH, USA). Magnetic targeting rations were calculated by dividing cell number of area with magnet (M+) with cell number of area without magnet (M-).

3.6. *In vitro* synthesis of modified mRNA

The establishment of modified mRNA (mmRNA) was based on the generation and evaluation of the enhanced green fluorescent protein (EGFP)(Figure 17). Any further processing of mmRNA was identical to EGFP, only diverging compositions will be mentioned afterwards.

3.6.1. Generation of DNA template for IVT

For the generation of EGFP and MyoD DNA template, pCS2+ expression vector was used (Figure 34). It contains, in addition to simian CMV IE94 DNA mammalian expression promotor (sCMV), a SP6 RNA polymerase promotor in the 5' untranslated region of the mRNA from the sCMV promotor. EGFP and MyoD sequences were introduced using XhoI (bp 107) and XbaI (bp 115) cloning sites (Figure 17B). The region of interest was amplified with PCR using the forward primer 5'-GTCGGAGCAAGCTTGATTAGG-3' and reverse primer 5'-T_{100}GTCTGGATCTACGTAATACG-3'. The PCR reaction was performed using Herculase enhanced proof-reading DNA polymerase (Agilent Technologies, USA) and the following cycle

conditions: initial denaturation at 95 °C for 2 min, 30 cycles with denaturation at 95 °C for 30 s, annealing at 59 °C for 60 s, elongation at 72 °C for 30 s and a final elongation step at 72 °C for 10 min with the MJ Mini™ thermal cycler. PCR purification was performed using the peqGOLD Cycle-Pure Kit (peqlab, UK) following the manufacturer's instructions. Purity and concentration was analyzed with NanoDrop 1000 Spectrophotometer.

3.6.2. *In vitro* synthesis

In vitro transcription (IVT) of desired transcription factor or EGFP gene was performed using either MEGAscript SP6 Kitor MEGAscript T7 Kit (both Ambion, USA) depending on the respective vector backbone. IVT of EGFP was realized with 500 ng purified DNA template and SP6 RNA poylermase. To generate mRNA modifications, modified ribonucleoside triphosphates were used during IVT performance. Uridine-triphosphate and cytidine-triphosphate were replaced with pseudouridine-5'-triphosphate and 5-methylcytidine-5'-triphosphate (both TriLink Biotechnologies, USA) in the indicated ratio. The optimal mRNA modification has to be defined for every cell type. Therefore, the following modifications of EGFP were used: unmodified mRNA, 100 % 5-methylcytidine-5'-triphosphate, 100 % pseudouridine-5'-triphosphate, 52 % 5-methylcytidine-5'- triphosphate + 52 % pseudouridine-5'-triphosphate and 100 % 5-methylcytidine-5'-triphosphate + 100% pseudouridine-5'-triphosphate with a final concentration of 5 mM per nucleoside. To obtain capped mRNA, a 3′-O-Me-m7G(ppp)G RNA cap structure analog (New England Biolabs, USA) was added through the IVT reaction while reducing guanosine-triphosphate in a ratio of 4:1. The reaction was incubated for 4 h at 37 °C. Following the IVT, mmRNA was treated with TurboDNase (contained in MEGAscript SP6 Kit) for 15 min at 37 °C to remove remaining DNA templates. The mmRNA was purified using the GeneJET RNA Purification Kit (Thermo Fisher Scientific Inc., USA) following the manufacturer's instructions. Purity and concentration was analyzed with NanoDrop 1000 Spectrophotometer.

3.7. Transfection procedures

3.7.1. Transfection with Plasmid DNA

mESCs were detached with trypsin for 3 min at 37 °C, centrifuged and counted in respective standard growth medium. They were seeded in a density of 5.4 x 10^5 per cm^2 in a TTP cell culture plate. 6 h after seeding, the cells were transfected using jetPEI® DNA transfection reagent (Polyplus transfection®, USA) according to the manufacturer's instructions. For the

generation of hNkx2.5 overexpressing clones, 20 µg nucleic acid was used per 5 x 10^6 cells. The first medium change was performed 24 h after transfection with the addition of respective antibiotics (Table 1). Subsequently, 24 clones were picked and cultured under antibiotic selection.

3.7.2. Transfection with modified mRNA

3.7.2.1. Single cell transfection with modified EGFP mRNA

Fibroblasts (n=3) and hMSCs (n=3) were detached with trypsin for 5 min at 37 °C, centrifuged and counted in respective standard growth medium. They were seeded in a density of 1.5 x 10^4 per cm^2 in a 24 well plate. 24 h after seeding, the cells were transfected using Lipofectamine2000 transfection reagent (Life Technologies GmbH, USA) according to the manufacturer's instructions. Therefore, respective standard growth medium was replaced with 100 µL prewarmed Opti-MEM® I Reduced Serum Medium (Life Technologies, USA). The cells were transfected with 500 ng modified EGFP mRNA. The nucleic acid-Lipofectamine2000-mixture was added to the cells and incubated for 4 h at 37 °C, 5 % CO_2, 20 % O_2. The medium was replaced with respective standard growth medium after the incubation time. Cells were cultured at 37 °C, 5 % CO_2 and 20 % O_2 and medium was chanced every second day.

3.7.2.2. Serial transfection with MyoD modified mRNA

C3H10T1/2 mouse fibroblasts were detached with trypsin for 5 min at 37 °C, centrifuged and counted in standard growth medium. Fibroblasts were seeded at a density of 5 x 10^3 per cm^2 in a 24 well plate (Figure 22). 4 h prior to the first transfection, medium was changed to transfection medium, DMEM supplemented with 200 ng/mL B18R (eBioscience, USA). Cells were transfected three times with 250 ng modified MyoD mRNA at intervals of 24 h (optimal modification carried out: 3.7.2.1). 24 h after the third transfection, medium was changed to transdifferentiation medium, DMEM containing 10% horse serum (Life Technologies, USA), 1 % non-essential amino acids and 1 % penicillin/streptomycin, for additional 72 h.

3.7.2.3. Serial transfection with Nkx2.5 modified mRNA

mESCs were detached with trypsin for 3 min at 37 °C, centrifuged and counted in cardiogenic differentiation medium. They were seeded in a density of 1.5 x 10^4 per cm^2 in a TTP cell culture plate. 4 h prior to the first transfection, medium was changed to transfection medium, cardiogenic differentiation medium supplemented with 200 ng/mL B18R (eBioscience, USA). Cells were

transfected three times with 500 ng modified hNkx.25 mRNA at intervals of 24 h (optimal modification carried out: 3.7.2.1). The standard differentiation procedure (3.2.2) starts 24 h after the third transfection. Therefore, cells were detached with trypsin for 3 min at 37 °C, centrifuged and counted in cardiogenic differentiation medium. Hereinafter, standard differentiation protocol was used (3.2.2).

3.7.3. miRNA/PEI/MNP transfection system

3.7.3.1. Formation of polyplexes and transfection

The establishment of miRNA/PEI/MNP complexes was previously reported and was used as described for the transfection of $CD133^+$ SCs [327, 328].

The miRNA/PEI/MNP complexes consists of the following compounds: I) Cy3™ dye-labeled Pre-miR Negative Control #1 (Ambion, USA) a double-stranded RNA molecule which mimics endogenous mature miRNAs, II) biotionylated branched polyethylenimine (molecular weight of 25 kDA, Sigma-Aldrich GmbH, Germany) (PEI) and III) Streptavidin MagneSphere® Paramagnetic Particles (Promega Corporation, USA) (MNPs). First, miRNA and PEI were diluted in equal volumes of 5 % glucose (MP Biomedicals, Germany) and mixed in accordance to the desired PEI nitrogen/ miRNA phosphate (N/P) ratio. MNPs were incubated in an ultrasonic bath before use. miRNA/PEI complexes were incubated separate before bringing together with prepared MNPs in different concentrations.

Freshly isolated $CD133^+$ HCs were seeded at a density of 2.5 x 10^3 per cm^2 in a 24 well plate in standard growth medium (3.2.5). The transfection with respective complexes was performed immediately after seeding and cells were cultured at 37 °C, 5 % CO_2 and 20 % O_2 for 18 h until further investigation (3.4.1.2, 3.4.2.5, 3.4.3, 3.5.4).

3.7.3.2. Magnetic particle spectroscopy

The quantification of magnetic iron loading of $CD133^+$ SCs was performed using magnetic particle spectroscopy (MPS; Bruker Biospin, Germany) in cooperation with the Physikalisch-Technische Bundesanstalt, Berlin. For this, 5 x 10^5 $CD133^+$ SCs were transfected with 20 pmol miRNA, N/P 7.5 and 3 µg/ml MNPs and hereinafter fixed with 1 % FA. The analysis was performed under magnetic field B_{drive} = 25 mT and a frequency f_0 = 25 kHz. The determination is based on the non-linear dynamic of magnetic moments of the sample at higher (odd) harmonics of f_0. The iron quantification of the samples is carried out by the third harmonic A_3 of the MPS-

spectrum which is normalized to the corresponding $A_{3,ref}$ of the MNP reference sample of known iron amount (3.2 µg for MNPs only reference and 2.5 µg for the CD133 MicroBeads reference) [330]. The ratio of the fifth to third harmonic A_5/A_3 is used as a characteristic finger print to identify the magnetic nanoparticle type in the sample.

3.8. Statistical analysis

3.8.1. Statistical analysis of mESC experiments

Statistical analysis of mESC experiments was performed using OriginPRO 2016G (OriginLab Corporation, USA). All data are reported as mean ± SEM. One Way Analysis of Variance (ANOVA) was performed for multiple comparisons with Bonferroni post hoc test. $P < 0.05$ was considered statistically significant.

3.8.2. Statistical analysis of mmRNA experiments

Statistical analysis of mmRNA experiments was performed using SigmaPlot software version 11.0 (Systat Software Inc., USA). All data are reported as mean ± SEM. Differences in EGFP expression, dead cells and mean fluorescence were analysed for every time point. Analyses of differences between modified mRNAs were performed after the Normality Test (Shapiro-Wilk) and the Equal Variance Test. One Way Analysis of Variance (ANOVA) was employed for normally distributed data with equal variance. In case of $p < 0.05$, significantly differing groups were determined using Bonferroni as a post hoc test for multiple comparisons. In case of nonnormally distributed data or unequal variance, One Way Analysis of Variance on Ranks (Kruskal-Wallis) test was employed using Dunn's test for post hoc multiple comparisons. $P < 0.05$ was considered statistically significant.

3.8.3. Statistical analysis of $CD133^+$ experiments

Statistical analysis of $CD133^+$ HSCs experiments was performed using the SigmaPlot software version 11.0. All data are reported as mean ± SEM. The evaluation was done using Student's *t*-test. $P < 0.05$ was considered statistically significant. The respective experiments were performed with different BM donors (n).

4. Results

4.1. Results Part I – cardiac differentiation of mESC

mESCs were cultured and differentiated according to a standardized protocol. This was adapted for the purpose to generate ventricular subtype cardiomyocytes. A general overview is displayed in Figure 4, which shows the different morphology stages during this protocol.

4.1.1. mESC culture

4.1.1.1. Generation of hNkx2.5 clones

This section contains a detailed characterization of the murine embryonic stem cells (W4) [324] which were subsequently used for cardiac differentiation. The present mESCs had previously been transfected with a pGK-hygro αMHC-puromycin cassette [155]. The clone (W4 αMHC #15; control), from which most spontaneously beating single cells could be obtained was selected for further studies.

Next, to achieve a specific ventricular-subtype differentiation, an exogenous introduction of hNkx2.5 through application of pEF-DEST51-hNkx2.5 plasmid and subsequent separation and cultivation of the resulting clones (W4 αMHC #15 hNkx2.5 #A – T) was performed (plasmid map pEF-DEST51: supplement Figure 35). The relative expression analysis of hNkx2.5 obtained by qPCR (Figure 5A) displayed significant differences in the expression of hNkx2.5 on the mRNA level among all clones under investigation. W4 αMHC #15 hNkx2.5 #F (0.95 ± 0.03) and #L (0.94 ± 0.05) presented significantly higher expression in relation to several other clones. The clone with the lowest expression is W4 αMHC #15 hNkx2.5 #N (0.02 ± 0.007).

To achieve an overview of different Nkx2.5 mRNA expression levels, several clones were picked for further analysis, this includes W4 αMHC #15 as well as W4 αMHC #15 hNkx2.5 #D, #F and #L, which will be presented in the following.

Immunohistochemical investigations were performed with selected clones (W4 αMHC #15 hNkx2.5 #D, #F and #L) and control cells (W4 αMHC #15) (Figure 5B). Stainings revealed embryonic stem cell clusters consisting of individual cells marked by actin. Exogenous expression of hNkx2.5 was strongly present in the nucleus of W4 αMHC #15 hNkx2.5#F and #L and mode in W4 αMHC #15 hNkx2.5 #D. The control cells exhibited no protein expression of Nkx2.5.

In order to maintain integrity of Mhy6-puro/PGK-hygro as well as pEF-DEST51 selection pressure was applied using hygromycin and blasticidin, according to Table 1.

W4
W4 αMHC #15
W4 αMHC #15 hNkx2.5 #D
W4 αMHC #15 hNkx2.5 #F
W4 αMHC #15 hNkx2.5 #L
cultivation under appropriate AB pressure (Table 1)
co-cultivation with SNL-feeder
EB formation d3

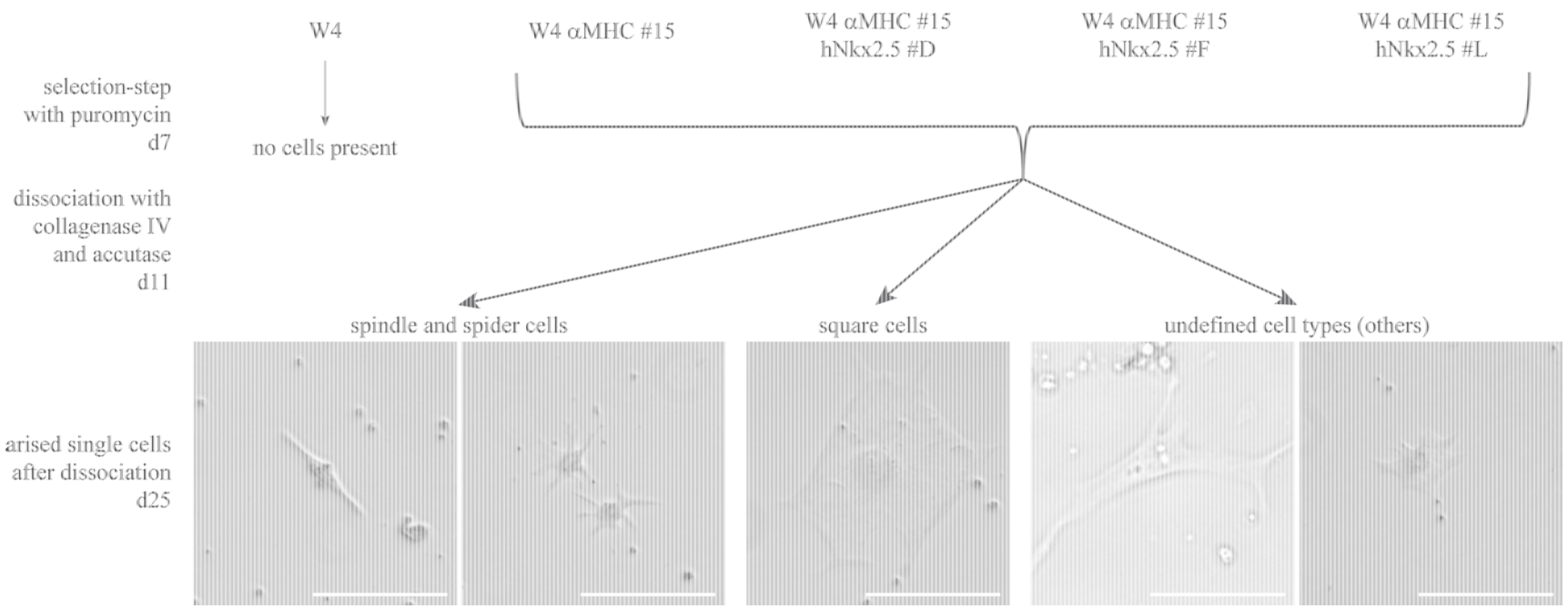

Figure 4: General view of Nkx2.5 forced cardiac differentiation of W4 mESCs

Representative visualization of cardiogenic differentiation of W4 mESCs clones. W4: original unaltered control culture; W4 αMHC #15: manipulated with pGK-hygro αMHC-puromycin cassette; W4 αMHC #15 hNkx2.5 #D-L: manipulated with pGK-hygro αMHC-puromycin cassette and the additional exogenous introduction of hNkx2.5 through application of pEF-DEST51-hNkx2.5 plasmid. Starting with mES cultivation in LIF supplemented medium with appropriate antibiotic pressure (#15: hygromycin; #D-L: hygromycin and blasticidin). Afterwards, cells were co-cultured with mitotically inactivated murine STO cell line-derived SNL 76/7 [139]. Specific ventricular subtype differentiation was introduced through EB formation and subsequent culturing in differentiation medium. Antibiotic selection using puromycin led to generation of single cells, whereby control W4 exhibit no cells, which indicates a successful selection procedure. All other clones give rise to single cells with the following morphogenic classification: spindle and spider like cells, large round and large square cells or an undefined cell population including large longitudinal and small round cells. Scale bar: 100 µm

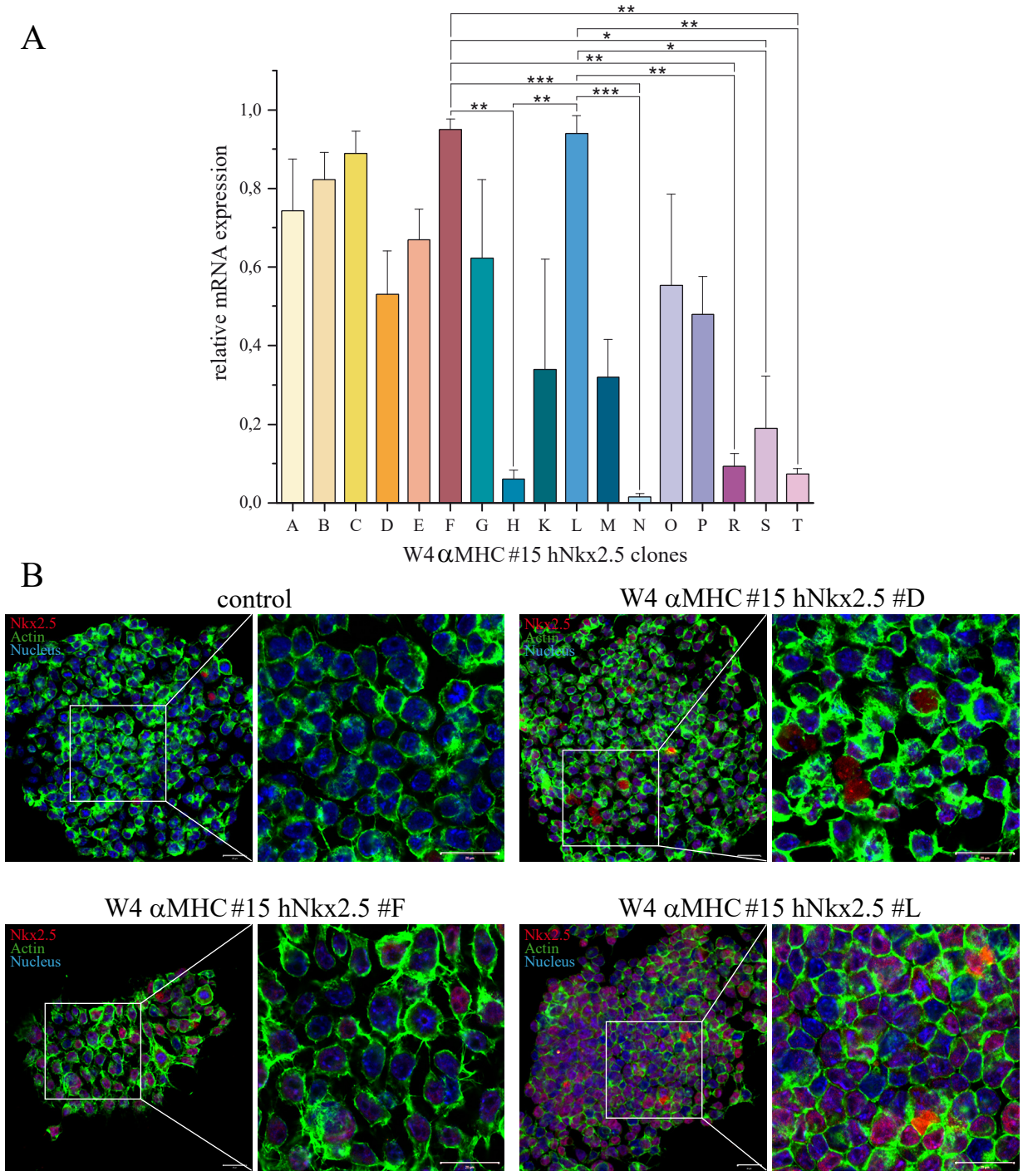

Figure 5: Exogenous hNkx2.5 expression in W4 αMHC clones

Analysis of hNkx2.5 expression on mRNA (A) and protein level (B) at day 0 of differentiation. (A) Relative expression of hNkx2.5 among all obtained W4 αMHC clones performed by qPCR. Normalized to mHprt and mPolr2a. Values are presented as mean ± SEM; n=3; statistic was performed as multiple comparison of mean (ANOVA), *p ≤ 0.05, **p ≤ 0.01, ***p ≤ 0.001. Not all statistically significant values are displayed, focus towards subsequent used clones (W4 αMHC#15 hNkx2.5 #D, F, L). (B) Protein expression of control (W4 αMHC#15) and W4 αMHC#15 hNkx2.5 #D, F, L clones; hNkx2.5 (red), actin (green) and nucleus (blue); scale bar: 20 µm. (parts of

the figure appear in the Bachelor thesis of Vivien Krebs who was supervised by F. Hausburg and submitted to the Journal of Cellular Physiology and Biochemistry.)

4.1.1.2. Maintenance of pluripotency

Undifferentiated mESCs were continuously cultured with leukemia inhibitory factor (LIF) [133, 134] to maintain a pluripotent state. The cell cluster formations remain similar between the cell clones. They appeared in flat clusters with sharp edges in varying degrees and size (Figure 4). Furthermore, partial differentiation has already started as indicated by thin extensions on the edges.

Prior to cardiogenic differentiation, mESCs were co-cultured with mitotically inactivated murine embryonic fibroblasts derived from the line SNL 76/7 [138] for seven days. Thereafter, clusters appeared in a more 3-dimensional form with obvious bright edges. Moreover, no false differentiation was observed (Figure 4).

Cells were additionally cultured under selection pressure after they had been separated from the feeder cell culture for two days. Afterwards, on day 0 of differentiation, all clone clusters displayed a normal morphology with a high nucleus / cytoplasm ratio.

Analysis on mRNA level using qPCR (Figure 6A) showed no significant difference of pluripotency marker expression (mOct4, mNanog and mSsea1) between Nkx2.5 clones and control (expression analysis relativized to W4 αMHC#15 (set: 1)). All clones revealed a tendentially higher expression of mOct4 (between 1.18 ± 0.12 and 1.27 ± 0.13). Whereas W4 αMHC #15 hNkx2.5 #L was the only clone with limited expression of the pluripotency markers mNanog (0.76 ± 0.30) and mSsea1 (0.85 ± 0.22) as well as both early cardiac markers investigated, mIsl1 (0.72 ± 0.20) and mMesP1 (0.75 ± 0.27).

However, no significant differences are discernible in early cardiac marker expression. Whereby all Nkx2.5 clones revealed a slight decrease of mMesp1 (between 0.75 ± 0.27 and 0.99 ± 0.13) compared to control. Present circumstances are owned by a large standard deviation.

In contrast, certain differences among the clones become obvious on the protein level (Figure 6B). Immunohistochemical investigations were performed with the pluripotency marker Oct4. The protein expression of Oct4 was present in all clones, with only a minor decrease in the control cluster.

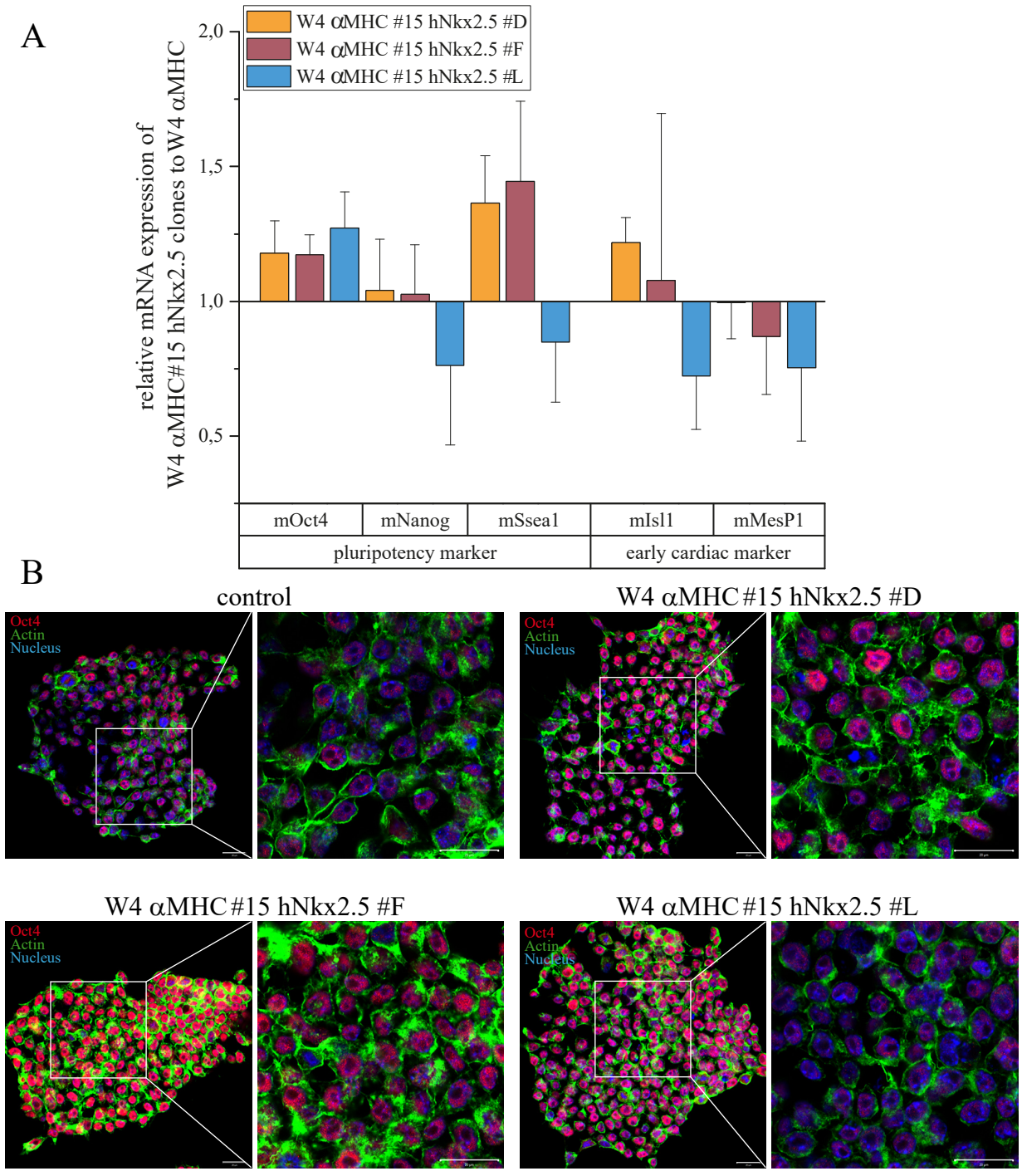

Figure 6: Pluripotency and early cardiac marker expression

Analysis of pluripotency and early cardiac marker expression on mRNA (A) and protein level (B) at day 0 of differentiation. (A) Relative expression among all obtained W4 αMHC clones performed by qPCR. Values normalized to mHprt and mPolr2a and relativized to W4 αMHC#15 (set: 1). Values are presented as mean ± SEM; n=3; statistic was performed as multiple comparison of mean (ANOVA), *p ≤ 0.05, **p ≤ 0.01, ***p ≤ 0.001. (B)

Protein expression of control (W4 αMHC#15) and W4 αMHC#15 hNkx2.5 #D, F, L clones; Oct4 (red), actin (green) and nucleus (blue); scale bar: 20 µm. (parts of the figure appear in the Bachelor thesis of Vivien Krebs who was supervised by F. Hausburg and submitted to the Journal of Cellular Physiology and Biochemistry.)

4.1.2. Cardiac differentiation of mESCs

As described above, three hNkx2.5 clones were selected for further specific ventricular subtype differentiation (W4 αMHC #15 hNkx2.5 #D, F, L). W4 αMHC #15 and unaltered W4 cells were used as references.

4.1.2.1. Protocol optimization

To achieve the optimal results, it is essential to optimize the entire differentiation protocol. Therefore, mESCs were brought to cardiac differentiation through EB formation and subsequent suspension culture.

At first, from day 7 on, cells were split in two different oxygen concentrations (1 % O_2 and 20 % O_2) and were thereafter examined with regard to their spontaneous beating activity and quantity (Figure 7A). No significant difference could be found using multiple comparison of means (ANOVA) among all clones at any specific time. All clones started to beat on day 8 of differentiation (1 % O_2: W4: 0.25 ± 0.21; W4 αMHC #15: 0.60 ± 0.2; W4 αMHC #15 hNkx2.5 #D: 0.1 ± 0.05; W4 αMHC #15 hNkx2.5 #F: 0.5 ± 0.17; W4 αMHC #15 hNkx2.5 #L: 0.56 ± 0.21 and 20 % O_2: W4: 0.3 ± 0.21; W4 αMHC #15: 0.59 ± 0.21; W4 αMHC #15 hNkx2.5 #D: 0.38 ± 0.12; W4 αMHC #15 hNkx2.5 #F: 0.89 ± 0.21; W4 αMHC #15 hNkx2.5 #L: 0.61 ± 0.20) and the number of beating areas per EB increased over time until day 18 (Figure 7B). From this point, beating areas synchronized themselves. W4 αMHC #15 hNkx2.5 #D showed a significant increase of beating areas at day 16 (2.2 ± 0.29) and W4 αMHC #15 hNkx2.5 #F at day 17 (3.07 ± 0.5) at 20 % O_2. Whereas W4 αMHC #15 hNkx2.5 #L showed no significant difference at 20 % O_2 conditions, at 1 % O_2 a significant difference from day 12 on (2.55 ± 0.51) was recorded. The largest significant difference was observed with W4 αMHC #15 hNkx2.5 #F on day 20 (4.09 ± 1.26).

Second, the optimal time for antibiotic selection was determined using similar separation into both oxygen concentration groups. Clones were treated at five different times (day 7, 9, 11, 13 and 15) with equal concentration of puromycin. EBs were dissociated four days after puromycin treatment and the number of obtained single cells was determined 16 days after treatment (Figure 8A). Unmanipulated W4 cells were used as control to comprehend the effectiveness of the

antibiotic reagent, which has become apparent if no single cells were present after the dissociation step (Figure 4). This could be confirmed in every attempt. In addition, a morphologic categorization was performed (detailed single cell number: Figure 33) inspired by Jung *et al.* [153]. They were subsequently classified in: spindle and spider cells [153], square cells and an undefined cell population (includes dying round shaped cells) (see 4.1.2.2). Under both conditions (1 % O_2 and 20 % O_2), W4 αMHC #15 has yielded exceedingly few cells, but due to a large standard deviation, without a significant difference at nearly all times (using multiple comparison of means, Figure 8B).

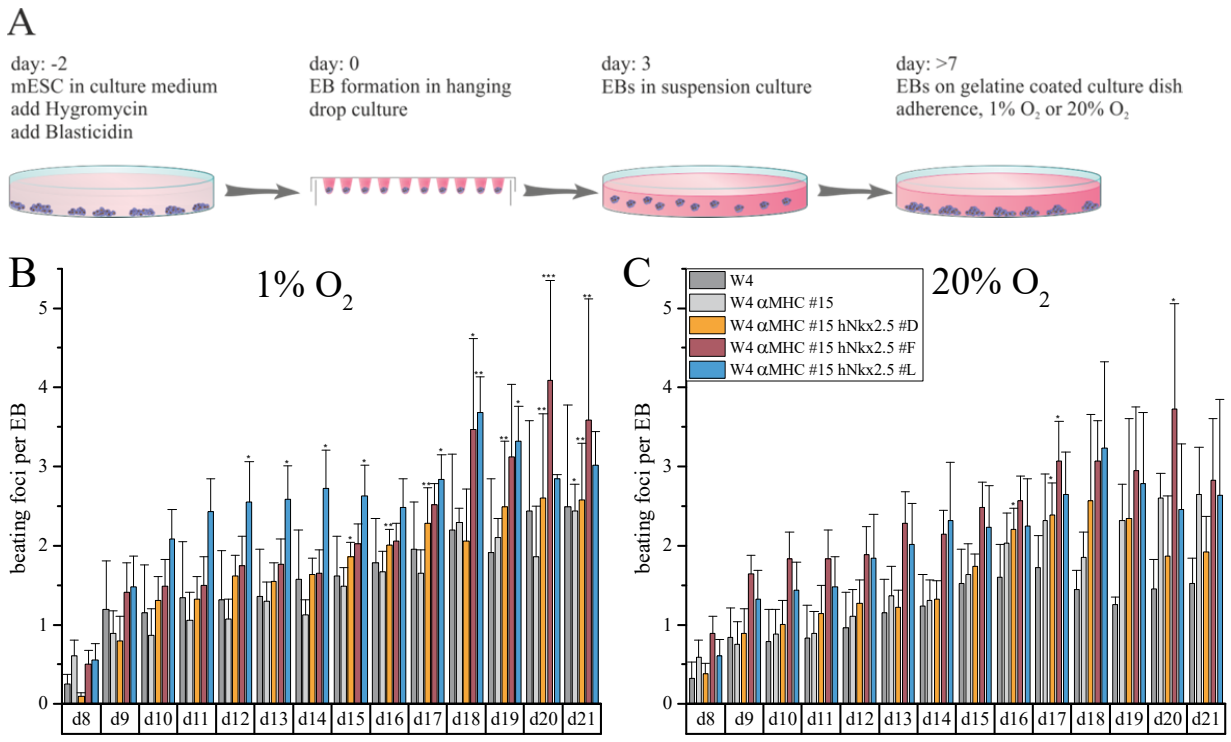

Figure 7: Quantitative determination of spontaneously beating areas per EB

Quantitative analysis of beating areas per EB during cardiogenic differentiation of W4 αMHC clones. (A) Experimental setup and (B) enumerated beating areas per EB under 1 % O2 and 20 % O2 oxygen conditions. Values are presented as mean ± SEM; n=7 (d8-d17), n=3 (d18-d21); statistic was performed as multiple comparison of mean (ANOVA) within one clone against day 8 of differentiation (start of beating), *p ≤ 0.05, **p ≤ 0.01, ***p ≤ 0.001. (parts of the figure appear in the Bachelor thesis of Christin Völkner who was supervised by F. Hausburg and submitted to the Journal of Cellular Physiology and Biochemistry.)

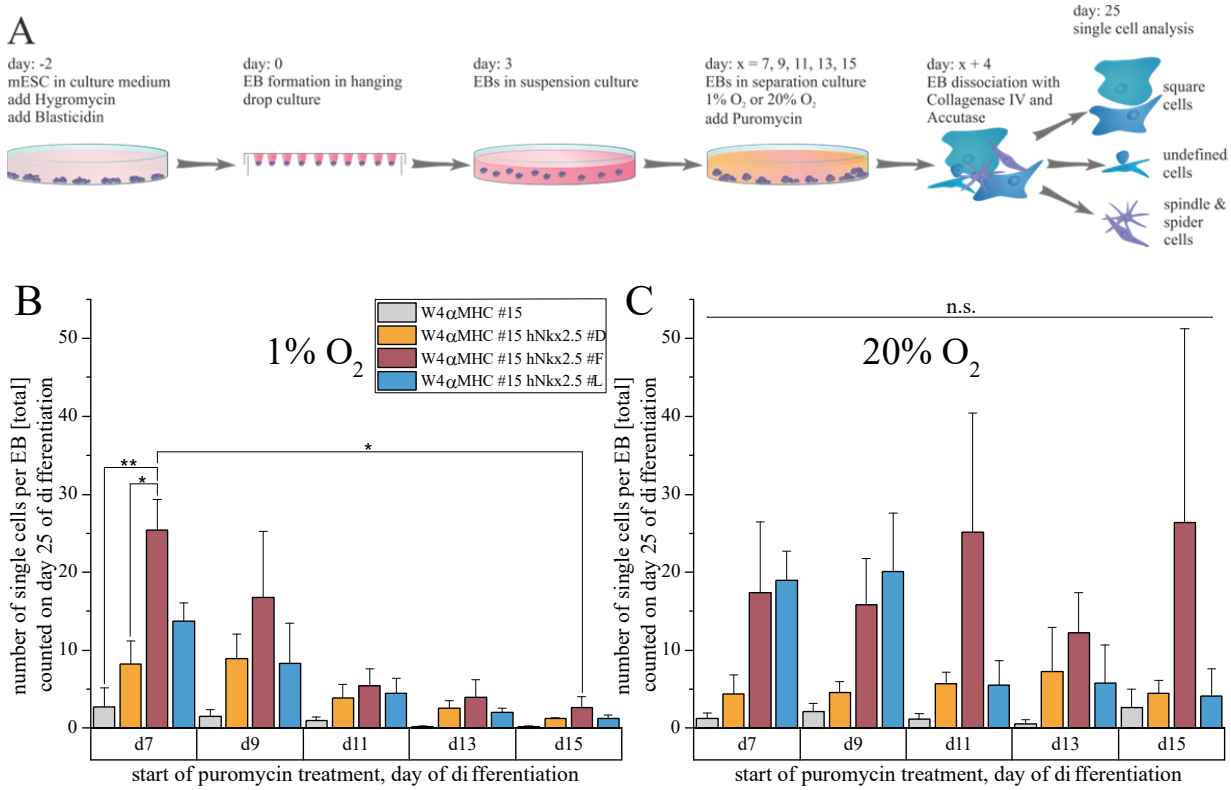

Figure 8: Quantitative determination of the optimal time point for antibiotic selection

Quantitative analysis of antibiotic selection during cardiogenic differentiation of W4 αMHC clones. (A) Experimental setup and (B) enumerated single cells per EB under 1 % O_2 and 20 % O_2 oxygen conditions. Values are presented as mean ± SEM; n=3; statistic was performed as multiple comparison of mean (ANOVA), *p ≤ 0.05, **p ≤ 0.01, ***p ≤ 0.001. (parts of the figure appear in the Bachelor thesis of Christin Völkner who was supervised by F. Hausburg and submitted to the Journal of Cellular Physiology and Biochemistry.)

The efficiency ranged from 0.01 % (0.02 cells/EB ± 0.07) to 1.35 % (2.7 cells/EB ± 2.45). The total number of single cells was significantly different under 1 % O_2 conditions between W4 αMHC #15 hNkx2.5 #F (25.4 ± 3.96) and W4 αMHC #15 (2.72 ± 2.45) as well as W4 αMHC #15 hNkx2.5 #D (8.22 ± 3.0). Moreover, a significant reduction was observed under 1 % O_2 conditions within W4 αMHC #15 hNkx2.5 #F from day 7 to day 15 (2.6 ± 1.49). Most cells could be generated under 20 % O_2 conditions and W4 αMHC #15 hNkx2.5 #F at day 15 (26.38 ± 24.81), which is an efficiency of 13.19 %. This indicates a 9.77-fold higher yield compared to the best result obtained with W4 αMHC #15 (at day 7 under 1 % O_2 conditions).

As neither W4 αMHC #15 hNkx2.5 #F nor W4 αMHC #15 hNkx2.5 #L displayed an adjusted cell number with low standard deviation, and no significant difference in total numbers of all four clones, 20 % O_2 and day 7 was selected for further experiments.

4.1.2.2. Cardiomyocyte characteristics

Single cells received using the aforementioned protocol (4.1.2.1) have been analyzed with regard to their cardiomyocyte characteristics, signified morphology, protein expression, spontaneous beating frequency and their response to pharmacological substance administration, respectively.

4.1.2.2.1. CM-like cells present specific myogenic characteristics

It should be noted, that all clones under investigation give rise to equal cell shapes. A morphologic categorization inspired by Jung *et al.* [153] led to the subsequent classification: spindle and spider cells [153], large round and large square cells and an undefined cell population (includes large longitudinal and small round cells). The only difference consists in the total amount of yielded cells (Figure 8). Spindle cells are characterized by a thin spindle-shape with two opposed extensions and an approximately cell size of 18 x 73 µm (n=36). Whereas spider cells possess five or more extensions, in all directions (54 x 68 µm, n=20). Both cell types showed a raised cell body. The second cell population is defined by a flat round or squared shape, with or without extensions. These cells exhibit the largest population with a cell size approximately 86 x 118 µm (n=67). Cells which do not match the aforementioned categories were named as undefined cells, this also includes rounded in cell death situated but still beating cells (20 x 27 µm, n=26) as well as large longitudinal cells with a cell size of approximately 36 x 74 µm (n=107). However, the cell size difference of the clones is only modest, whereby W4 αMHC #15 represents the smallest population with approximately 34 x 62 µm (n=28) and W4 αMHC #15 hNkx2.5 #F the largest with approximately 59 x 102 µm (n=81). W4 αMHC #15 hNkx2.5 #D: 45 x 79 µm (n=68) and W4 αMHC #15 hNkx2.5 #L: 43 x 76 µm (n=79).

To investigate a potential cardiogenic phenotype, structural proteins of myofibril and sarcomere as well as gap junctions were immune-labeled on day 25 of differentiation. Therefore, equal stainings were performed for each clone within one differentiation approach to ensure same conditions.

The labeling of mMyh6 (Figure 9) revealed a weak and unstructured expression in W4 αMHC #15 hNkx2.5 #D (Figure 9B) and only partial in W4 αMHC #15 (Figure 9A) as well as W4 αMHC #15 hNkx2.5 #F (Figure 9C). The thin cells of W4 αMHC #15 (Figure 9A) exhibited a striped structure along the cell boundary of the extensions, whereas mMyh6 in W4 αMHC #15

hNkx2.5 #F (Figure 9C) were predominantly expressed around the nucleus. In contrast, the ghost cell of W4 αMHC #15 hNkx2.5 #L (Figure 9D) revealed unambiguous A-bands, consisting of the thick filament spread over the whole cell.

All hNkx2.5 clones exhibit mMhy7 protein expressions (Figure 10B-D), the second myosin heavy chain isoform existing in vertebrates. On the other hand, no expression of mMyh7 was achieved in single cells of the control clone (Figure 10A). Labeled actin was marked by intersecting structures as well as thin strings toward the periphery. W4 αMHC #15 hNkx2.5 #D revealed polynuclear cells with striated actin and thin strings toward the periphery, which are present in the whole cell body (Figure 10B). Only one cell, lying on top of the others exhibits mMyh7. The striped expression of mMyh7 is co-localized with actin. The two co-localized components of the muscle sarcomere became apparent in a large square cell of W4 αMHC #15 hNkx2.5 #F (Figure 10C) and W4 αMHC #15 hNkx2.5 #L (Figure 10D), whereby mMyh7 marked the M-band consisting of the thick filament and actin marked the I-band consisting of the thin filament. Actin filaments were tethered to the Z-lines through the microfilament protein α-actinin, which was expressed in all clones (Figure 11). However, neither hNkx2.5 clones nor the control displayed a complete mature myosin arranged α-actinin structure. Most likely, spider-like cells of W4 αMHC #15 hNkx2.5 #F (Figure 11C) revealed a well-organized structure with a striped expression.

The troponin complex, consisting of three subunits (T, C, I), is co-localized to the actin filament. Cardiac troponin T (cTnT) binds the complex to tropomyosin and therefore provides the connection between actin and myosin. As well as α-actinin, cTnT is present in two different forms, either streaked or thin strings toward the periphery in all clones (Figure 12). For this, it makes no difference whether these are spindle and spider cells, ghost cells or another morphologic cell type. The expression of Connexin 43 (Cx43) and hyperpolarization-activated cyclic nucleotide-gated cation channels (Hcn4) were evaluated with regard to the accordance of subtype specifications.

W4 αMHC #15 hNkx2.5 #L was the only clone expressing the gap junction protein Connexin 43 on its surface of a single ghost cell (Figure 9D) and beyond this between adjacent cells (Figure 12D). This localization of strong Cx43 expression was also present in cell complexes of W4 αMHC #15 hNkx2.5 #D (Figure 9B and Figure 12B) as single dots in apparent gaps. This

confirmed the special function of gap junctions as functional connection between neighboring cells.

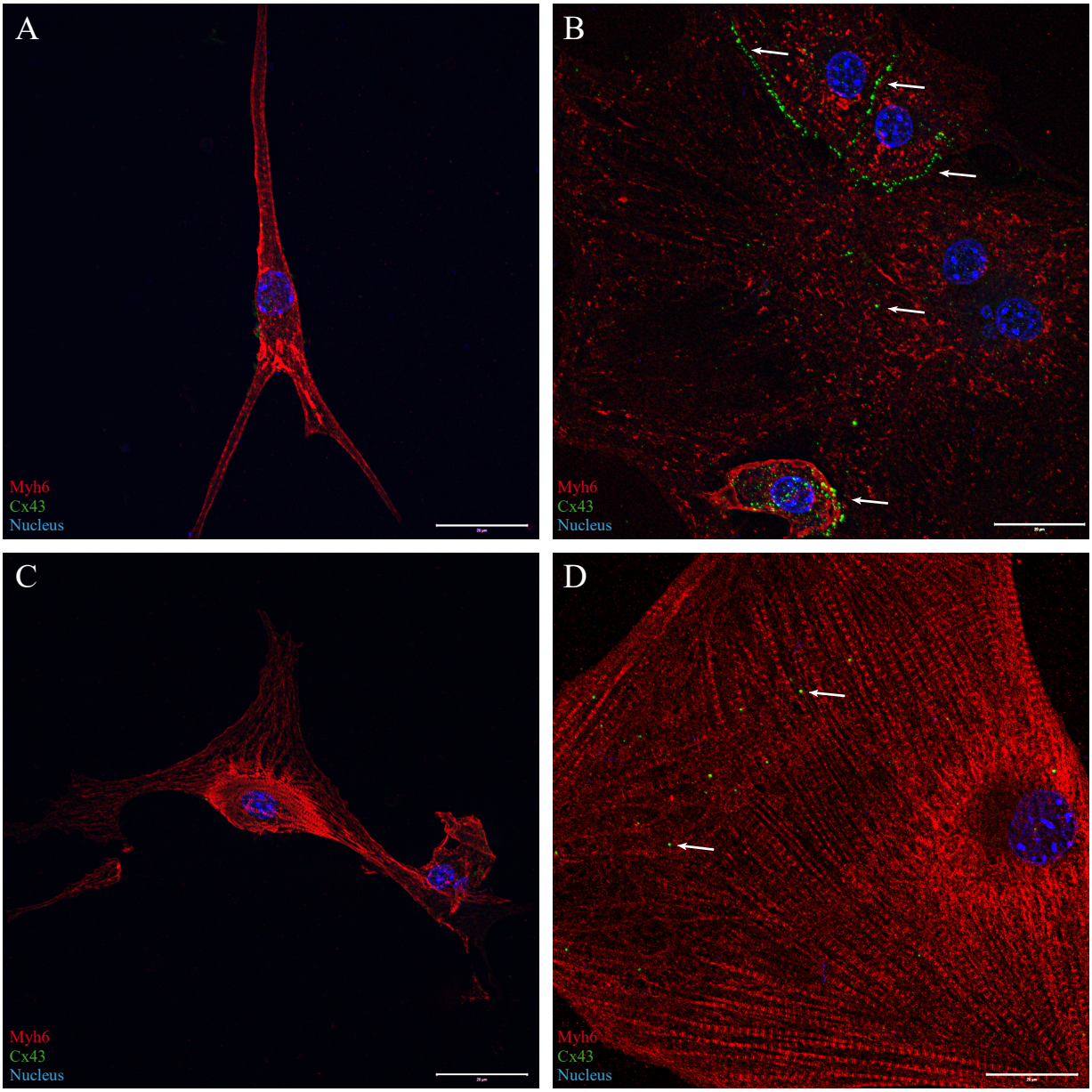

Figure 9: Expression of Myh6 and Connexin 43 in CM-like single cells

Immunostaining of obtained CM-like single cells on day 25 of differentiation. (A) W4 αMHC #15, (B) W4 αMHC #15 hNkx2.5 #D, (C) W4 αMHC #15 hNkx2.5 #F, (D) W4 αMHC #15 hNkx2.5 #L, Myh6 (red), Cx43 (green) and nucleus (blue). The arrows indicating the Cx43 expression, which is nonexistent in (A) and (C), scattered spotted in (D) and strongly expressed between cells in (B); scale bar: 20 µm

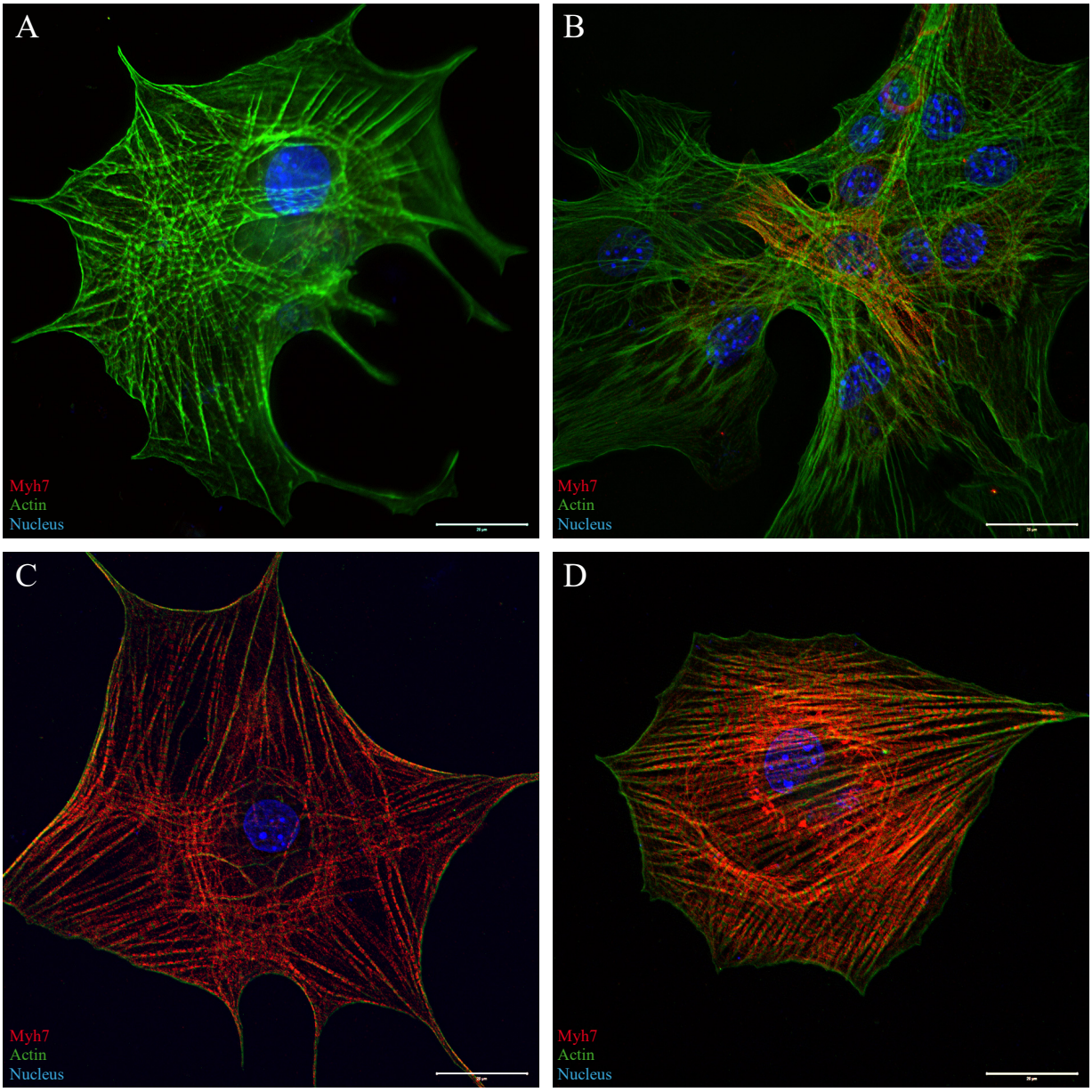

Figure 10: Expression of Myh7 and actin in CM-like single cells

Immunostaining of obtained CM-like single cells on day 25 of differentiation. (A) W4 αMHC #15, (B) W4 αMHC #15 hNkx2.5 #D, (C) W4 αMHC #15 hNkx2.5 #F, (D) W4 αMHC #15 hNkx2.5 #L, Myh7 (red), Actin (green) and nucleus (blue); scale bar: 20 µm

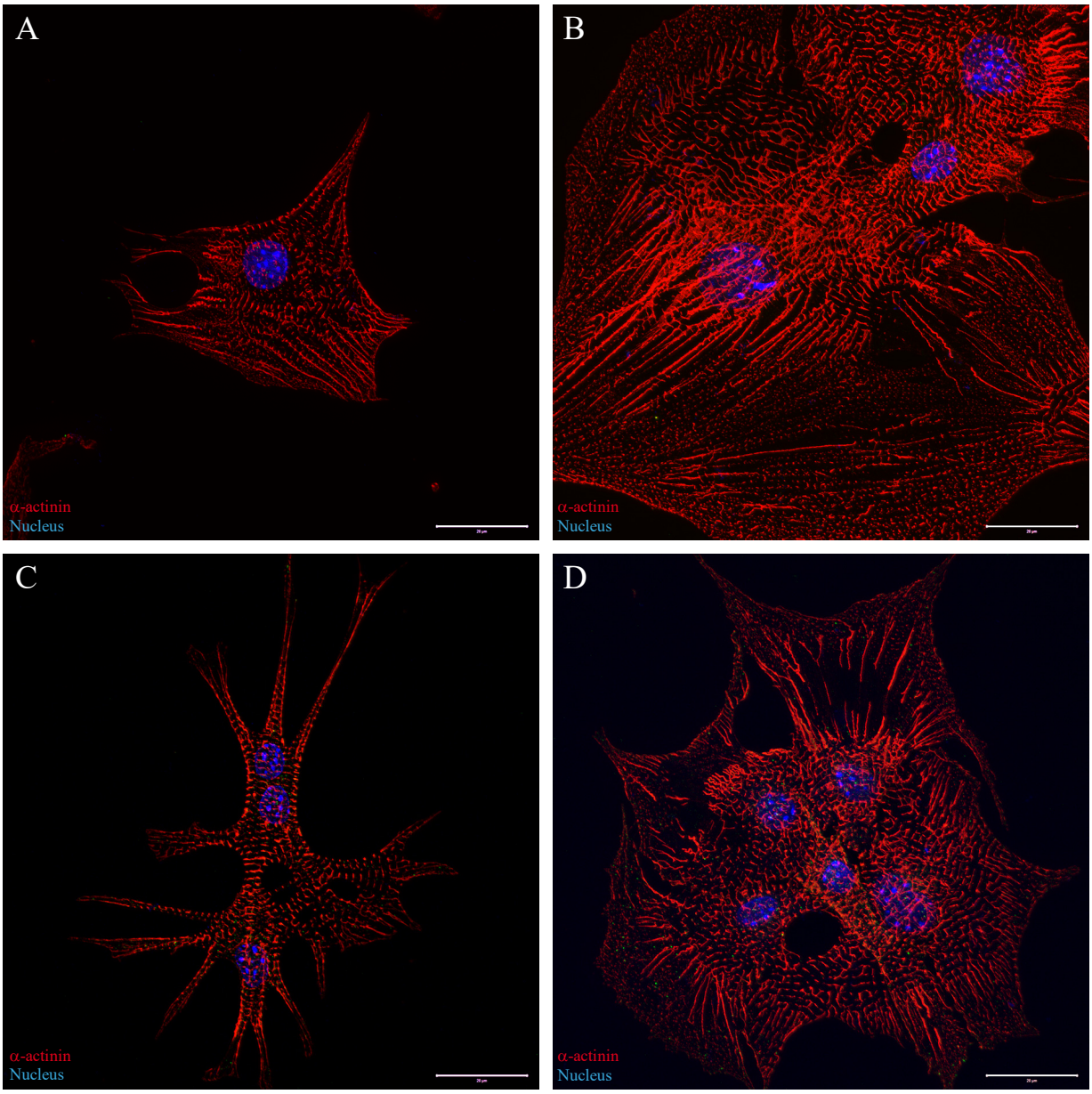

Figure 11: Expression of α-actinin in CM-like single cells

Immunostaining of obtained CM-like single cells on day 25 of differentiation. (A) W4 αMHC #15, (B) W4 αMHC #15 hNkx2.5 #D, (C) W4 αMHC #15 hNkx2.5 #F, (D) W4 αMHC #15 hNkx2.5 #L, α-actinin (red) and nucleus (blue); scale bar: 20 µm

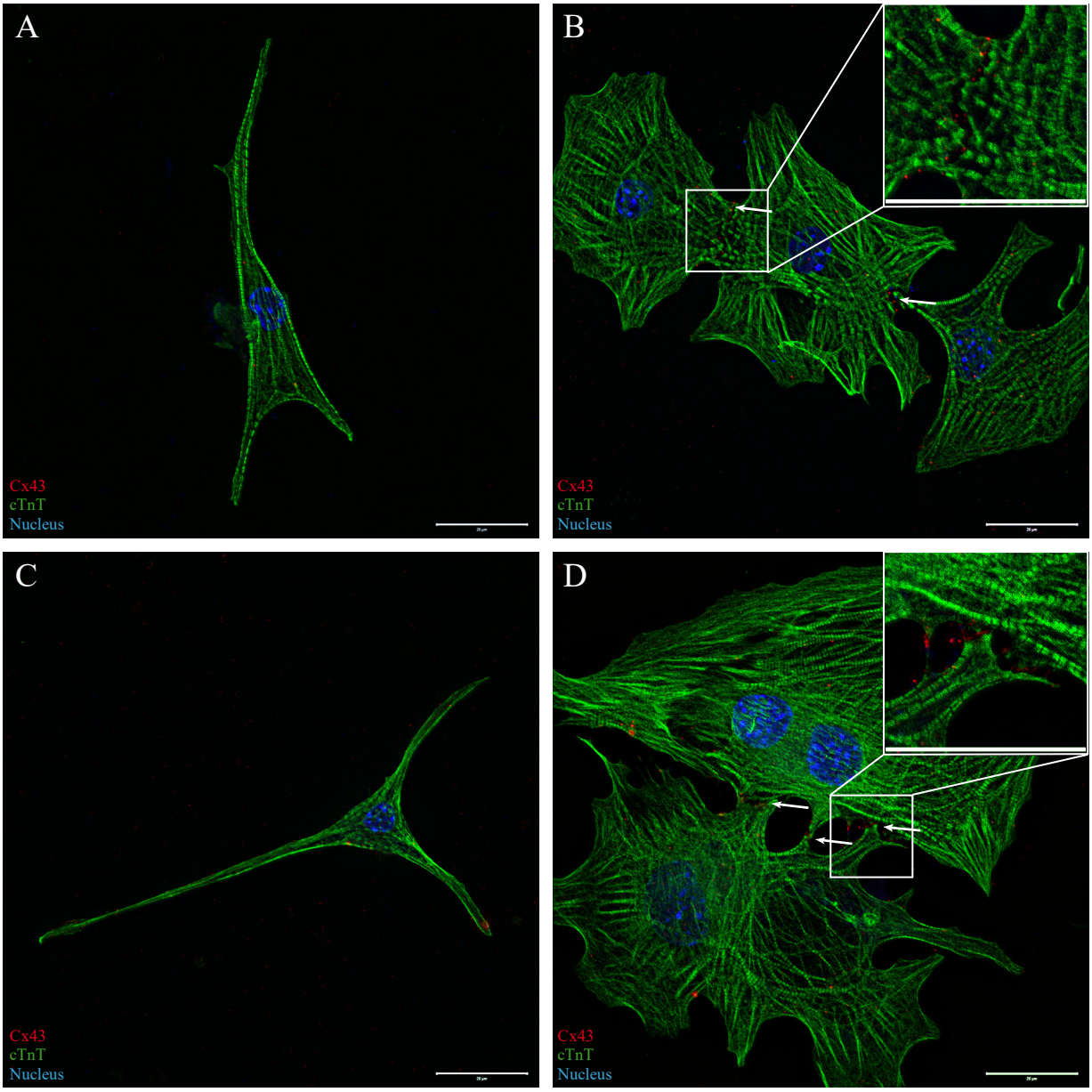

Figure 12: Expression of cardiac Troponin T and Connexin 43 in CM-like single cells

Immunostaining of obtained CM-like single cells on day 25 of differentiation. (A) W4 αMHC #15, (B) W4 αMHC #15 hNkx2.5 #D, (C) W4 αMHC #15 hNkx2.5 #F, (D) W4 αMHC #15 hNkx2.5 #L, Cx43 (red), cTnT (green) and nucleus (blue). The arrows indicating the Cx43 expression, which is nonexistent in (A) and (C), and strongly expressed between cells in (B) and (D); scale bar: 20 µm (parts of the figure appear in the Bachelor thesis of Vivien Krebs who was supervised by F. Hausburg and submitted to the Journal of Cellular Physiology and Biochemistry.)

4.1.2.2.2. CM-like cells possess spontaneous beating activity

Another characteristic of cardiomyocytes, the ability of self-contained contractions, was evaluated on day 25 of differentiation in comparison to murine neonatal cardiomyocytes (mnCM).

The cells were cultured under the previously described protocol and the spontaneous beating activity was determined using a 37 °C incubator to avoid temperature influences. It should be considered that not all single cells exhibited autonomous beating activity and a large amount of large square cells lose their capacity over time. Dying round beating cells were not used for the calculation comparing all clones (Figure 13A).

To exactly determine the frequency after recording, regions of interest (ROI) were fixed at one position on the cell using the ZEN2011 software (Figure 13C). Change in light intensity at the respective ROI correlates with the contraction of the cell and reflect the spontaneous beating frequency (Figure 13D).

In Figure 13A the beating frequencies per min of the control cells, hNkx2.5 clones without dying small round cells and mnCMs are depicted. However, only mnCMs were considered as representing a closed group, shown by a compact and evenly distributed bf within all analyzed cells (30 – 174 beats min^{-1}). On the other hand, W4 αMHC #15 (36 – 378 beats min^{-1}), W4 αMHC #15 hNkx2.5 #D (18 – 432 beats min^{-1}) and W4 αMHC #15 hNkx2.5 #F (12 – 414 beats min^{-1}) exhibited a wide variety, with some cells not fitting to the cell population. This might be due to the fact that the generated cells present an inconsistent subtype population. This was expected with cells derived from the W4 αMHC #15 clone, and therefore causes the most outliers. Single cells derived from the W4 αMHC #15 hNkx2.5 #L clone show a heterogeneous population (0 – 426 beats min^{-1}) but the beating frequency is still significantly faster than mnCMs. However, cell populations of different morphologies exhibit different – more homogenous – beating frequencies, exemplarily shown for W4 αMHC #15 hNkx2.5 #L (Figure 13B). The largest cell population of large square and large round cells exhibit the slowest beating frequency between 0 – 228 beats min^{-1} with significant difference to small round (174 – 474 beats min^{-1}) and spindle like (36 – 408 beats min^{-1}) cells.

Furthermore, adjacent cells synchronize their respective beating frequencies between themselves, which confirmed the ability of functional connections given by formation of gap junctions (Figure 9 and Figure 12).

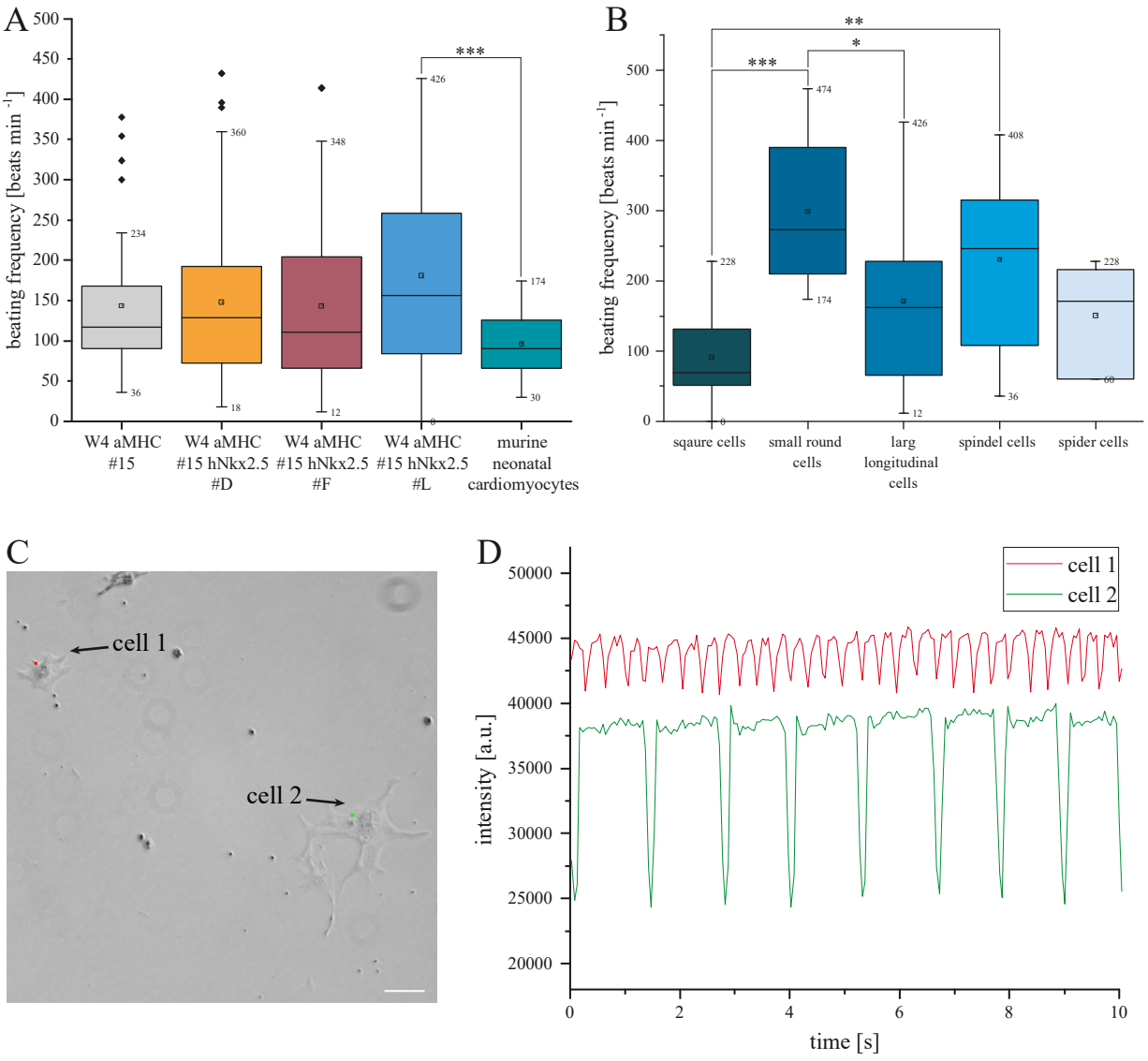

Figure 13: Beating frequency of CM-like single cells

Analysis of beating frequencies of obtained CM-like single cells on day 25 of differentiation. (A) beating frequencies of single cells (excluding small round dying cells) and (B) W4 αMHC #15 hNkx2.5 #L subdivided by morphology (including small round dying cells) displayed as boxplot, with 25 %- and 75 %-quantil, coeff. 1.5, outliers marked, horizontal line indicates media, square indicates mean;; statistic was performed as multiple comparison of mean (ANOVA), *p ≤ 0.05, **p ≤ 0.01, ***p ≤ 0.001. A:n=38, 86, 86, 88, 32 and B: n=16, 8, 33, 16, 6. (C) and (D) exemplary depiction of data acquisition with ZEN2011 software. Region of interests are marked (red: cell 1 and green: cell 2). Scale bar: 50 µm

4.1.2.2.3. Pharmacological substance administration on CM-like cells

Pharmacological investigations were performed referring to ion channel availability within the cell population of the respective clones as well as mnCMs in culture under administration of the following reagents: Noradrenaline (NA, 1 µM), Acetylcholine (ACh, 10 µM), Tetrodotoxin (TTX, 10 µM), potassium rich extracellular fluid (K^+, 20 mM), Mibefradil (Mibe, 10 µM) and Verapamil (Vera, 10 µM).

To analyze the impact of relevant substances, initial state (t0) of beating frequency was recorded as described above (see 4.1.2.2.2) (Figure 14A). Subsequently, recording was performed which serves the following issues: application of respective substance, time points t1 (10 s after application) and t2 (1 min after application) (Figure 14B). After an incubation period of 5 min (t3) a closing recording was performed to determine the final effect (Figure 14C).

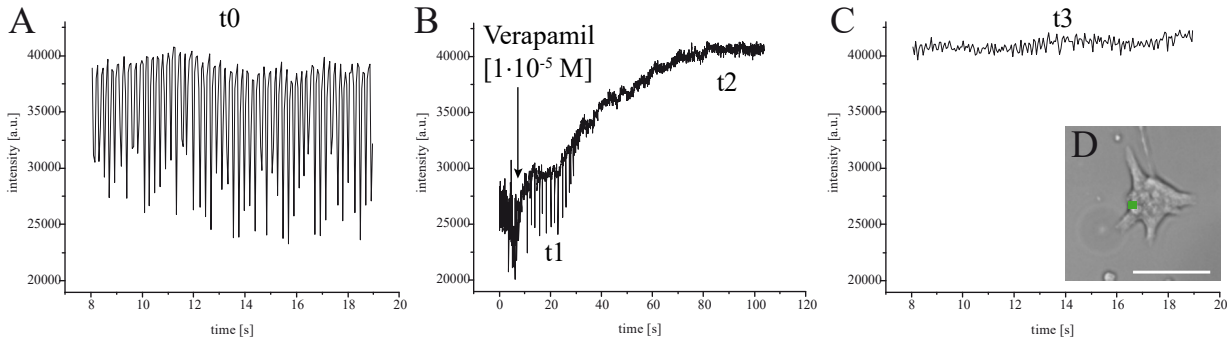

Figure 14: Exemplary depiction of data for administration of Verapamil

Exemplary depiction of data acquisition with ZEN2011 software. (A) Beating frequency of t0 indicates the initial state, (B) administration of Verapamil [$1 \cdot 10^{-5}$ M] and following time points t1 (10 sec after application) and t2 (1 min after application), and (C) t3 (5 min after application). (D) Associated cell, region of interests is marked (green). Scale bar: 50 µm

Figure 15B-F depicts the shift of beating frequencies (t1-t3) compared to the initial state (t0). Here it became apparent that cells derived from W4 αMHC #15 clone as expected represent an inconsistent population, reacting to each parameter with a large standard deviation (Figure 15B). Cells derived from W4 αMHC #15 hNkx2.5 #D clone exhibit the same inhomogeneous behavior (Figure 15C). MnCMs served as positive control in order to avoid methodological

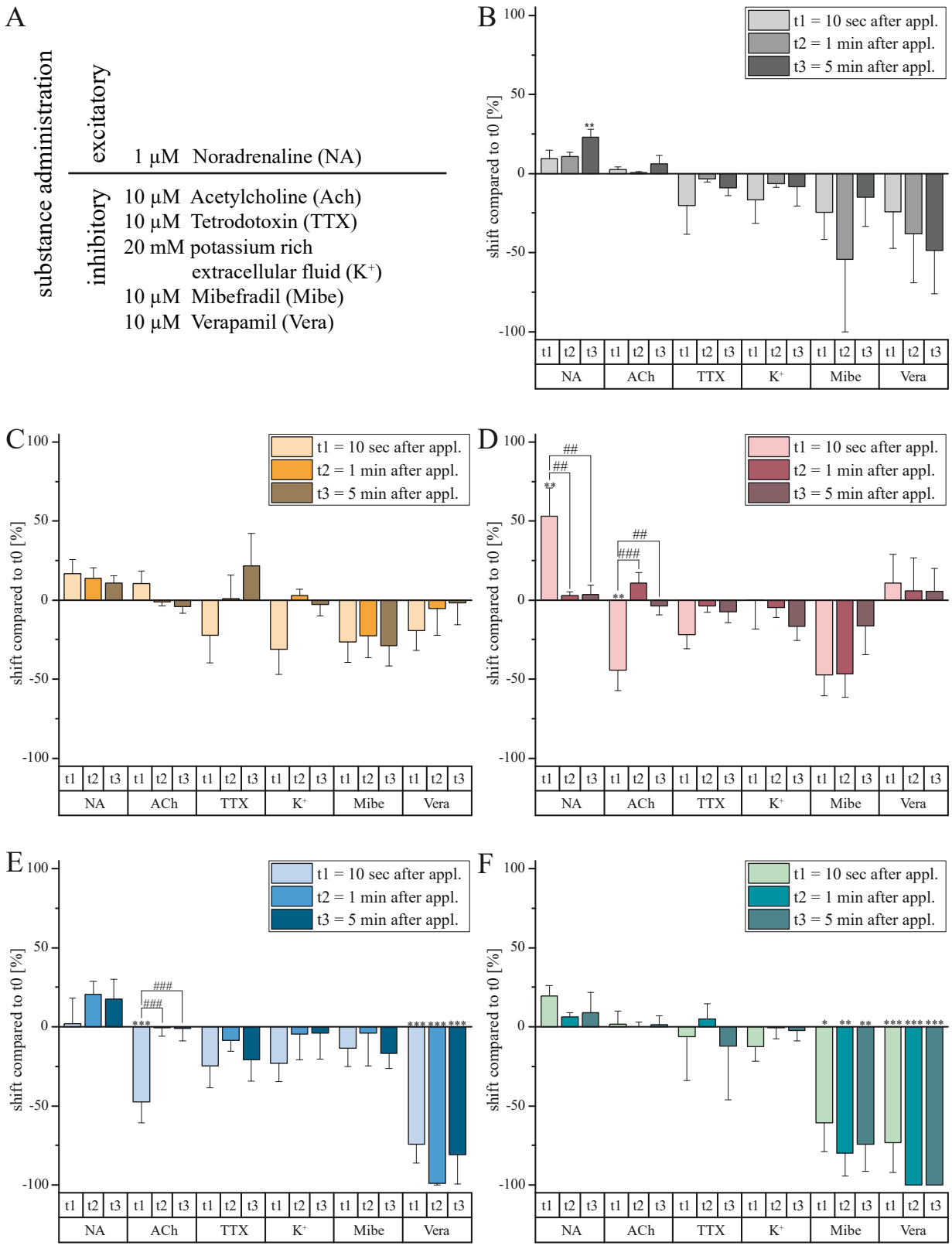
A
substance administration
excitatory
1 µM Noradrenaline (NA)
inhibitory
10 µM Acetylcholine (Ach)
10 µM Tetrodotoxin (TTX)
20 mM potassium rich extracellular fluid (K+)
10 µM Mibefradil (Mibe)
10 µM Verapamil (Vera)
B
C
D
E
F
t1 = 10 sec after appl.
t2 = 1 min after appl.
t3 = 5 min after appl.
shift compared to t0 [%]
100
50
0
-50
-100
t1 t2 t3
NA
ACh
TTX
K+
Mibe
Vera

Figure 15: Substance administration on CM-like single cells

Quantitative analysis of beating activity in relation to the respective substance administration. (A) Administration of inhibitory and excitatory pharmacological substance on obtained single cells of (B) W4 αMHC #15, (C) W4 αMHC #15 hNkx2.5 #D, (D) W4 αMHC #15 hNkx2.5 #F, (E) W4 αMHC #15 hNkx2.5 #L, and (F) monolayer mnCMs. Data represent the shift of beating frequencies compared to t0 (t0 set 0) (Figure 14). Values are presented as mean ± SEM; n=3-17; statistic was performed as multiple comparison of mean (ANOVA), */#$p \leq 0.05$, **/##$p \leq 0.01$, ***/###$p \leq 0.001$. (* comparison to t0, # comparison within all time points) (parts of the figure are submitted to the Journal of Cellular Physiology and Biochemistry.)

errors. It could be confirmed that mnCMs displayed a heterogeneous population reacting significantly to Mibefradil, an inhibitor of T-type calcium channels typically expressed in pacemaker cells, as well as highly significant to Verapamil, an inhibitor of L-type calcium channels typically expressed in cells of the contractile system (Figure 15F). However, the analyzed cells showed only a slight response to essential channel modulators NA, ACh, TTX and K^+.

In contrast, cells derived from W4 αMHC #15 hNkx2.5 #F clones demonstrated a significant beating activity after administration of NA and Ach (Figure 15D). Directly after application of NA, beating frequency increased significantly, but however, a time dependent significant decrease could be recorded. A similar behavior was shown after application of ACh, here, beating frequency is significantly decreased directly after application, but however, a time dependent significant increase could be registered. Furthermore, cells only slightly response to the administration of TTX, K^+, Mibefradil and Verapamil. There is an apparent negative influence on the beating frequency after the application of Mibefradil but not to a significant level.

Cells derived from W4 αMHC #15 hNkx2.5 #L clone exhibit a significant decrease of beating frequency within all time points recorded after application of Verapamil to the initial state (Figure 15E), exemplarily demonstrated in Figure 14. The cells react significantly to the application of ACh with a decrease of beating activity, as it was shown for W4 αMHC #15 hNkx2.5 #F, and time dependent behavior was observed. Furthermore, cells only slightly respond to the administration of NA, TTX, K^+ and Mibefradil.

Therefore, the W4 αMHC #15 hNkx2.5 #L clone was selected for further investigations because these cells come closest to the pattern of mnCM with a strong response on Verapamil an inhibitor of L-type calcium channels typically expressed in cells of the contraction system and almost no

reaction on Mibefradil as an inhibitor of T-type calcium channels typically expressed in pacemaker cells.

4.1.2.2.4. Cardiac marker expression on mRNA level

According to the selection of the W4 αMHC #15 hNkx2.5 #L clone, single cells at day 25 of differentiation were analyzed using qPCR to examine their cardiac marker expression on mRNA level (expression analysis relativized to W4 αMHC#15 (set: 1), Figure 16).

It could be demonstrated that cells derived from W4 αMHC #15 hNkx2.5 #L clones displayed a tendency of higher expression of cardiac structural markers, such as mMyh6, mMyl2 and mcTnT. There is no apparent difference in the expression of Connexin 43 expression between the two cell populations. However, the expression of mHcn4, a channel prominently expressed in pacemaker cells, is significantly lower in cells derived from W4 αMHC #15 hNkx2.5 #L clones.

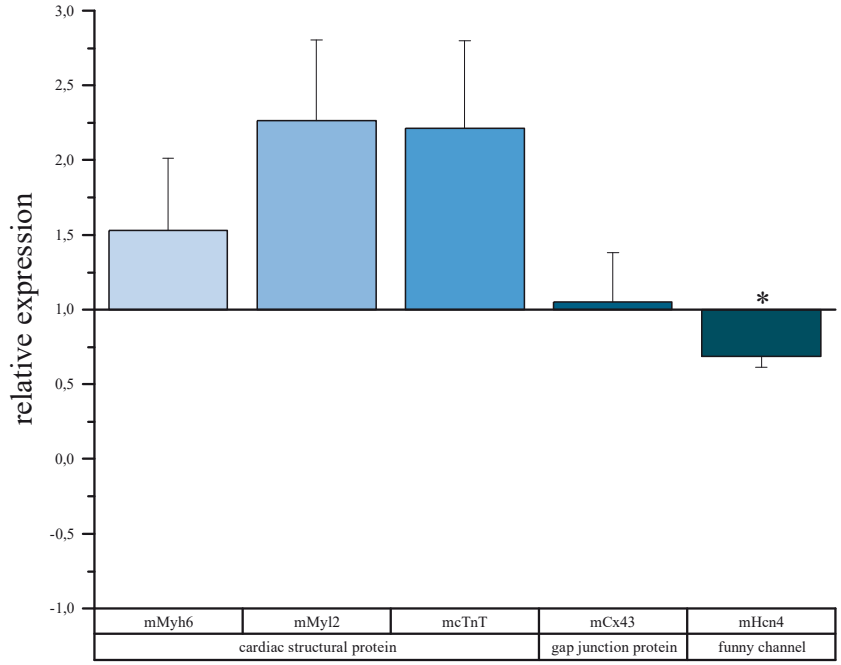

Figure 16: Late cardiac marker expression

Analysis of cardiac structural proteins, gap junction protein and funny channel expression on mRNA level. Relative expression of W4 αMHC #15 hNkx2.5 #L was performed by qPCR. Values normalized to mHprt and mPolr2a and relativized to W4 αMHC#15 (set: 1). Values are presented as mean ± SEM; n=3; statistic was performed as t-test, *p ≤ 0.05.

Overall, this part of the thesis has shown that a combined forced exogenous overexpression of Nkx2.5 [151] and a αMHC promotor-based antibiotic selection [155] using murine ESCs, is

sufficient to generate a pure αMHC^{+} cell population with augmented maturation towards ventricular but yet immature CM-like cells.

4.2. Results Part II – establishment of modified mRNA

4.2.1. Protocol establishment – Generation of modified EGFP mRNA

The focus for this project was set on the generation of highly reproducibly modified mRNA (mmRNA) using an accelerated PCR-based protocol (Figure 17A).

Therefore, the pCS2+ expression vector (plasmid map pCS2+: supplement Figure 34) containing the EGFP-ORF sequence was used to establish a standardized method allowing an appropriate verification on protein level. The generation of a linear DNA template for subsequent *in vitro* mod-mRNA synthesis relies on proof-reading polymerase-based PCR amplification of the respective sequence of interest. Therefore a forward primer upstream of the SP6 promotor sequence and a reverse primer, containing a poly(T) overhang of 100 thymidine-triphosphate, downstream of the EGFP sequence were used (Figure 17B; Table 9).

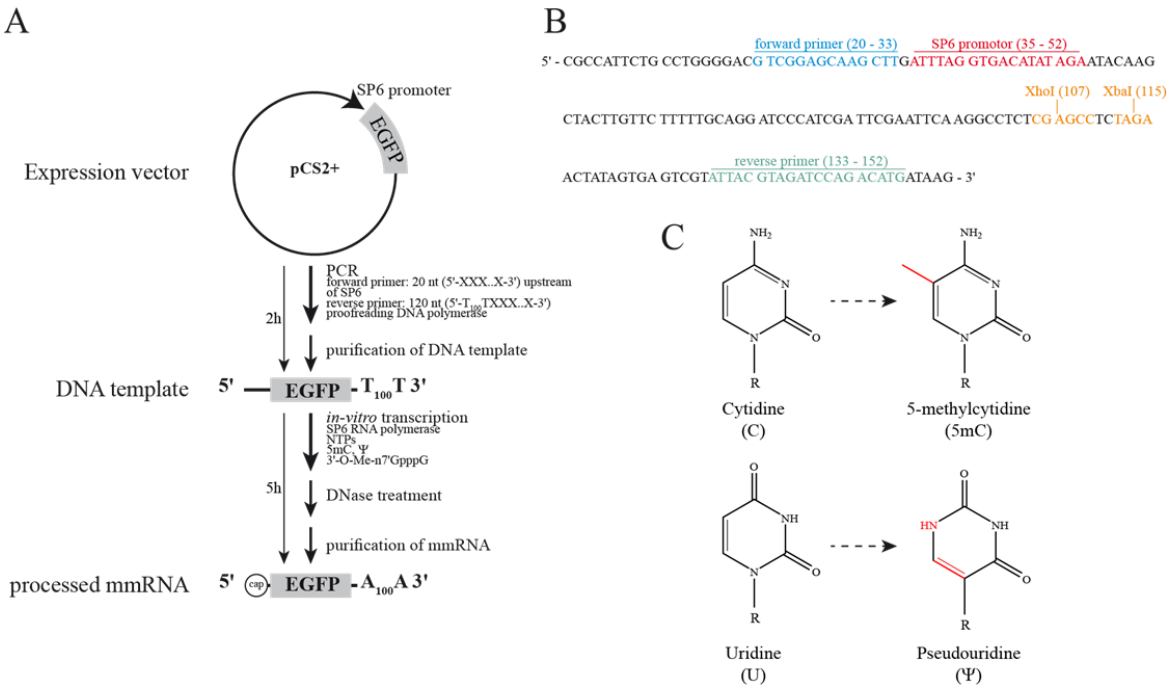

Figure 17: Procedure model of modified mRNA generation

Conception for *in vitro* synthesis of chemical modified mRNA, exemplarily EGFP. (A) Flow-chart, elucidating generation of mmRNA. Expression vector pCS2+ was used as DNA-template for the amplification of EGFP sequence, using proofreading DNA polymerase and self-designed reverse primer (containing poly(T) tail). IVT was performed using SP6 RNA polymerase with the incorporation of modified bases 5mC and Ψ as well as a methylated RNA cap. (B) pCS2+ expression vector sequence (bp 1 to 160) indicating binding sequences of forward (bp 20 – 33) and reverse (bp 133 - 152) primer, SP6 RNA polymerase promotor (bp 35- 52) as well as restriction sequence of XhoI (107) and Xba I (115) for the integration of EGFP sequence. (C) RNA nucleoside molecules with their chemical modified counterparts used for IVT. Modified positions marked in red, R: ribose. Adapted from [276]

The following *in vitro* transcription (IVT) was performed using the commercially available MEGAscript SP6 kit. However, crucial changes in the composition were applied. In order to improve translation efficiency and stability of the mRNA, a methylated 3′-O-Me-m7G(ppp)G RNA cap structure analog and modified nucleosides were added to the IVT reaction. Both ribosyl pyrimidines (Cytidine and Urdine) were replaced by their chemically modified counterparts, 5-methylcytidine (5mC) and pseudouridine (Ψ), in the respective ratio (Figure 17C).

This standardized process ensures a mmRNA, comprising i) a 5'-cap, ii) a modified sequence of interest and iii) a 3' poly(A) tail. The obtained modified EGFP mRNAs were subsequently used for the delivery into various cell types.

4.2.2. Introduction of mEGFP mRNA into various cell types

For the following experiments, the lipid-based Lipofectamine2000 reagent was used for non-viral delivery of mmRNA into all cell types under investigation. As described above (Figure 17), pyrimidines were replaced by their chemically modified counterparts, 5mC and Ψ, in the following ratios: unmodified, 100 % 5mC, 100 % Ψ, 52 % 5mC + 52 % Ψ and 100 % 5mC + 100 % Ψ. Transfections were performed 24 h after cell seeding in a 24 well plate with 500 ng of the respective mRNA modification. The analysis of EGFP expression, mean fluorescence intensity and cell viability was verified 4 h, 12 h, 24 h, 48 h and 72 h after the transfection with flow cytometry and microscopy.

4.2.2.1. Optimization of mRNA modification for monkey fibroblasts

The well-established cell line COS7 was used to initially evaluate the mmRNA-mediated protein expression of five different EGFP mRNA modifications.

All mRNA modifications exhibit a fast translation, indicated by a EGFP protein expression between 22.9 ± 5.6 % and 47.7 ± 4.6 % after 4 h, whereby only 100 % 5mC + 100 % Ψ (22.9 ± 5.6 %) displayed a significantly lower expression compared to unmodified mRNA (43.5 ± 1.8 %) (Figure 18A). This is also indicated by the fact, that all modifications lead to a peak in expression at 12 h (except 100 % 5mC + 100 % Ψ, peak at 24 h), whereas 100 % Ψ (89.4 ± 2.2 %) is the most efficient modification, at the same time exhibiting the highest mean fluorescence intensity per cell and low toxicity (Figure 18B and D). Modifications in which uridine was

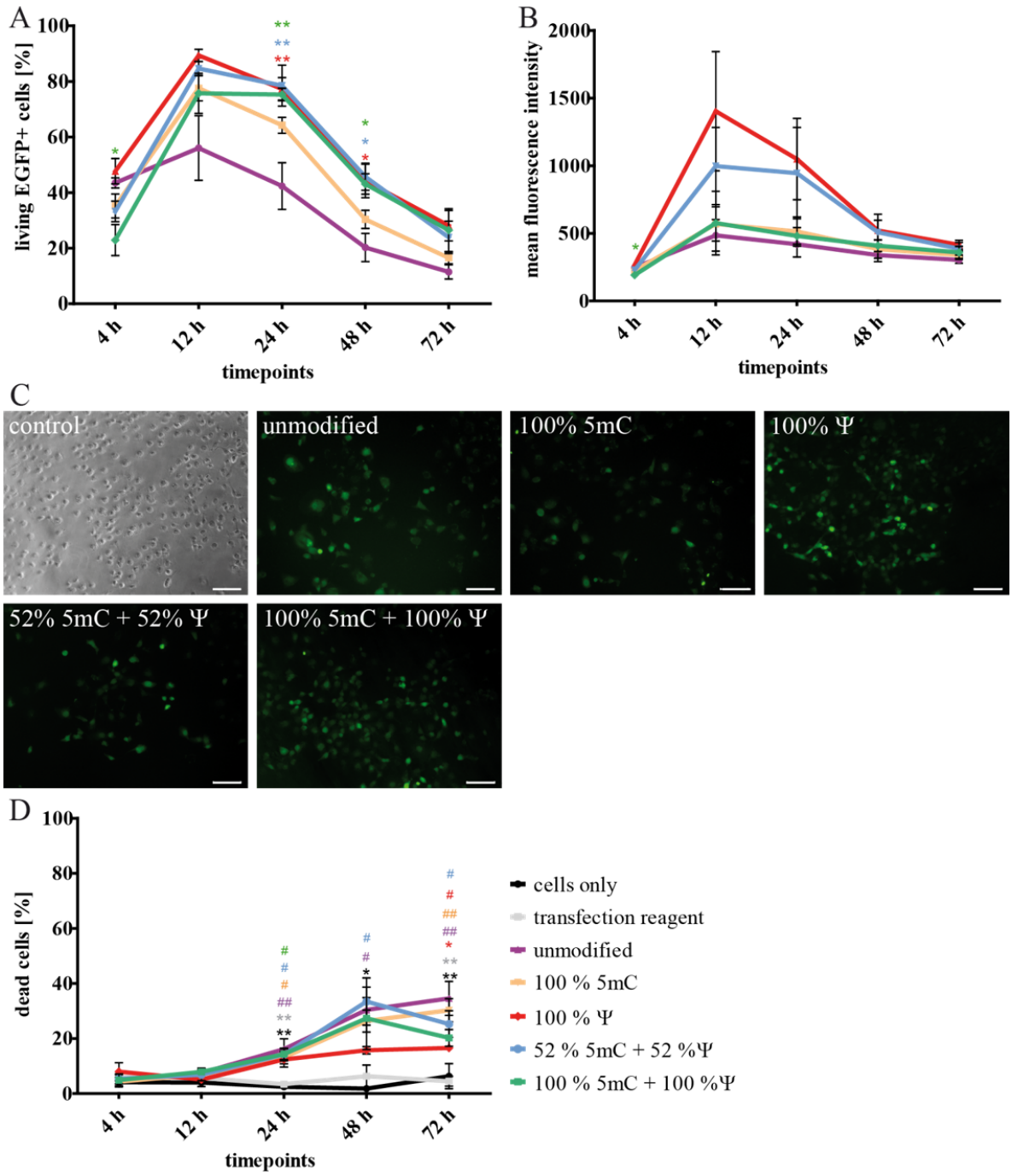

Figure 18: Transfection of monkey fibroblasts COS7 with modified EGFP mRNA

Analysis of monkey fibroblasts COS7 in order to determine (A) living EGFP expressing cells, (B) mean fluorescence intensities of living EGFP expressing cells and (D) toxicity as measured by flow cytometry. Data represent mean ± SEM, n = 3. Statistics was performed in multiple comparisons versus unmodified mRNA: *p ≤ 0.05, **p ≤ 0.01 and versus untransfected cells: #p ≤ 0.05, ##p ≤ 0.01, ###p ≤ 0.001. (C) Microscopy images 24 h after transfection with unmodified, 100 % 5mC, 100 % Ψ, 52 % 5mC + 52 % Ψ, 100 % 5mC + 100 % Ψ and transfection reagent (Lipofectamine2000) as control, stained with FITC-conjugated anti- GFP antibody. Scale bar: 100 µm. Taken from [276] (parts of the figure appear in the Bachelor thesis of Silke Naß who was supervised by F. Hausburg)

completely or partially replaced by pseudouridine led to a significantly higher protein expression after 24 h and 48 h compared to unmodified mRNA. However, EGFP expression decreases over time within all used modifications, but persists at a level of 11.5 ± 2.5 % – 28.1 ± 5.5 % at 72 h, with no evident difference. Only 100 % 5mC + 100 % Ψ displayed no significant difference with regard to long term viability compared to untransfected cells 72 h after transfection.

Therefore, 100 % Ψ and 100 % 5mC + 100 % Ψ were selected as the most promising modifications for the monkey COS7 fibroblast cell line.

4.2.2.2. Transfer to human fibroblasts and human mesenchymal stem cells

Investigations on human cells were performed in order to verify the capability of mmRNA as therapeutic application in the clinic. To this end, the newborn foreskin fibroblast cell line BJ as well as adult bone marrow derived mesenchymal stem cells (MSCs) were examined.

As demonstrated in COS7, using the complete replacement of uridine with Ψ, has led to the highest EGFP protein expression as well as mean fluorescence intensity in human BJs (Figure 19A, B). Along with a complete replacement of both ribosyl pyrimidines, the modifications: 100 % Ψ and 100 % 5mC + 100 % Ψ displayed a significant higher expression after 48 h and 72 h compared to unmodified EGFP. It is also shown, that all mRNA modifications exhibit fast translation, indicated by EGFP protein expression between 21.4 ± 4.0 % and 48.6 ± 10.3 %after 4 h, hereinafter peak between 12 h and 24 h. Whereby 100 % Ψ displayed the highest EGFP expression 12 h after transfection with 76.3 ± 4.9 %. Unlike COS7 cell line, the protein expression remained constant over time with a level between 29.6 ± 11.1 % and 60 ± 4.6 %. However, again only 100 % 5mC + 100 % Ψ revealed no significant difference with regard to long term viability compared to untransfected cells 72 h after transfection.

Therefore, 100 % Ψ and 100 % 5mC + 100 % Ψ were selected as the most promising modifications for the human BJ fibroblast cell line.

The replacement of cytidine alone or partly in combination with Ψ did not result in an improvement in hBJs as well as human MSCs (Figure 19 and Figure 20). The tendency in protein expression is continuing in hMSCs, 100 % Ψ displayed the highest EGFP expression over

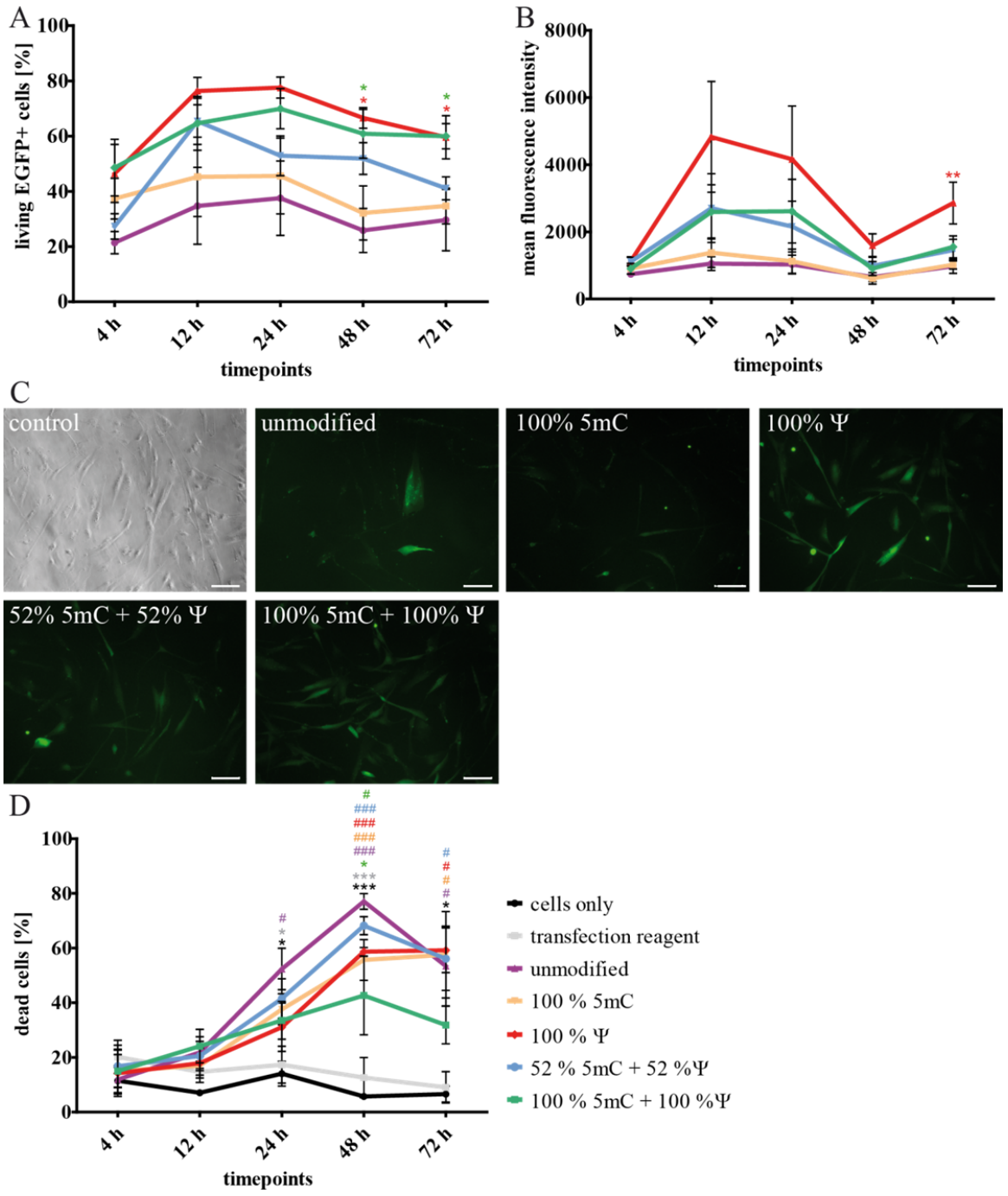

Figure 19: Transfection of human fibroblasts BJ with modified EGFP mRNA

Analysis of human foreskin fibroblasts BJ in order to determine (A) living EGFP expressing cells, (B) mean fluorescence intensities of living EGFP expressing cells and (D) toxicity as measured by flow cytometry. Data represent mean ± SEM, n = 3. Statistics was performed in multiple comparisons versus unmodified mRNA: *p ≤ 0.05, **p ≤ 0.01 and versus untransfected cells: #p ≤ 0.05, ##p ≤ 0.01, ###p ≤ 0.001. (C) Microscopy images 24 h after transfection with unmodified, 100 % 5mC, 100 % Ψ, 52 % 5mC + 52 % Ψ, 100 % 5mC + 100 % Ψ and transfection reagent (Lipofectamine2000) as control, stained with FITC-conjugated anti- GFP antibody. Scale bar: 100 µm. Taken from [276] (parts of the figure appear in the Bachelor thesis of Silke Naß who was supervised by F. Hausburg)

time with a peak 24 h after transfection (54 ± 7.5 %) and the highest mean fluorescence 12 h after the transfection (Figure 20A, B). Remarkably, protein expression appears even in this slowly proliferating adult stem cells very rapidly, already 4 h after transfection between 15.7 ± 5.7 %

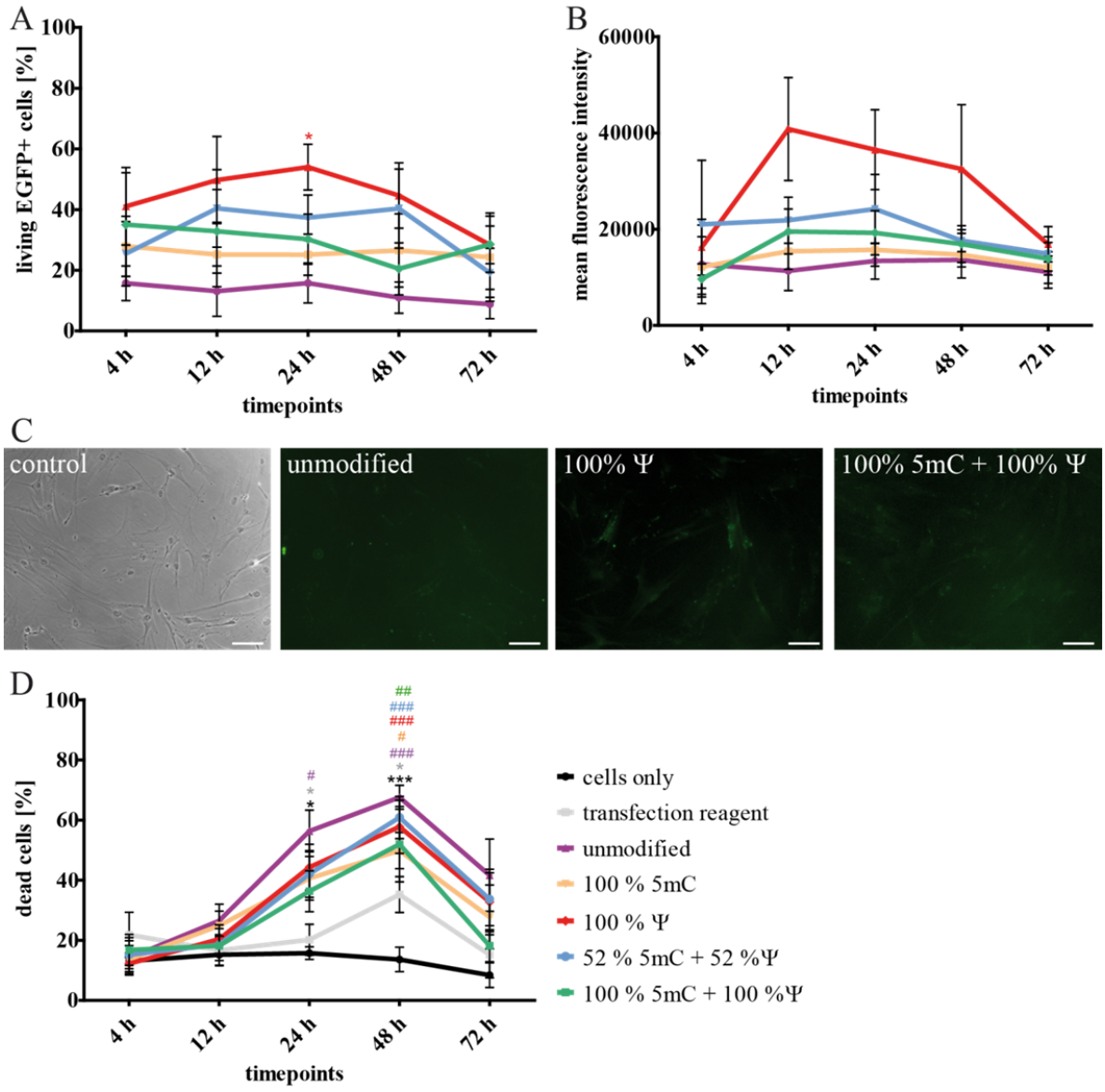

Figure 20: Transfection of human MSCs with modified EGFP mRNA

Analysis of human adult mesenchymal stem cells in order to determine (A) living EGFP expressing cells, (B) mean fluorescence intensities of living EGFP expressing cells and (D) toxicity as measured by flow cytometry. Data represent mean ± SEM, n = 3. Statistics was performed in multiple comparisons versus unmodified mRNA: *p ≤ 0.05, **p ≤ 0.01 and versus untransfected cells: #p ≤ 0.05, ##p ≤ 0.01, ###p ≤ 0.001. (C) Microscopy images 24 h after transfection with unmodified, 100 % Ψ, 100 % 5mC + 100 % Ψ and transfection reagent (Lipofectamine2000) as control, stained with FITC-conjugated anti- GFP antibody. Scale bar: 100 µm. Taken from [276] (parts of the figure appear in the Bachelor thesis of Silke Naß who was supervised by F. Hausburg)

and 41 ± 12.8 % of the cells are EGFP positive. However, all modifications revealed no significant difference with regard to long term viability compared to untransfected cells 72 h after transfection, though the highest amount of dead cells appeared with unmodified mRNA (56 ± 8.9 % after 24 h and 67.9 ± 4 % after 48 h) (Figure 20D).

Therefore, 100 % Ψ were selected as the most promising modifications for the adult bone marrow derived mesenchymal stem cells.

4.2.3. mmRNA as a tool for cell fate conversion

In order to demonstrate the application potential of mmRNA in cell reprogramming and gene therapy approaches, the murine fibroblast C3H10T1/2 cell line as an established *in vitro* system for transdifferentiation into skeletal myoblasts was selected [214].

To ensure optimal mRNA-mediated protein expression combined with the highest cell viability, we initially tested the aforementioned EGFP mRNA modifications (4.2.2). It appeared, that the translation is as fast as in all other cell types under investigation 4 h after transfection with protein expression between 33.9 ± 13.5 % and 41.4 ± 16.8 % and a peak 12 h after transfection (Figure 21A, C). However, only 100 % Ψ displayed comparably good expression levels (highest at 12 h with 56.2 ± 11.8 %) like hMSCs. Yet taking all modification over time into consideration, C3H10T1/2 cells exhibit the lowest protein expression with a fast decrease after 12 h. All modifications show a similar trend of protein expression over time with no statistically significant difference compared to unmodified mRNA. There is almost no EGFP expression detectable after 72 h, whereby 100 % 5mC + 100 % Ψ showed the highest expression with 7.7 ± 4.2 % simultaneously with low toxicity (Figure 21D).

Therefore, 100 % 5mC + 100 % Ψ was selected as most promising for murine C3H10T1/2 with regard to its best cell viability during long term cultivation combined with a high transfection efficiency and good fluorescence intensity.

Subsequently, MyoD mRNA with the incorporation of 100 % 5mC + 100 % Ψ was used for cell reprogramming. For this purpose, C3H10T1/2 cells were seeded and cultured in standard growth medium, which was changed 4 h prior the first mmRNA transfection to medium supplemented with the recombinant protein B18R to increase cell viability (Figure 22A). Thereafter, cells were transfected three times with 250 ng mMyoD mRNA in an interval of 24 h.

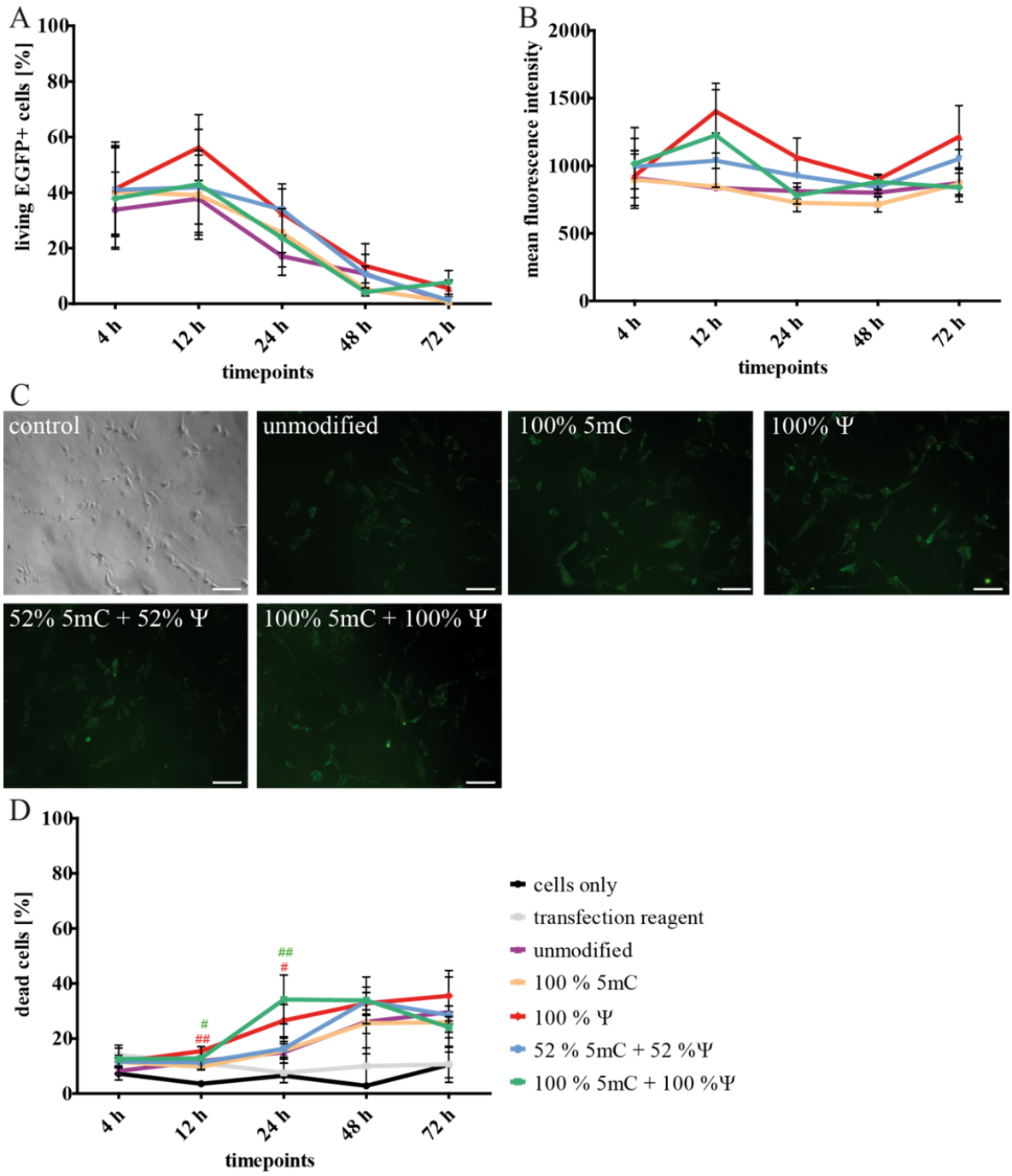

Figure 21: Transfection of murine fibroblasts C3H10T1/2 with modified EGFP mRNA

Analysis of murine fibroblasts C3H10T1/2 in order to determine (A) living EGFP expressing cells, (B) mean fluorescence intensities of living EGFP expressing cells and (D) toxicity as measured by flow cytometry. Data represent mean ± SEM, n = 3. Statistics was performed in multiple comparisons versus unmodified mRNA: *p ≤ 0.05, **p ≤ 0.01 and versus untransfected cells: #p ≤ 0.05, ##p ≤ 0.01, ###p ≤ 0.001. (C) Microscopy images 24 h after transfection with unmodified, 100 % 5mC, 100 % Ψ, 52 % 5mC + 52 % Ψ, 100 % 5mC + 100 % Ψ and transfection reagent (Lipofectamine2000) as control, stained with FITC-conjugated anti- GFP antibody. Scale bar: 100 µm. Taken from [276] (parts of the figure appear in the Bachelor thesis of Silke Naß who was supervised by F. Hausburg)

This was followed by an incubation time of three days in serum reduced medium, to support transdifferentiation. Cell fate conversion towards myoblast-like cells was demonstrated by staining of typically expressed myosin heavy chain (MyHC) (Figure 22B). Control cells, which underwent the same cultivation conditions failed to reveal any expression. This proves the effectiveness and ability of mmRNA to directly alter cell identity.

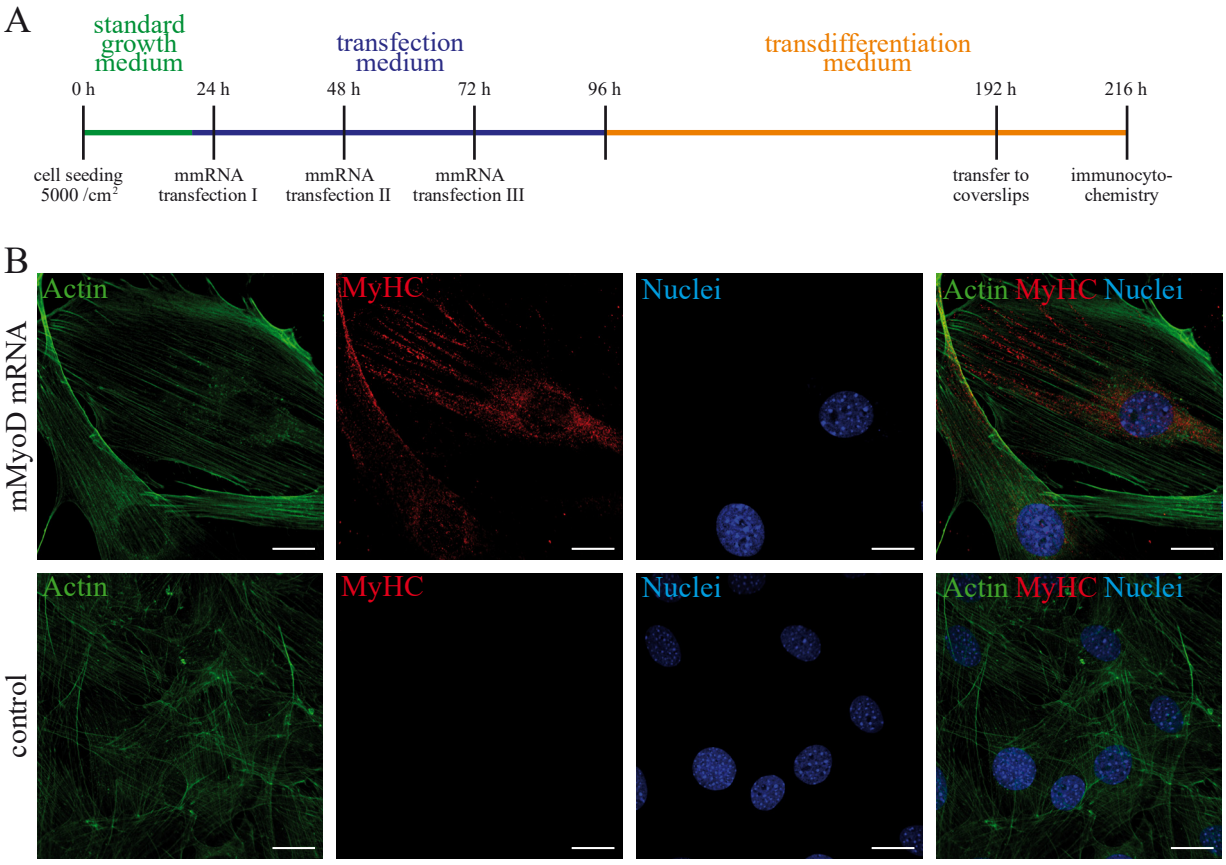

Figure 22: Cell fate conversion induced by modified MyoD mRNA

Direct cell reprogramming of murine fibroblasts C3H10T1/2 towards myoblast-like cells. (A) Flow chart of cell reprogramming procedure, cells were seeded (5 x 10^3 cells/cm^2) in standard growth medium. Transfection was performed with 250 ng mMyoD mRNA three times (every 24 h) in transfection medium supplemented with B18R. Additional cultivation was performed for three days in serum reduced medium. (B) mRNA-derived myoblast-like cells, expression of the muscle marker myosin heavy chain (MyHC) in C3H10T1/2 cell derivatives after transfection with mMyoD mRNA and negative control. Actin (green), MyHC (red), Nuclei (blue). Scale bar: 20 µm. Taken from [276]

4.2.4. mmRNA as a tool for cardiac cell differentiation

To establish mmRNA as a suitable equivalent to DNA introduction, Nkx2.5 mRNA with the incorporation of 100 % 5mC + 100 % Ψ was used to differentiate murine embryonic stem cells toward a cardiac phenotype.

For this purpose, W4 αMHC #15 were seeded and cultured in cardiogenic differentiation medium, which was supplemented 4 h prior the first mmRNA with the recombinant protein B18R to increase cell viability (Figure 23). Thereafter, cells were transfected three times with 500 ng mNkx2.5 mRNA in an interval of 24 h. Subsequently, cells were cultured according to the standard cardiac differentiation protocol, which implies EB formation, αMHC selection and dissociation to obtain single cells.

The determination of beating frequencies was performed in accordance to 4.1.2.2.2 (Figure 13B). Figure 23B depict the beating frequencies per min of control (W4 αMHC #15) and mRNA programmed CM-like cells. W4 αMHC #15 displayed a homogenous cell population with values (24 -132 beats min^{-1}). Cells generated with a boost exogenous force of Nkx2.5 reveal a heterogeneous population with a fast beating outlier (24 – 396 beats min^{-1}). Both cell populations did not differ significantly from each other.

Furthermore, calcium oscillation within the cells was analyzed using X-Rhod-1 dye. Exemplary presented cells (Figure 24) exhibit a regular but for every cell individual calcium transient, usually originating from the middle of the cell and spread over the cell through the periphery.

These first indications have proven the ability of mmRNA to be a suitable equivalent to DNA while performing forward cardiac programming of mESCs.

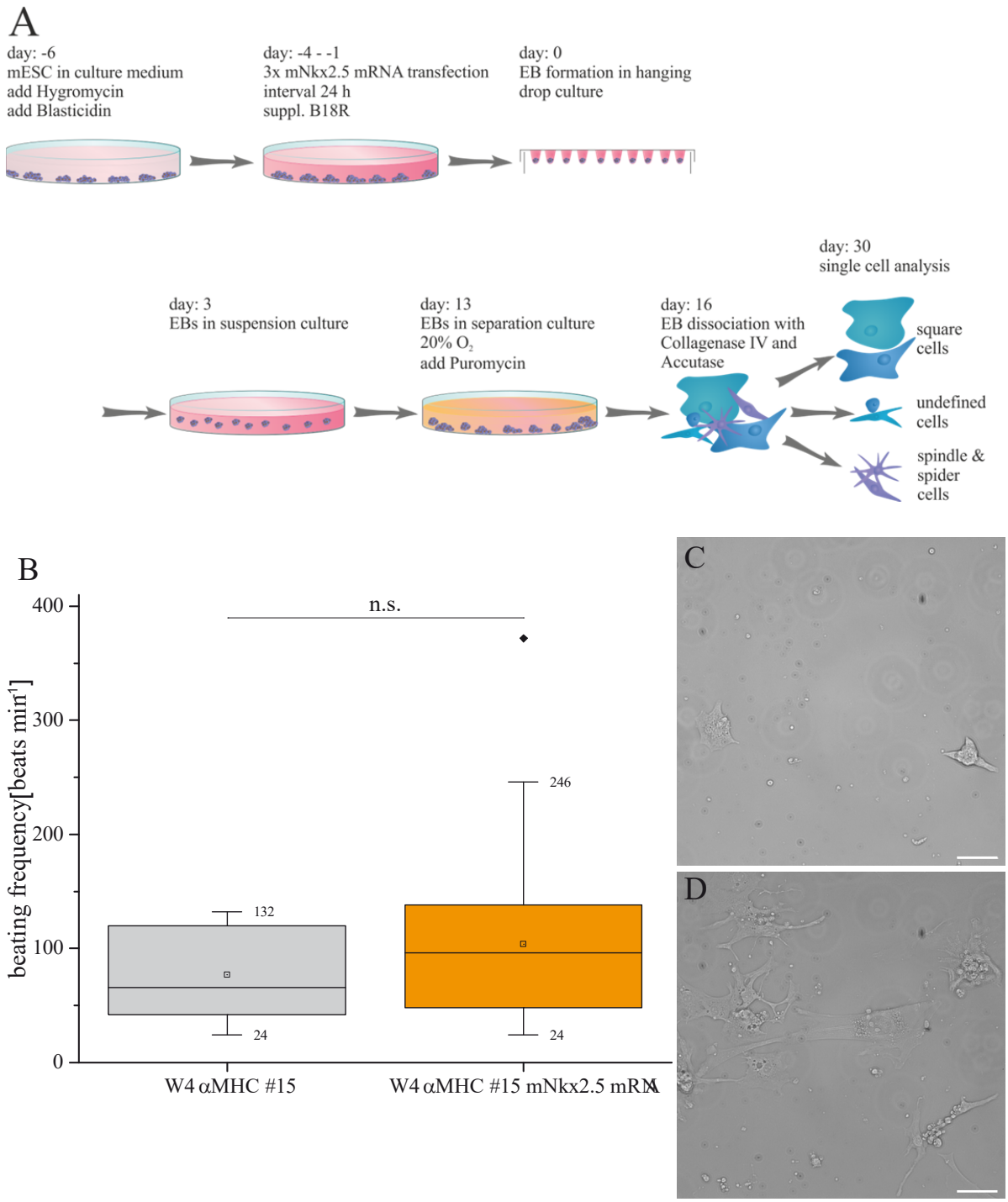

Figure 23: Cardiac differentiation induced by modified Nkx2.5 mRNA

Forward programming of murine embryonic stem cells towards a cardiomyocyte-like phenotype. (A) Experimental setup, starting with three successive transfections of modified Nkx2.5 mRNA and subsequent cardiac differentiation according to the standard protocol, including EB formation and antibiotic selection. (B) Analysis of beating frequencies, displayed as boxplot, with 25 %- and 75 %-quantil, coeff. 1.5, outliers marked, horizontal line indicates media, square indicates mean; n=14, 57; statistic was performed as t-test. Representativ visualization of cell morphologies of (C) control cells and (B) cells using mNkx2.5 mRNA. Scale bar: 50 µm

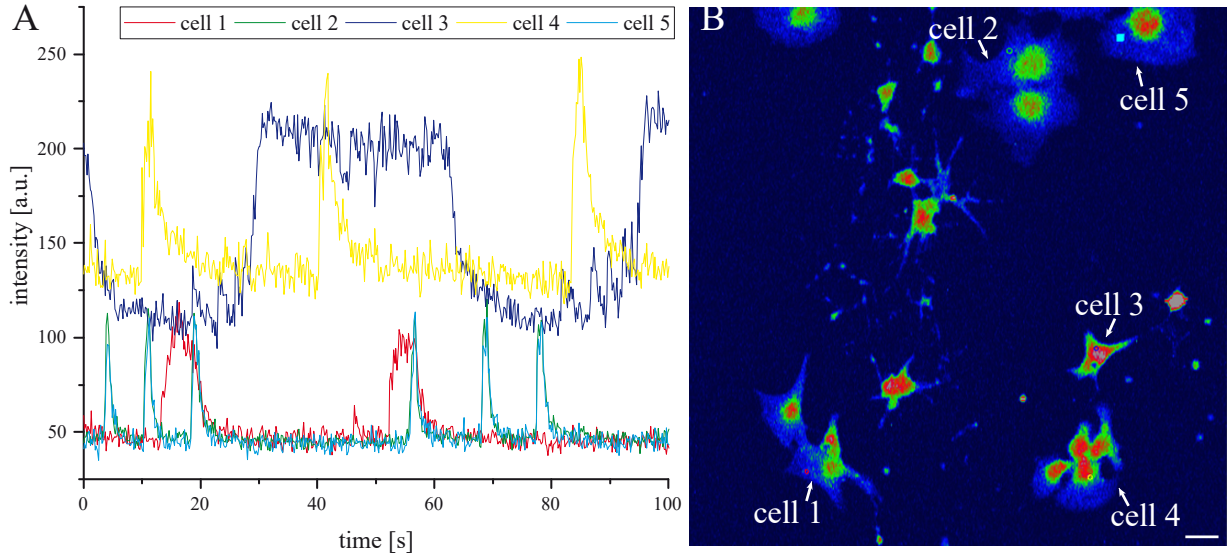

Figure 24: Calcium transient of mmRNA iCM-like cells

Analysis of calcium oscillation of obtained mmRNA iCM-like single cells on day 25 of differentitation. (A) and (B) exemplary depiction of data acquisition with ZEN2011 software. Region of interests are marked (red: cell 1, green: cell 2, dark blue: cell 3, yellow: cell 4 and cyan: cell 5). Scale bar: 50 µm

4.3. Results Part III – modification of CD133$^+$ hSCs

A potential modification of human CD133$^+$ stem cells was evaluated using superparamagnetic polymer-based non-viral delivery of miRNA with respect to a gentle and safe strategy (Figure 25). The results have been equally compiled by N. Voronina, P. Müller and F. Hausburg.

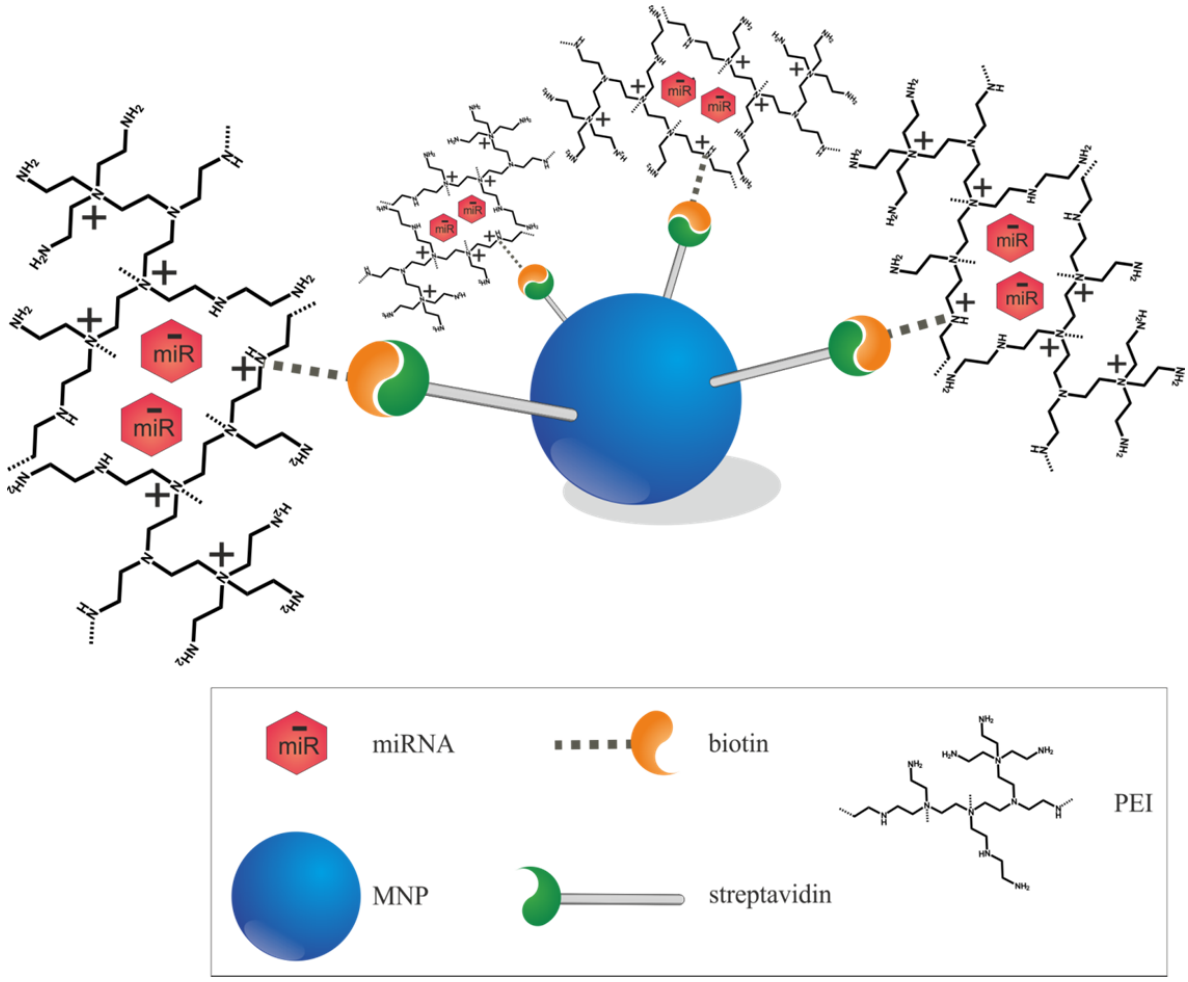

Figure 25: Schematic structure of superparamagnetic polymer-based complexes for a non-viral delivery of miRNA

Transfection complexes are composed of a streptavidine-coated magnetic iron oxide nanoparticle (MNP) and biotinylated polyethylenimine (PEI), which condenses miRNA through electrostatic interactions. Taken from [328]

4.3.1. Defining the optimal miR/PEI/MNP complex composition suitable for CD133$^+$ stem cell transfection

In order to optimize miR/PEI/MNP complexes most suitable for an efficient CD133$^+$ stem cell transfection, Cy3-labeled miRNA was used to obtain qualitative evidence using flow cytometry.

To exclude cytotoxic effects of isolation and cultivation procedures, untransfected cells were used as control.

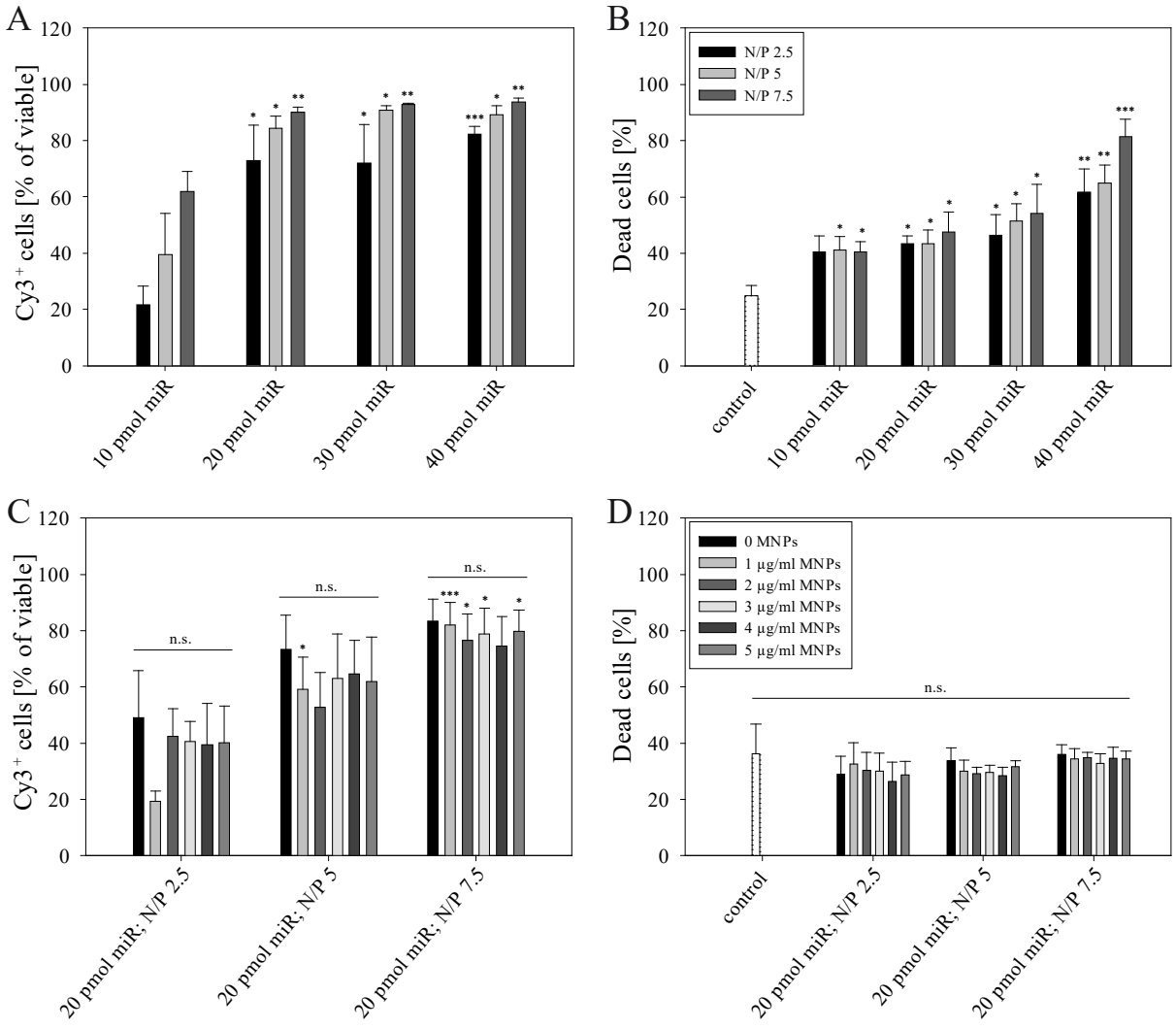

Figure 26: Optimization of miR/PEI/MNP complexes for efficient CD133$^+$ stem cell transfection

Transfection optimization analyzed 18 h after transfection by flow cytometry using Cy3-labeled miRNA. (A) And (B) present optimization of miRNA/PEI complexes using four different miRNA amounts (10, 20, 30 and 40 pmol) and three different N/P ratios (2.5, 5 and 7.5). Uptake efficiency (A) and cytotoxicity (B) were measured. Untransfected cells were used as control. Values are presented as mean ± SEM; n = 4; statistic was performed vs. 10 pmol miR with respective N/P ratio (A) and vs. control (B); *p ≤ 0.05, **p ≤ 0.01, ***p ≤ 0.001. (C) And (D) present optimization of miRNA/PEI/MNP complexes using 20 pmol miR, three different N/P ratios (2.5, 5 and 7.5) and six different MNP amounts (0, 1, 2, 3, 4 and 5 µg/ml). Uptake efficiency (A) and cytotoxicity (B) were measured. Untransfected cells were used as control. Values are presented as mean ± SEM; n = 4; statistic was performed vs. 20 pmol miR, N/P ratio 2.5 with respective MNP amount (indicated as *) or within the same N/P ratio (A) and vs. control (B); *p ≤ 0.05, **p ≤ 0.01, ***p ≤ 0.001. Adapted from [328]

The best miR/PEI compositions were determined first by testing four different miRNA amounts (10, 20, 30 and 40 pmol per 5 x 10^4 cells) and three different N/P ratios (2.5, 5 and 7.5) with regard to uptake efficiency and cytotoxicity (Figure 26A and B). Complexes with a low amount of miRNA (10 pmol) revealed the lowest uptake efficiency (between 21.7 ± 6.6 % and 62 ± 7.1 %) and only a modest increase of dead cells (between 40.3 ± 3.8 % and 41.2 ± 4.6 %). In contrast, using highest amount of miRNA (40 pmol) led to significantly higher uptake efficiency within all N/P ratios used (e.g. 40 pmol miRNA; N/P 7.5: 93.8 ± 1.3 %) but at the same time to a significantly higher cytotoxicity (e.g. 40 pmol miRNA; N/P 7.5: 81.3 ± 6.4 %). Therefore, complexes comprising 20 pmol miRNA were used for further evaluation, as they exhibit high uptake efficiency (between 72.8 ± 12.7 % and 90 ± 1.9 %) and reasonable cytotoxicity between 43.3 ± 4.9 % and 47.5 ± 7.1 % compared to untransfected cells (24.8 ± 3.8 %).

Next, selected miR/PEI complexes were mixed with MNPs in six different concentrations (0, 1, 2, 3, 4 and 5 µg per ml of prepared miR/PEI mixture) and tested with regard to uptake efficiency and cytotoxicity (Figure 26C and D). In particular, the introduction of MNPs has no significant effect on uptake efficiency compared to respective miR/PEI complexes (0 MNP) within all N/P ratios tested. However, variation of N/P ratios led to rising uptake efficiency, e.g. 20 pmol miRNA; 1 µg/ml MNPs: N/P 2.5: 19.4 ± 3.5 %; N/P 5: 59.2 ± 11.4 %; N/P 7.5: 82.1 ± 7.9 %. Furthermore, no significant difference in cytotoxicity could be observed among all transfection complexes (between 26.3 ± 7 % and 36.1 ± 3.5 %) and control cells (36.2 ± 10.6 %).

Therefore, superparamagnetic polymer-based complexes comprising of 20 pmol miRNA, N/P ratio 5 and 7.5, with 3 and 5 µg/ml MNPs were selected as most promising for human $CD133^+$ stem cells with regard to their highest uptake efficiency combined with a low cytotoxicity.

4.3.2. Maintenance of viability and surface marker pattern of modified $CD133^+$ stem cells

In order to prove the influence of superparamagnetic polymer-based complexes themselves and cultivation procedures on $CD133^+$ stem cell characteristics, cell viability and surface marker patterns were evaluated using flow cytometry 18 h after transfection (Figure 27). To this end, Boolean gating strategy was adapted on the ISHAGE guidelines for $CD34^+$ cells.

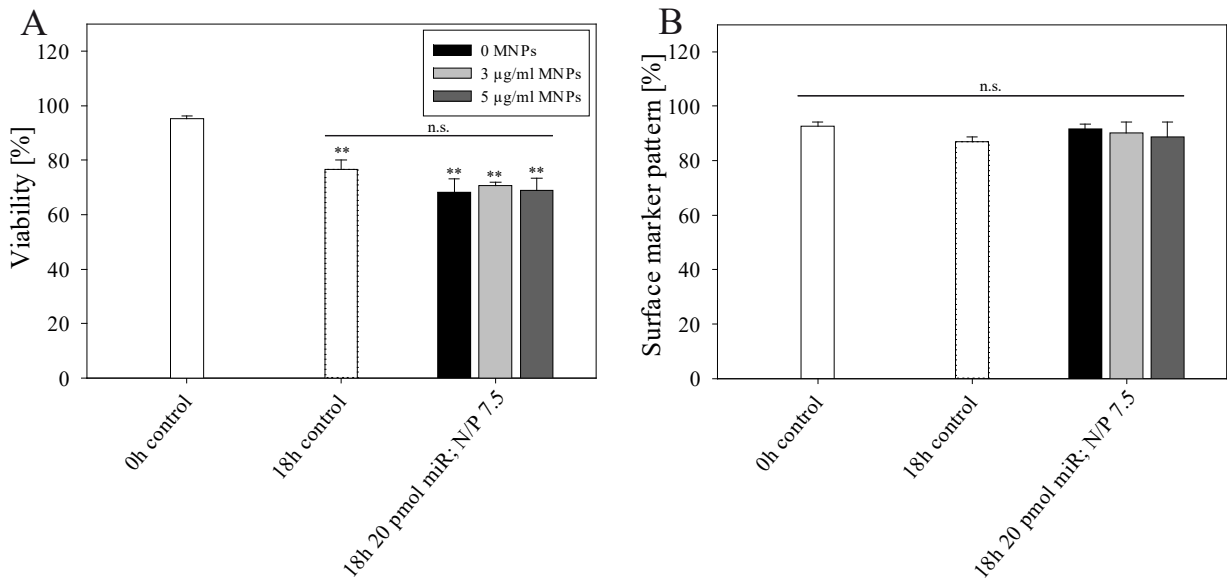

Figure 27: Viability and surface marker pattern 18 h after transfection

Evaluation of CD133$^+$ haematopoietic stem cell characteristics 18 h after transfection by flow cytometry using Cy3-labeled miRNA. Transfection complexes consisting of 20 pmol miRNA, N/P ratio 7.5 and three different MNP amounts (0, 3 and 5 µg/ml) were used. (A) Viability and (B) surface marker pattern (composed of the expression of CD45, CD34, and CD133) were measured. Untransfected cells (0 h and 18 h) were used as control. Values are presented as mean ± SEM; n = 3; statistic was performed vs. 0 h control (indicated as *) or vs. 18 h control; *p ≤ 0.05, **p ≤ 0.01, ***p ≤ 0.001. Adapted from [328]

It has been demonstrated that 18 h *in vitro* cultivation of CD133$^+$ stem cells led to a significant decrease of cell viability from 95.2 ± 0.9 % (0 h, control) to 76.7 ± 3.3 % (18 h, control). However, neither miRNA/PEI (68.2 ± 4.9 %) nor miRNA/PEI/MNPs (3 µg/ml MNPs: 70.5 ± 1.4 % and 5 µg/ml MNPs: 68.9 ± 4.5 %) complexes displayed a significant difference in viability, proving the gentle and mild transfection conditions.

Moreover, no significant difference in surface marker patterns (CD45, CD34 and CD133) could be observed after 18 h cultivation among all transfection complexes (between 88.8 ± 5.3 % and 91.8 ± 1.6 %) and control cells (87.1 ± 1.7 %). As expected, 0 h control cells displayed with 92.6 ± 1.5 % a homogenous and pure cell population. Likewise, modified cells are considered to be a homogenous and pure cell population, maintaining haematopoietic stem cell characteristics.

4.3.3. Maintenance of haematopoietic differentiation potential of modified CD133$^+$ stem cells

Next, to prove the influence of superparamagnetic polymer-based complexes themselves and cultivation procedures on CD133$^+$ haematopoietic stem cell characteristics, multipotent

differentiation potential was evlaluated using haematopoietic CFU assay (CFU-H). For this purpose, transfected cells as well as untransfected controls were reseeded 18 h after transfection in MethoCult™ H4434 Classic. After an incubation period of 14 days, formed colonies were counted and determined according to a standardized protocol. No significant difference was detected in the amount of formed CFU-erythroid (CFU-E), Burst-forming unit-erythroid (BFU-E), CFU-granulocyte, erythroid, macrophage, megakaryocyte (CFU-GEMM), and CFU-granulocyte, macrophage (CFU-GM), and among all cells under investigation. Moreover, CFUs formed by transfected cells had no morphological abnormalities (Figure 28B-E). Here again, modified cells are considered to maintain haematopoietic stem cell characteristics, indicated by their haematopoietic differentiation potential.

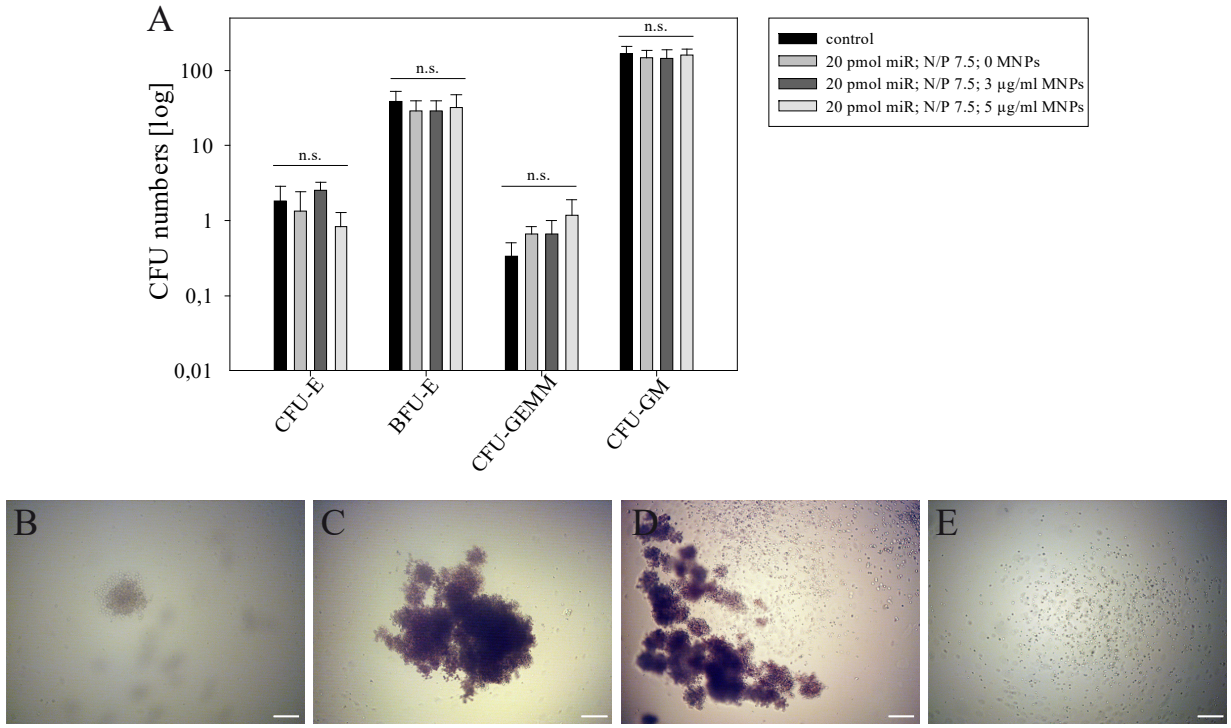

Figure 28: Haematopoietic differentiation potential 18 h after transfection

Evaluation of $CD133^+$ haematopoietic stem cell characteristics 14 d after transfection by CFU-H assay. Transfection complexes consisting of 20 pmol miRNA, N/P ratio 7.5 and three different MNP amounts (0, 3 and 5 µg/ml) were used. (A) Enumerated formed colonies and (B-E) example images representing cell morphologies of (B) CFU-E, (C) BFU-E, (D) CFU-GEMM and (E) CFU-GM. Untransfected cells were used as control. Values are presented as mean ± SEM; n = 3; statistic was performed within respective units; n.s. not significant. Scale bar 200 µm. Adapted from [328]

4.3.4. Magnetic guidance of miR/PEI/MNP-modified CD133$^+$ stem cells

In order to demonstrate the opportunity of cell targeting with modified CD133$^+$ stem cells carrying superparamagnetic nanoparticles, optimized transfection complexes (4.3.1) with Cy3-labeled miRNA were used. Untransfected cells served as control to preclude effects of magnetic MACS CD133 MicroBeads.

For this purpose, CD133$^+$ stem cells were transfected with previously selected miR/PEI/MNP complexes and after 18 h washed and reseeded on a new well plate (Figure 29A). In addition, a magnet was applied locally under the well plate for 24 h. The ratio of targeted to untargeted cells was calculated based on images acquired in the field with and without magnet. It has been shown that control cells displayed almost the same number in both fields, indicating a negligible effect of MACS MicroBeads (Figure 29B). In contrast, cells transfected with any complex composition led to an increased targeting efficiency compared to control. Whereby complexes composed of 20 pmol miRNA, N/P 7.5 (3 µg/ml MNPs: 2.6 ± 0.2 and 5 µg/ml MNPs: 2.2 ± 0.1) exhibited a significantly higher magnetic targeting ratio compared to control (1 ± 0.12) and complexes composed of 20 pmol miRNA, N/P 5 (3 µg/ml MNPs: 1.6 ± 0.1 and 5 µg/ml MNPs: 1.9 ± 0.02).

Therefore, superparamagnetic polymer-based complexes comprising of 20 pmol miRNA, N/P ratio 7.5, with 3 and 5 µg/ml MNPs were selected as most promising for targeting of human CD133$^+$ stem cells in a magnetic field.

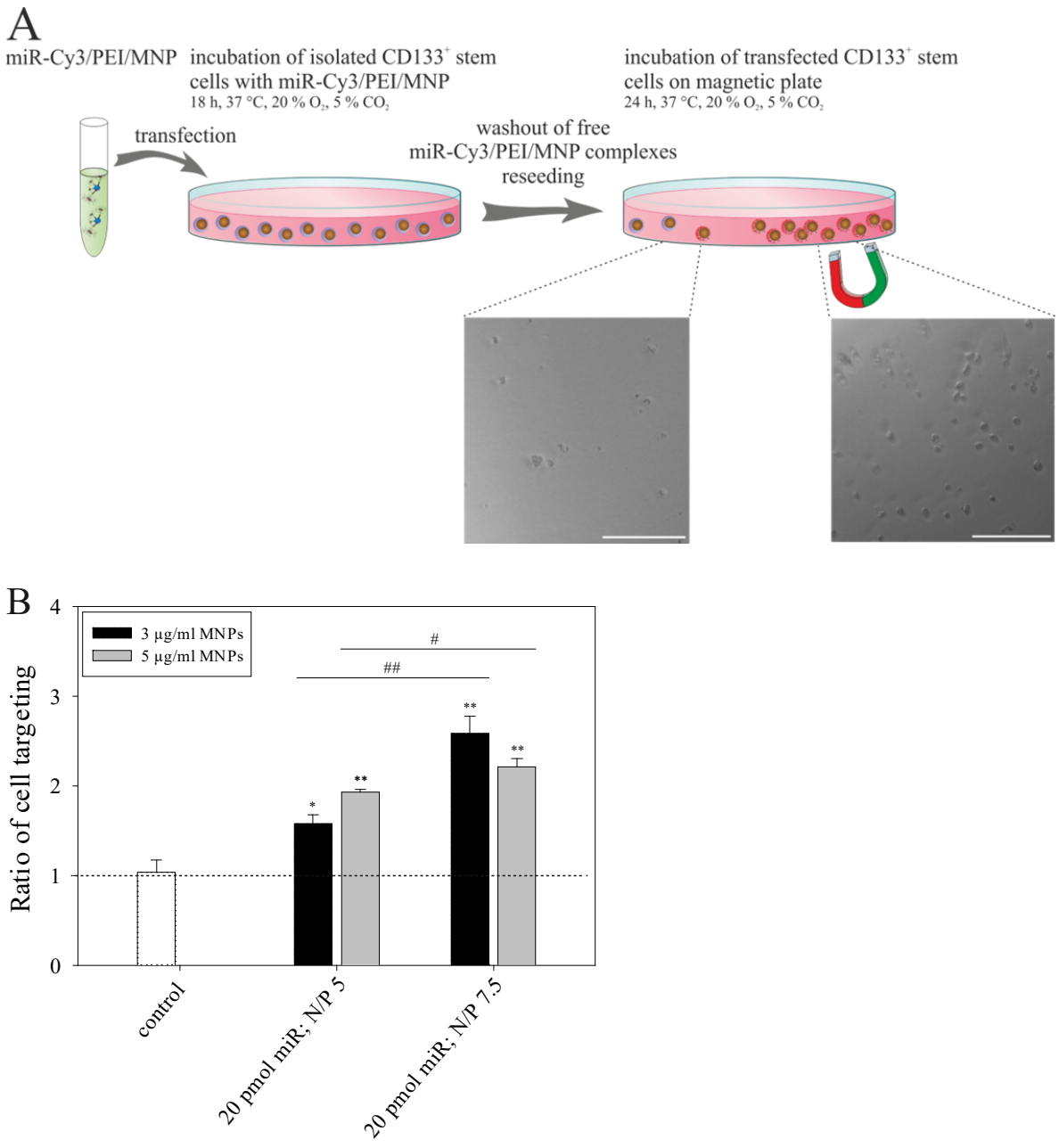

Figure 29: Efficient magnetic guidance of modified CD133$^+$ stem cells

Evaluation of magnetic targeting using magnetic transfection complexes. (A) Experimental setup; transfection complexes consisting of 20 pmol miRNA, two different N/P ratios (5 and 7.5) and MNP amounts (3 and 5 µg/ml) were used. 18 h after transfection, a local magnetic field was applied locally using a magnetic plate for additional 24 h. Images were acquired in the field with and without magnet and subsequently analyzed. Scale bar 100 µm. (B) Enumerated CD133$^+$ stem cells; ratio of cell number present in the field with magnet to cell number present in the field without magnet. Untransfected cells were used as control. Values are presented as mean ± SEM; n = 3; statistic was performed vs. control (indicated as *) or within respective MNP amounts (indicated as #); */#p ≤ 0.05, **/##p ≤ 0.01, ***/###p ≤ 0.001. Adapted from [328]

4.3.5. Intracellular iron concentration

The amount of intracellular iron in CD133$^+$ SCs using 20 pmol miRNA; N/P ratio: 7.5 and 3 µg/ml MNPs was determined using MPS. It has been shown, that 0.155 ± 0.0419 pg iron was uptaken from each cell. The associated A_5/A_3 value of 20.5 ± 3.1 % represents a unique fingerprint, avoiding false positive signals emanating from CD133 magnetic cell isolation MicroBeads (A_5/A_3 value: 27 to 30 %).

4.3.6. Intracellular visualization of superparamagnetic polymer-based complexes

To verify the intracellular distribution of superparamagnetic polymer-based complexes z-stack images were performed using laser scanning confocal microscopy and SIM technology, for which 5 x 10^4 CD133$^+$ SCs were transfected with optimal conditions: 20 pmol miRNA; N/P ratio: 7.5; 3 µg/ml MNPs and either labeled with Cy3 (Figure 30) or, using SIM: Cy5-labeled miRNA was complexed with Oregon Green® 488 labeled PEI and Atto 565 labeled MNPs(Figure 31).

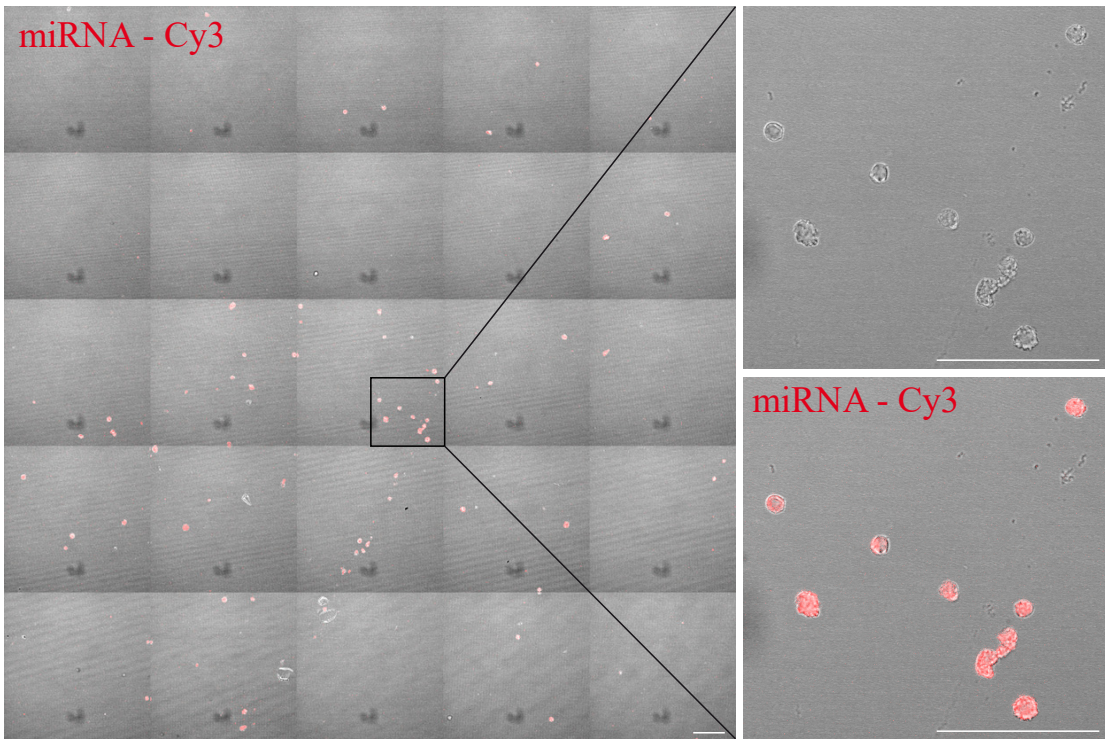

Figure 30: Visualization of CD133$^+$ SC transfected with Cy3 labeled miRNA

Representative visualization of CD133$^+$ SCs transfected with 20 pmol miRNA; N/P ratio: 7.5; 3 µg/ml MNPs 18 h after transfection using laser scanning confocal microscopy. miRNA labeled with Cy3 (red). Scale bar 50 µm. Adapted from [328]

The microscopic analyses confirmed the successful uptake of transfection complexes after 18 h (Figure 30, Figure 31). Furthermore, complexes are predominantly present in the cytoplasm. Whereby all components are localized at the perinuclear region in spatial proximity to each other. It has to take into account, that the observed complexes and nuclei are spatially located on different planes, discovered using z-stack methodology. Formed complexes exhibit a size of approximately 100 - 400 nm.

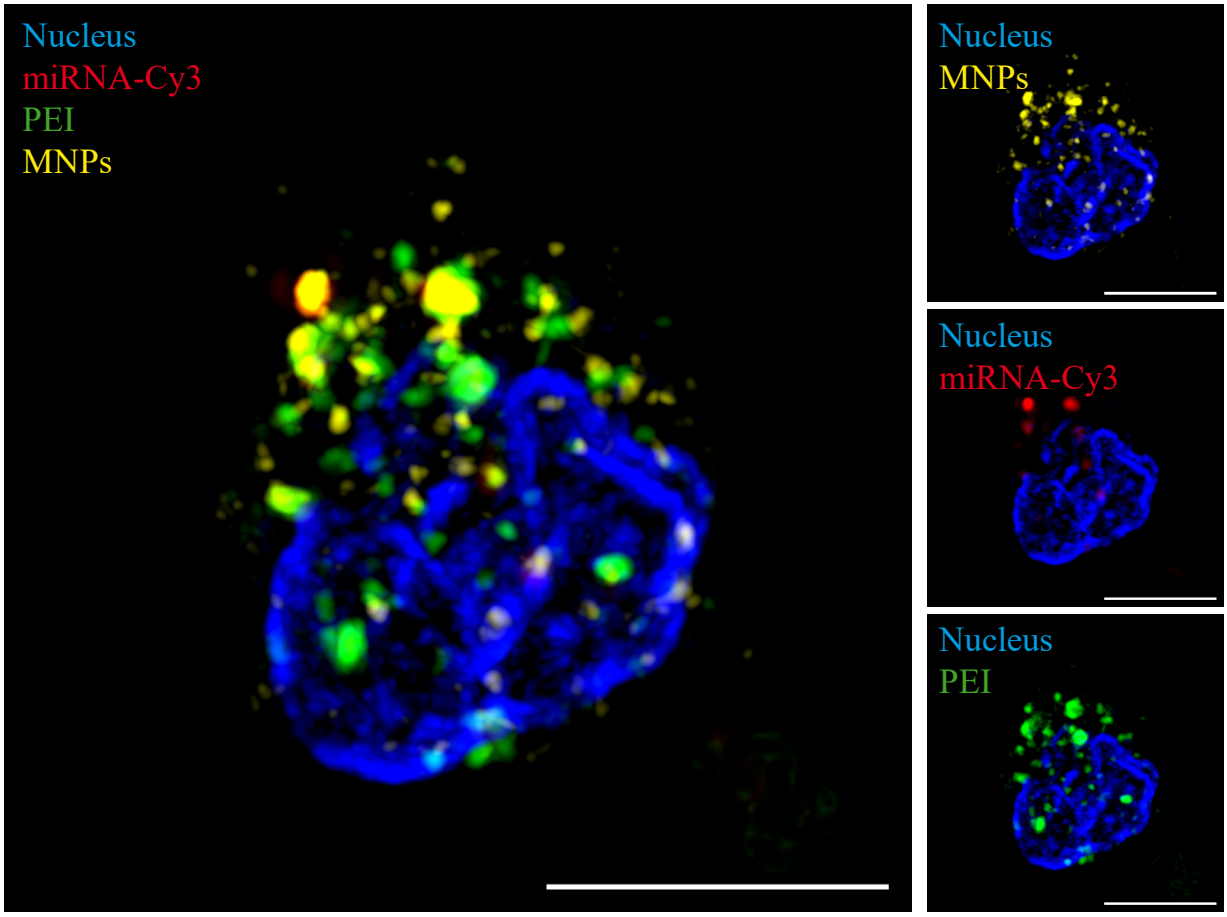

Figure 31: Intracellular visualization of transfection complexes

Representative visualization of CD133^{+} SCs transfected with 20 pmol miRNA; N/P ratio: 7.5; 3 µg/ml MNPs 18 h after transfection using structured illumination microscopy. miRNA staining was performed with Cy5 dye (red), PEI was labeled with Oregon Green 488 (green), MNPs were stained with Atto 565 (yellow) und Nucleus was counterstained with DAPI (blue). Scale bar 5 µm. Adapted from [328]

4.3.7. CD133 cell characteristics and transfection efficiency in cytokine-supplemented culture medium

To improve cell viability of CD133$^+$ SCs in culture, received data obtained from the aforementioned establishment of the miRNA/PEI/MNP transfection system were used in combination with culture medium representing a more clinically relevant scenario.

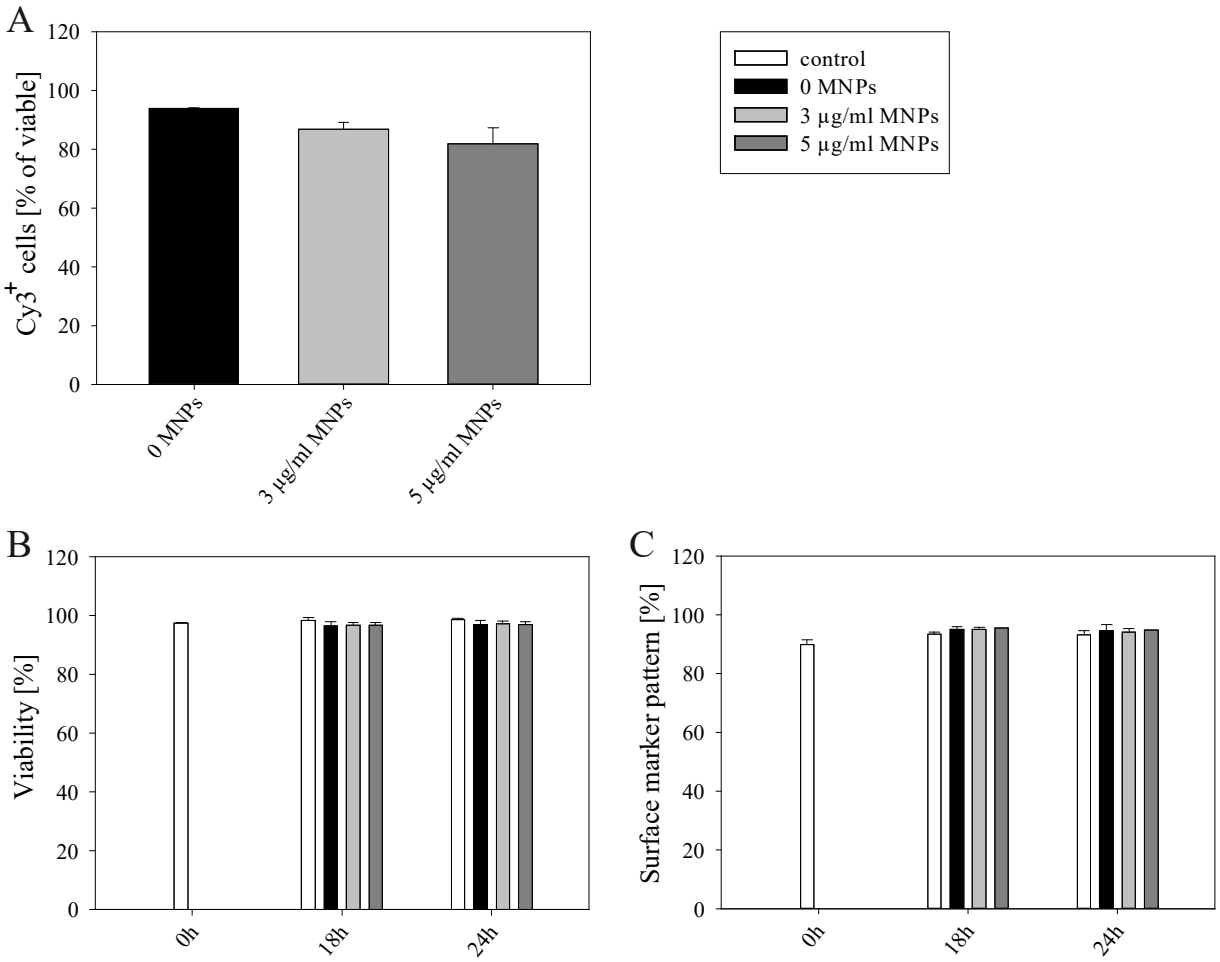

Figure 32: miRNA/PEI/MNP delivery system under cytokine-supplemented culture conditions

Evaluation of miRNA/PEI/MNP transfection of CD133$^+$ SC under cytokine-supplemented culture conditions (StemSpan™ H3000 supplemented with StemSpan™ CC100) by flow cytometry using Cy3-labeled miRNA. (A) uptake efficiency 18 h after transfection. (B) viability and (C) surface marker pattern (composed of the expression of CD45, CD34 and CD133) were measured directly after isolation (0 h) as well as 18 h and 24 h after transfection. Untransfected cells were used as control. Values are presented as mean ± SEM; n = 2. Taken from [328]

Optimal transfection conditions (20 pmol miRNA; N/P ratio: 7.5; 3 and 5 µg/ml MNPs) were finally test in culture medium suitable for haematopoietic stem cells: StemSpan™ supplemented with StemSpan™ CC100. It could be demonstrated that despite the complex medium composition, 87 ± 2 % and 82 ± 5 % of $CD133^+$ SCs had incorporated labeled miRNA (Figure 32A) after 18 h incubation time. Moreover, using StemSpan™ cell viability was unaffected 18 h and 24 h after transfection, in control as well as transfected cells, which highlights the use of StemSpan™ for clinical application and long-time culturing experiments (Figure 32B). Equally to the transfection in DMEM, StemSpan™ caused no changes in the expression of stem cell surface markers (CD45, CD34 and CD133) (Figure 32C).

5. Discussion

Cardiovascular diseases are the leading cause of dead worldwide. However, conventional therapeutic options encounter their limits supplying adequate and comprehensive support for every patient. So far, following an end-stage CVD, in most cases heart transplantations remains the only promising therapeutic option [331]. Currently, merely 604 donor organs were engrafted successfully in Europe in 2015 [332]. Nonetheless, 1140 patients are on the active Eurotransplant waiting list, whereby in 2015 209 recipients deceased before they received the crucial transplant.

Therefore, new innovative therapeutic opportunities must be explored to ensure health and appropriate quality of life. Basic research in the field of developmental biology paves the way for the comprehension of regenerative strategies which requires more detailed understanding of cell fate during cardiac development as well as their possible manipulation.

5.1. mESCs as valid basis for *in-vitro* modelling and manipulation of cardiac development

In order to study key cellular and molecular mechanisms of early heart development, pluripotent cells provide a suitable cell source. Due to the fact that the use of human ESCs is hampered by their limited availability and ethical concerns, research focuses on widely similar murine ESCs [122–124]. Veerman *et al.*, 2015 collected evidence for so far unfeasible complete terminal cardiac differentiation of PSC towards specific cardiomyocytic subtypes *in vitro* [6]. Major efforts should be undertaken to improve purity, yield and safety of physiologically functional PSC-derived CM. In addition, even commercially available PSC-derived cardiomyocytes, such as murine Cor.At or human Cor.4U (both Axiogenesis AG, Germany) display indeed a 100 % pure cardiac population, however, with only a 60 % pure ventricular cell population. Therefore, it is of major interest to identify suitable differentiation methodologies and to begin stepwise optimization of protocols using murine.

For this purpose, an adjusted protocol was established based on forward programming of murine ESCs with the cardiomyocyte key transcription factor Nkx2.5, which could be shown to have an impact on specific cardiac differentiation[144, 151, 333] combined with an αMHC-promotor-based antibiotic selection step [155] for further purification resulting in a pure αMHC^{+} cell population.

5.1.1. Manipulation of mESCs

Forced exogenous overexpression of the lineage specific TF Nkx2.5 has been achieved by introduction of either DNA (4.1.1.1) as stated before from David *et al.* [151] and Dorn *et al.* [144] or mRNA (4.2.4), thus defining a new strategy.

The subsequent discussion section refers to the manipulation of mESCs with plasmid DNA pEF-DEST51-hNkx2.5; the use of modified mRNA will be discussed in 5.2.

The relative expression analysis of hNkx2.5 obtained by qPCR (Figure 5A) has led to a selection of three different clones (W4 αMHC #15 hNkx2.5 #D, #F and #L) demonstrating different expression levels of hNkx2.5 expression to verify the impact on further cardiac differentiation as was demonstrated by Jung *et al.* using Tbx3 as pacemaker specific TF [154].W4 αMHC #15 and W4 αMHC #15 hNkx2.5 #L were used for publication.

The expression on the mRNA level was confirmed with data achieved by immunohistochemical investigation (Figure 5B). These indications point to a relatively high expression of exogenous hNkx2.5 in W4 αMHC #15 hNkx2.5 #F and #L and a moderate expression in W4 αMHC #15 hNkx2.5 #D as well as a lack of any hNkx2.5 expression in the control cells.

In order to maintain the pluripotency of murine ESCs and assure an equal starting point, used cells were continuously cultured with leukemia inhibitory factor (LIF) [133, 134] and prior to differentiation additionally co-cultured with the mitotically inactivated murine embryonic fibroblast-derived cell line SNL 76/7 [138]. However, only the combination with a SNL feeder co-culture lead to compact cell clusters of the same size, without starting differentiation fringes at the periphery of colonies (Figure 4). All clones display a normal morphology with a high nucleus:cytoplasm ratio. Furthermore, all clones exhibit another key prerequisite of the pluripotent state, the stable expression of pluripotency markers Oct4 and Nanog as stated by Niwa *et al.* [334], as no significant difference appeared among the three clones tested and the control on the mRNA level, despite the exogenous expression of hNkx2.5 (Figure 6A). In accord with mRNA expression, mOct4 is less strongly expressed in the control cells and equal among the three clones, however without any effect on pluripotent cell behavior. No significant differences could be observed in early cardiac marker expression of mIsl1 and mMesP1. The data are accompanied by large standard deviations owing to experimental circumstances. Nevertheless, W4 αMHC #15 hNkx2.5 #L presents a tendency of decreased mIsl1 expression

which could go along with *in vivo* observation during FHF progenitor differentiation, representing Nkx2.5 as direct responsible mediator of Isl1 repression [144]. However, it is unclear why W4 αMHC #15 hNkx2.5 #F with a comparable Nkx2.5 mRNA expression exhibit different marker expression of mIsl1 and mMesP1. A co-cultivation of mouse embryonic fibroblasts (MEFs) could better maintain the stemness of ESCs, as stated by Park *et al.* [138] compared to a feeder cell line; thus reducing marker expression variants.

Thus selected and characterized clones were used for further specific ventricular subtype differentiation. W4 αMHC #15 as well as unaltered W4 cells were used as references.

Murine ES cells are most likely able to differentiate toward a cardiac phenotype using a specific cardiac differentiation protocol including EB formation and special medium, containing among others ascorbic acid [149]. This process leads also with the used W4 ES cell line to a spontaneous beating activity of formed EBs in suspension and later on as adherent cells. However, in contrast to the work of Jung *et al.* [154], using Tbx3 as specific pacemaker lineage inducer, different Nkx2.5 mRNA expression levels had no impact on the amount of beating areas, even without any significant difference to the control clones (Figure 7).

In order to increase the purity of separated cells arising, an antibiotic selection step was inserted in the protocol using puromycin under the control of Mhy6 promotor [153, 155, 335–337] to achieve a pure αMHC^{+} cell population. As opposed to Jung *et al*. [153], initially, the optimal time was evaluated to achieve the best recovery (Figure 8). It could be demonstrated that an early puromycin treatment yielded a higher single cell amount on day 25 of differentiation, either under 1 % or 20 % oxygen conditions. It is noticeable, that both clones with a high Nkx2.5 mRNA and protein expression level revealed the highest cell amounts, demonstrating an enhanced may also sooner cardiomyocytic differentiation outlined by a more rapid αMHC expression. The genetic selection resulted in a 9.77-fold higher amount of CM-like cells compared to control clones, demonstrating the positive effect of Nkx2.5 expression toward a myocardial phenotype.

5.1.2. Nkx2.5 as crucial factor for cardiomyocyte differentiation of mESCs

All clones presented single cells with differently shaped morphology. So far, no single cell morphological classification is currently discussed in the literature. Therefore, inspired from single cell characterization of pacemaker cells [153], cell morphologies were classified as spindle and spider cells [153], large round and large square cells which are not described after pacemaker

cell differentiation and an undefined cell population including large longitudinal and small round cells (Figure 4, Figure 33). The newly classified cell type is defined by flat round or squared shape, with or in most of cases without extensions and a cell size approximately 83 x 116 µm, which presents the largest cell population under investigation. It has been demonstrated, that already the specific cardiac differentiation protocol performed with the W4 α-MHC control clone give rise to all possible cell shapes in an equal ratio to Nkx2.5 overexpressing clones. Nonetheless, single cells of Nkx2.5 overexpressing clones are in comparison to control cells larger, this is especially due to the fact that obtained square cells appear larger.

The generated single cells of all tested clones as well as control cells indicate a partially organized sarcomeric structure in longitudinal myofibrils (Figure 9, Figure 10, Figure 11, Figure 12) as well as gene expression of structural proteins, demonstrated for one clone (W4 αMHC #15 hNkx2.5 #L compared to control cells; Figure 16). They demonstrate both intertwining filament structures, the thin actin filament (Figure 10) as well as two isoforms of thick myosin filaments (Figure 9 and Figure 10).

Nonetheless, mere W4 αMHC #15 hNkx2.5 #F and #L display distinct striped expression of α-myosin as well as β-myosin in co-localization with actin. The distribution of the ventricular myosin isoforms is temporally regulated during development. Whereas αMHC is predominantly expressed in adult hearts and βMHC abundant in late fetal development in small species such as mouse and rat [338, 339], the distribution is reversed in large mammals (rabbits and pigs): αMHC is only transiently predominantly expressed neonatal and βMHC returned after three weeks and is most abundant in adult hearts [340]. Furthermore, adult dogs, cattles and humans express only βMHC isoform [340]. Since both isoforms are present in iCM-like cells of high Nkx2.5 expressing clones the assumption exists, that this cells are immature and still in a late embryonic stage. It is noteworthy that not all cells exhibit the βMHC isoform (estimation: 10 %) and it was not possible to detect any signal of βMHC expression in control cells, whereby αMHC could be detected in all cells. Thus, it could be possible, that cells of Nkx2.5 expressing clones at day 25 of differentiation are stated in a more immature ventricular developmental stage.

The linking troponin complex is delineated through staining of the complex compound cTnT (Figure 12). Additionally, mRNA analysis reveal a slightly higher cTnT expression in W4 αMHC #15 hNkx2.5 #L compared to control cells, vicariously for overexpressing clones (Figure 16).

Troponin T binds the complex to tropomyosin, which entwine the actin filament. An incoming Ca^{2+} signal is recorded through binding on complex compound cTnC, thereafter, tropomyosin frees the binding site of myosin at the actin filament. α- and βMHC isoforms have a varying impact on actin filament activation through cTnT [341], which also lead to a different calcium sensitivity and heart rates. Moreover, αMHC confers a high Ca^{2+}-ATPase activity, whereby β-MHC confers a low Ca^{2+}-ATPase activity [338, 342]. These combined causes engender cells with fast cycling αMHC isoforms [339] which have fast heart rates (650 – 800 bpm, [343]) and slow cycling βMHC isoforms [339] which have slow heart rates (60 – 120 bpm, [343]). However, a significant difference of beating frequencies could not be determined among the clones (Figure 13A). Yet, subdivision into morphologically different populations revealed a significant difference (Figure 13B), whereby large square and large round cells are the slowest population which goes along with the observation of βMHC expression detected in this cells (Figure 10).

The actin filaments are attached through the z-disc via the microfilament protein alpha-actinin, which partly revealed a well-organized structure (Figure 11) and are comparable to data from David *et al.* [151].

An intracellular communication between neighboring cells during embryonic development as well as in embryonic and adult tissues and organs is mainly mediated through gap junctions [344, 345]. These specialized cell-cell junctions enable the direct transfer of ions, metabolites, second messengers and molecules, less than 1 kDa [346–349]. The transmission of positive ions results in slight voltage changes which depolarize the proximal sodium voltage-dependent channels, thus initiating action potential. The absence of gap junctions would therefore cause several cardiac disorders. As shown in Figure 9 and Figure 12, if cells be located in close proximity to each other, gap junctions are formed in existing gaps, stained through gap junction component connexin 43. The impact of Nkx2.5 as homeodomain-containing TF on Cx43 is under controversial discussion. Homeobox proteins act in the promotor region thereby directly regulating target genes. Nkx2.5 probably have binding sites in the proximal promotor P1 of the rat Cx43 genes [345]. However, gain- and loss-of-function experiments indicate an activative [350, 351] as well as repressive [352, 353] impact on Cx43 occurrence. Nevertheless, additional analysis of Cx43 on mRNA level displayed no difference between the control and Nkx2.5 overexpressing clone W4 αMHC #15 hNkx2.5 #L (Figure 16).

Liang and co-works demonstrated, that HCN4 is a marker of early FHF progenitor cells and specifically expressed in late cardiac conduction system [74], which was confirmed in *in vitro* experiments by Jung *et al.* in ESC forward programming using Tbx3 overexpression [153]. Data obtained by qPCR analysis underlines the use of Nkx2.5 for ventricular specific differentiation demonstrating a significant decrease of HCN4 mRNA expression in W4 αMHC #15 hNkx2.5 #L cells compared to only αMHC selected cells (Figure 16). Moreover, these corroborate previous research using Nkx2.5 overexpression by David *et al.* [151].

Not merely beating frequencies revealed a heterogeneous population (Figure 13) likewise pharmacological substance administration evinced a discordant and immature behavior of CM-like single cells (Figure 15). Even distribution of ion channels is necessary to ensure a transient change in ion conductance across the cell surface membrane. Therefore, the occurrence of ion channels involved in the generation of action potential was determined using excitatory (Noradrenaline) as well as inhibitory (Acetylcholine, Tetrodotoxin, potassium rich extracellular fluid, Mibefradil, Verapamil) substances (Figure 15).

A sympathetic stimulation of β-adrenergic receptors through noradrenaline mediate a positive chronotropic effect, which result in a shortened depolarization phase and became obvious in W4 αMHC #15 hNkx2.5 #F and control cells as a significant increase of the beating frequency. In literature reports it is described that the stimulation results in an increased Ca^{2+} influx through L-type calcium channels, which in turn increases the Ca^{2+} release from ryanodine receptors located in the sarcoplasmic reticulum [354, 355]. The documented response provides a first indication for partially functional cells.

Additionally, only cells of W4 αMHC #15 hNkx2.5 #F and #L responded significantly to acetylcholine; which has impact on the ligand-dependent muscarinic acetylcholine receptor type M2. The G protein activated inwardly rectifying K^{+}-channels (Kir3.x) are most abundant in the atria as well as sinoatrial- and atrioventricular nodes, where they are involved in vagal regulation of the heart rate [356, 357]. The activation through acetylcholine increases the potassium conductance, which leads to potassium efflux and is followed by a hyperpolarization of the cell membrane. This hampers the excitability of cells and leads to reduced action potential frequency, which transiently became obvious in W4 αMHC #15 hNkx2.5 #F and #L beating frequencies.

The most important current, depolarizing the cell surface from appr. -85 mV to appr. +25 mV within 10th of milliseconds, is mediated through sodium channels [358–360]. Among them, the neuronal voltage-gated sodium channels possess a high sensitivity to tetrodotoxin [361], opposed to the primary TTX-resistant cardiac $Na_v1.5$ isoform, and makes up to 15 % of the total sodium current of isolated rat ventricular cells [362]. Recent studies have proven the presence in murine sinoatrial nodal cells as well as myocardium [363–367] and support the appearance in close proximity to the transverse tubulus thereby coupling depolarization of the cell surface membrane (electrical excitation) to contraction of the myocardium [366, 368] due to regulation of Ca^{2+} release from sarcoplasmic reticulum [369]. In contrast to literature data, a concentration of 10 µM does not lead to an inhibition of both, TTX-sensitive (1 - 100 nM) and TTX-resistant (2 - 6 µM) sodium channel isoforms, only a slight reduction of beating frequencies could be observed. This may indicate a major presence of strongly TTX-resistant cells in immature iCM like cells as well as in neonatal CM, whereas cells with a total reduction of beating frequency are merely rare. However, like K^+, TTX could also be complexed and thereby masked.

An analysis of potassium in form of potassium rich extracellular fluid with a concentration of 20 mM was unsuitable due to the high buffer capacity of the used differentiation medium. Chelating agents like ascorbic acid or glucose complexate the metal ions K^+. Preliminary data suggest complete cessation of beating activities with higher concentrations (data not shown). An appropriate medium for *in-vitro* testing would be a physiological solution of NaCl. A highly concentrated potassium solution is used to induce a cardioplegic cardiac arrest to perform, e.g. a bypass surgery.

Voltage-dependent Ca^{2+}-channels are responsible for Ca^{2+} influx due to depolarization of the cell membrane mediated by sodium, thereby determining excitation and contraction. The high voltage-activated long-lasting L-type Ca^{2+}-channel is abundant and ubiquitously expressed at the whole heart [370]. The resulting calcium current, together with sodium and potassium, is responsible for the long action potential plateau phase and pass as a chemical signal of intercellular Ca^{2+} release of the sarcoplasmic reticulum [371]. One type of Ca^{2+}-channel antagonists are phenylalkylamines, e.g. verapamil, which inhibits L-type as well as T-type Ca^{2+}-channels [372]; which then results in a stoppage of beating frequencies in W4 αMHC #15 hNkx2.5 #L and neonatal CM. However, all other cell clones display only a minor response. In contrast, the low-voltage-activated transient T-type Ca^{2+}-channel opens at a low membrane

potentials and inactivate rapidly, triggering the action potential originated by the sinus node [373]. During embryonic development T-type Ca^{2+}-channel are functionally expressed, but disappear after birth and are predominantly expressed in sinoatrial nodal cells in the adult heart [374]. Mibefradil is more selective and preferentially blocks T-type Ca^{2+}-channel by a factor of 10 to 15 [375, 376]. The presence could be confirmed with its minor effect on the immature iCM-like cells, represented in all clones. An explanation for the stronger response of the control cells to the Mibefradil application may be the lack of the specific Nkx2.5 ventricular differentiation force.

It would be of great interest to transfer the achieved physiological results to patch clamp subtype distinction shown by several groups for electrophysiologically functional cardiomyocytes [144, 151, 153]. Through this, precise classification of obtained single cells in ventricular-, atrial- and nodal-like as well as intermediate cells would be possible.

The data indicate an immature cardiomyocyte phenotype with cells being situated in a late embryonic stage with ventricular-like characteristics. Nevertheless, some issues such as the heterogeneity within one clone as well as the wide variation emerging from different Nkx2.5 expression profiles in the ESC initial state remain serious reasons for concern and further improvement. On this account, it should be stated that one transcription factor alone appears insufficient to generate a homogenous population of fully functional mature ventricular cardiomyocytes using murine ESCs as starting material. These findings validate previous results and debates of so far inefficient cardiac differentiation of PSCs *in vitro* [6]. However, the forced exogenous overexpression of the Nkx2.5 TF combined with a Myh6-antibiotic-selection step resulted in a population of αMHC^{+} spontaneously beating CM-like cells with typical sarcomere structural proteins and essential electrophysiological properties.

5.2. Modified mRNA as a reliable tool for cell fate alteration

So far, various opportunities of mRNA in respect to their universal applicability still lay dormant. Despite technological progress many unanswered issues need to be clarified before it becomes possible to widely exploit the scientific knowledge.

5.2.1. Generation of highly reproducible modified mRNA

In order to generate highly reproducible mmRNA, a PCR-based protocol was established and verified with EGFP protein expression in several cell types, including fibroblasts and hMSCs

(4.2), which was published in *Cellular Physiology and Biochemistry*, 2015 [276]. During the data collection, one article was published which describes several transfection reagents and transfection conditions for an efficient translation [377, 378], which confirmed the usage of Lipofectamine 2000 in the present thesis. However, direct comparison of different modification compositions with respect to their translation efficiency and cell viability for long term cultivation in several cell types has not been studied before [276]. Later the same year, Andries *et al.* demonstrated another promising pseudouridine modification (N1-methylpseudouridine (m1Ψ)) [379] using the classical modifications, they present the same results and confirm the finding that optimal modification composition differs between cell types.

These positive modulations comprising i) a 5` cap analog, ii) a 3` poly A tail and iii) modified nucleosides became apparent in the present data. Previous studies were limited by the instability and low efficiency of utilized mRNA, which is no longer an obstacle. Through the use of mimicking properties, fast protein expression of EGFP with a peak between 12 h and 24 h after transfection and high durability for more than 72 h is documented in every cell type under investigation even for nucleoside-unmodified mRNA (Figure 18, Figure 19, Figure 20, Figure 21). Further improvements can be achieved with the incorporation or complete replacement of both pyrimidines (cytidine and uridine) with 5mC and Ψ. It has become evident, that the ratio of replacement should be tested for the desired cell type and purpose considering the different protein expression and viability results received. Any nucleoside modification led to higher translation efficiency and increased viability. Nevertheless, as Karikó and colleagues had reported [272], incorporation of Ψ led almost always to the best translation capacity indicated by $EGFP^+$ cells and mean fluorescence intensities which were often significantly higher than unmodified mRNA. However, the replacement of both pyrimidines resulted in good, partly significant higher protein translation but most importantly, to the best cell viability during long term cultivation, as stated by several groups [162, 165].

For this reason, 100 % 5mC + 100 % Ψ was selected as the most promising modification demonstrating the applicability of this non-viral DNA-free delivery technology.

5.2.2. Modified mRNA as a tool for cell fate conversion

As previously shown, mRNA is a potential tool for cell reprogramming strategies [162–166]. In order to prove the capability of self-synthesized mRNA apart from EGFP protein translation, an attempt based on the finding of Weintraub and colleagues was accomplished [214]. Murine fibroblasts were transdifferentiated towards a myoblast-like phenotype using mMyoD mRNA (Figure 22A). The obtained cells exhibit coarsely striped myosin heavy chain expression (Figure 22B), which is part of the contraction system [380], thereby demonstrating the effectiveness and ability of mmRNA to directly alter cell fate identity. These data were confirmed by Preskey *et al.* adapting the protocol for presenting multi-nucleic myotube-like cells [164].

Next, the opportunity to forward program murine ESCs was examined using the mNkx2.5 mRNA base. To date, no efficient method for the generation of fully mature ventricular cells is established; hence, a rethinking should take place. To overcome this obstacle, a spatiotemporally elusive stimulus could correspond to the endogenous embryonic development. Stringent molecular regulations in the developing organism engender specific progenitor cell fate behavior, consequently generating specialized somatic cells. The imitation of an early requirement of Nkx2.5 [81] could be achieved with a pulse-like exogenous overexpression of the TF. As opposed to DNA, mRNA demonstrated fast protein translation already 4 h after transfection and a peak between 12 h and 24 h with a time dependent decrease (4.2). Moreover, Chien and colleagues have shown that the application of VEGF-A displayed an increased efficacy by pulse-like delivery of mRNA in direct *in vivo* comparison with DNA [287].

Therefore, beforehand analyzed potential of Nkx2.5 (4.1 and 5.1) could be improved by applying the cardiac specific TF as mRNA. Comparatively, mRNA induced pluripotent stem cell reprogramming is even more efficient then DNA introduction [162].

Single cells obtained after triple transfection with mNkx2.5 and the subsequent cardiac differentiation appeared similar to that of DNA programmed iCM-like cells (Figure 4, Figure 23), whereas mRNA Nkx2.5 induced cells appear larger and more complex. Moreover, cells displayed spontaneous albeit heterogeneous beating activity, and an active calcium oscillation, which indicates functional iCM-like cells after modulation of mESCs with modified Nkx2.5 mRNA. Therefore, modified mRNA is a suitable tool to replace DNA modification to avoid circumstances accompanied with DNA insertion [276].

5.3. miRNA/PEI/MNP as a promising transfection system for slowly proliferating stem cells

Besides the development of new strategies mentioned above, already existing protocols regarding functional heart improvement after injury have been modified. For this purpose possible manipulations of bone-marrow derived $CD133^+$ SCs were examined. Their potential has been confirmed in several clinical trials (phase I and II) in recent years [381–393], however, substantial improvements are only imaginable if it is possible to overcome major obstacle arising by low retention in the area of interest and massive initial cell death [189–191]. These prominin-1 (highly conserved transmembrane antigen) expressing stem- and progenitor cells give rise to cells of the haematopoietic, endothelial and myogenic lineages and their derivatives [394–399]. Of particular interest is the promising muscle regeneration after skeletal muscle injury, demonstrated by several groups [400–404]. In contemplation of a successful transfer to cardiomyogenic regeneration, a promising approach based on precise manipulation of $CD133^+$ SCs could open up new opportunities.

To achieve this aim, a safe and gentle modification technology is still required [405]. To date, $CD133^+$ SCs rated as hard to manipulate cells, which is partly due to their sensitivity and their low proliferation potential, hampering the application of DNA. For this reason, miRNAs became an attractive alternative, supported by their operating area in the cytoplasm as well as their wide range as posttranscriptional regulators [406].

Therefore, a non-viral magnet-bead based polymer delivery system was established to propose a new manipulative treatment of $CD133^+$ SC in regenerative medicine [327, 328, 407–409]. PEI is an efficient delivery reagent, as it protects miRNA against degradation and supports cellular uptake and intracellular release [410, 411]. Moreover, PEI condenses miRNA through electrostatic interactions. The results have been equally compiled by N. Voronina, P. Müller and F. Hausburg.

5.3.1. miRNA/PEI/MNP as efficient delivery system for $CD133^+$ SC

To ensure an efficient transfection of miRNA into freshly isolated $CD133^+$ SCs, uptake efficiencies using Cy3-labeleld miRNA were evaluated. Hereafter, miRNA/PEI/MNP complexes consisting of 20 pmol miRNA, N/P ratio 5 and 7.5, with 3 and 5 µg/ml MNPs were selected as most promising for human $CD133^+$ stem cells with regard to their highest uptake efficiency combined with a low cytotoxicity. Efficient uptake using human MSCs could be achieved using a

lower amount of miRNA as well as PEI (10 pmol miRNA, N/P ratio 2.5), however with a lower overall efficiency of ~77 % [409]. In contrast, an efficient miRNA uptake using endothelial cells (HUVECs) could be reached with 5 pmol miRNA and an N/P ratio of 25 [327]. Additional application of MNPs causes a slight but not significant worsening, similar in $CD133^+$ SCs [328], hMSCs [409] as well as HUVECs [327]. This indicates the need for an individual optimization for the desired cell type considering the best miRNA uptake and a high viability.

The intracellular distribution of incorporated miRNA was visualized using laser scanning confocal microscopy and, for detailed images, SIM technology. The analyses confirmed the successful uptake of superparamagnetic polymer-based complexes 18 h after transfection (Figure 30, Figure 31). Complex components are predominantly present in the cytoplasm and localized at the perinuclear region in spatial proximity to each other.

As opposed to Ochi and colleagues [401, 412], cell targeting of freshly isolated $CD133^+$ SCs was insufficient, *in vitro* targeting experiments exhibit no effect of MACS CD133 MicroBeads alone (Figure 29). In contrast, an intracellular amount of 0.155 pg ± 0.0419 iron per cell demonstrated an efficient guidance 2.6-fold higher than untransfected cells (using 20 pmol miRNA; N/P ratio: 7.5 and 3 µg/ml MNP). The outcome consists in different field strengths (~3 T [401, 412] compared to 0.25 T [328]) generated through a portable superconducting bulk magnet system and to a neodymium permanent magnet. Efficient guidance and transfection depends on strength of the field source as well as its range and proximity relative to the target cells [413]. Furthermore, comparative studies demonstrate an improved transfection efficiency using an oscillating field compared to a static field [414]. However, uptake efficiency data obtained from $CD133^+$ SCs were generated without a direct application of a magnetic field [328]; thus it was no significant effect shown using magnet during transfection with MSCs [409]. The intracellular amount resemble the amount (0.37 pg iron per cell) which was shown to be sufficient for MRI detection using endothelial cells [327]. Hence, with the present approach an efficient uptake of miRNA and successful magnetic guidance of stem cells was achieved which can be used in future to improve cardiac regeneration.

5.3.2. miRNA/PEI/MNP transfection does not influence haematopoetic cell characteristics of $CD133^+$ SC

In order to prove the influence of superparamagnetic polymer-based transfection complexes and *in vitro* cultivation of $CD133^+$ stem cells, surface marker pattern, viability and multipotent

differentiation potential were evaluated. It could be demonstrated that the transfection procedure has no impact on $CD133^+$ stem cell characteristics, neither surface marker pattern (Figure 27) nor haematopoietic differentiation potential (Figure 28), which indicates a gentle and safe modification technology for $CD133^+$ SC. However, DMEM based transfection medium led to a significant decrease of $CD133^+$ cell viability after 18 h under standard culture conditions (Figure 27). Therefore, transfection procedures were performed using StemSpan™ supplemented with StemSpan™ CC100, which revealed no differences in cell viability, at the same time with high uptake efficiency comparable to DMEM (Figure 32). The observation confirmed previous data, which indicates a major role of cytokines, like SCF and Flt3L with IL-11 or Tpo for haematopoietic SC expansion [415, 416]. However, other studies stated underwhelming results for *ex vivo* stem cell expansion using only cytokine assistance, self-renewal and optimal HSC expansion requires a combination of several small molecules, cytokines, growth as well as transcription factors [276, 415].

6. Conclusions

This thesis aimed to overcome current hurdles in the field of cardiovascular regenerative medicine. Virus independent manipulations of various stem cell types, including adult and embryonic stem cells as well as of somatic fibroblasts were established to enable optimized cell programming.

In particular, data obtained from forced exogenous overexpression experiments with murine ESCs confirmed previous findings which showed that Nkx2.5 plays a crucial role during ventricular phenotype differentiation [144, 151, 417]. However, *in vivo* knock-down approaches suggest Nkx2.5 as essential cardiac TF in first and second heart field development [81, 333], which demonstrates the multifaceted spatiotemporally controlled mechanism of a variety of factors necessary to form a functional heart. It is therefore not surprising that one TF alone, in the present case Nkx2.5, is not sufficient to generate mature and fully functional ventricular cardiomyocyte subtypes. However, the addition of the Myh6-promotor-based antibiotic selection step [155] enhanced previous cardiac differentiation protocols [151] and gave rise to a cell population which possess typical sarcomere markers as well as they respond partially to crucial ion channel modulators. To improve aforementioned strategies, some modifications should be considered, such as changes in the maintaining of ESCs: One option may be to switch from STO to MEF co-culture [138] and another the optimization of the medium composition adjusted to the temporal requirements mimicking the endogenous developmental microenvironment.

New strategies with regard to the intrinsic spatiotemporal regulatory mechanisms should be based on more flexible modulation systems. Different variations of RNA, mRNA and miRNA molecules are suitable for pulse-like and comprehensive regulation of cell fate for numerous cell types. In addition, both lipid- and polymer-based delivery systems are benign and bear little risk of systemic alterations.

Initially presented experiments using modified TFs indicate an effective, but not yet fully refined technology to alter cell fate from murine fibroblasts with MyoD and cardiomyocyte-like phenotype originated from ESCs with Nkx2.5 to skeletal myoblasts. As was also shown in previous studies, a standardization of mmRNA production should be a key aspect in order to use GMP relevant mRNA in clinical scenarios [285, 286]. An important step in this direction was the

establishment of a highly reproducible PCR-based protocol to generate mmRNA in this dissertation [276]. However, a stringent purification procedure using HPLC should be performed in the future to eliminate short double stranded RNA as stated by Karikó *et al.* [284].

An efficient and mild transfection system was established for the hard to transfect and sensitive human $CD133^+$ SCs. Using the non-viral superparamagnetic polymer-based delivery system, miRNA could efficiently transferred into the cytoplasm of these slowly proliferating SCs. Furthermore, *in vitro* experiments demonstrated a huge advantage applying a magnetic field. The possibility of specific cell targeting may improve the so far marginal improvement of LVEF after autologous cell transplantation of $CD133^+$ SCs together with CABG surgery (~6 % after 6 months) [381]. The massive wash out of SCs during the first hour led to a retention of ~ 5 – 8 % of SCs in the heart evaluated in a mouse model and patient study, demonstrating a huge biodistribution into the lung and liver [418, 419]. Applying our innovative systems may offer the opportunity to improve the cardiovascular regeneration potential of SC transplantations. It also creates new options using miRNA to enhance cardiac reprogramming due to their wide posttranscriptional impact [292].

Overall, the presented strategies provide high potential for regenerative medicine and addresses hurdles towards a bench-to bedside translation for current *in vitro* models.

7. Danksagung

Mein Dank gilt all jenen die mich Toleranz, Offenheit und Neugier lehrten.

8. Selbstständigkeitserklärung

Ich versichere, die vorliegende Arbeit zum Thema „Optimisation of Stem Cell based Approaches towards cardiac Regeneration“ selbstständig verfasst und keine anderen Hilfsmittel, als die angegebenen benutzt zu haben. Stellen, die anderen Werken dem Wortlaut oder dem Sinn nach entnommen sind, habe ich in jedem einzelnen Fall durch Angabe der Quelle kenntlich gemacht.
Ich erkläre, meine wissenschaftliche Arbeit nach den Prinzipien der guten wissenschaftlichen Praxis gemäß der gültigen „Satzung der Universität Rostock zur Sicherung guter wissenschaftlicher Praxis“ angefertigt zu haben.

Ettringen, 11. Januar 2019

9. Appendix

I. References

1. **Bergmann O, Bhardwaj RD, Bernard S, Zdunek S, Barnabe-Heider F, Walsh S*, et al.*** Evidence for Cardiomyocyte Renewal in Humans. *Science*. 2009; 324: 98–102.
2. **Mollova M, Bersell K, Walsh S, Savla J, Das LT, Park S-Y*, et al.*** Cardiomyocyte proliferation contributes to heart growth in young humans. *Proceedings of the National Academy of Sciences of the United States of America*. 2013; 110: 1446–51.
3. **Jain A, Bansal R**. Applications of regenerative medicine in organ transplantation. *Journal of pharmacy & bioallied sciences*. 2015; 7: 188–94.
4. **Heidary Rouchi A, Mahdavi-Mazdeh M**. Regenerative Medicine in Organ and Tissue Transplantation: Shortly and Practically Achievable? *International journal of organ transplantation medicine*. 2015; 6: 93–98.
5. **Orlando G, Soker S, Stratta RJ, Atala A**. Will regenerative medicine replace transplantation? *Cold Spring Harbor perspectives in medicine*. 2013; 3.
6. **Veerman CC, Kosmidis G, Mummery CL, Casini S, Verkerk AO, Bellin M**. Immaturity of human stem-cell-derived cardiomyocytes in culture: fatal flaw or soluble problem? *Stem cells and development*. 2015; 24: 1035–52.
7. **Laflamme MA, Murry CE**. Heart regeneration. *Nature*. 2011; 473: 326–35.
8. **Bhatia SK**. Biomaterials for Clinical Applications. 2010.
9. **Whelan RS, Kaplinskiy V, Kitsis RN**. Cell death in the pathogenesis of heart disease: mechanisms and significance. *Annual review of physiology*. 2010; 72: 19–44.
10. **Anversa P, Kajstura J**. Myocyte Cell Death in the Diseased Heart. *Circulation research*. 1998; 82: 1231–33.
11. **Gottlieb RA, Burleson KO, Kloner RA, Babior BM, Engler RL**. Reperfusion injury induces apoptosis in rabbit cardiomyocytes. *The Journal of clinical investigation*. 1994; 94: 1621–28.
12. **Baines CP, Kaiser RA, Purcell NH, Blair NS, Osinska H, Hambleton MA*, et al.*** Loss of cyclophilin D reveals a critical role for mitochondrial permeability transition in cell death. *Nature*. 2005; 434: 658–62.
13. **Nakagawa T, Shimizu S, Watanabe T, Yamaguchi O, Otsu K, Yamagata H*, et al.*** Cyclophilin D-dependent mitochondrial permeability transition regulates some necrotic but not apoptotic cell death. *Nature*. 2005; 434: 652–58.
14. **Jennings RB, Sommers HM, Smyth GA, Flack HA, Linn H**. Myocardial necrosis induced by temporary occlusion of a coronary artery in the dog. *Archives of pathology*. 1960; 70: 68–78.
15. **Matsui Y, Takagi H, Qu X, Abdellatif M, Sakoda H, Asano T*, et al.*** Distinct roles of autophagy in the heart during ischemia and reperfusion: roles of AMP-activated protein kinase and Beclin 1 in mediating autophagy. *Circulation research*. 2007; 100: 914–22.

16. **Takagi H, Matsui Y, Hirotani S, Sakoda H, Asano T, Sadoshima J**. AMPK mediates autophagy during myocardial ischemia in vivo. *Autophagy*. 2007; 3: 405–07.
17. **Hamacher-Brady A, Brady NR, Gottlieb RA**. Enhancing macroautophagy protects against ischemia/reperfusion injury in cardiac myocytes. *The Journal of biological chemistry*. 2006; 281: 29776–87.
18. **Murry CE, Reinecke H, Pabon LM**. Regeneration gaps: observations on stem cells and cardiac repair. *Journal of the American College of Cardiology*. 2006; 47: 1777–85.
19. **Laflamme MA, Murry CE**. Regenerating the heart. *Nature biotechnology*. 2005; 23: 845–56.
20. **Hasenfuss G**. Animal models of human cardiovascular disease, heart failure and hypertrophy. *Cardiovascular Research*. 1998; 39: 60–76.
21. **Leor J, Palevski D, Amit U, Konfino T**. Macrophages and regeneration: Lessons from the heart. *Seminars in cell & developmental biology*. 2016.
22. **Ramos G, Hofmann U, Frantz S**. Myocardial fibrosis seen through the lenses of T-cell biology. *Journal of molecular and cellular cardiology*. 2016; 92: 41–45.
23. **Lighthouse JK, Small EM**. Transcriptional control of cardiac fibroblast plasticity. *Journal of molecular and cellular cardiology*. 2016; 91: 52–60.
24. **Saez P, Kuhl E**. Computational modeling of acute myocardial infarction. *Computer methods in biomechanics and biomedical engineering*. 2016; 19: 1107–15.
25. **Richardson WJ, Clarke SA, Quinn TA, Holmes JW**. Physiological Implications of Myocardial Scar Structure. *Comprehensive Physiology*. 2015; 5: 1877–909.
26. **Frangogiannis NG**. Pathophysiology of Myocardial Infarction. *Comprehensive Physiology*. 2015; 5: 1841–75.
27. **Garbern JC, Lee RT**. Cardiac Stem Cell Therapy and the Promise of Heart Regeneration. *Cell stem cell*. 2013; 12: 689–98.
28. **Senyo SE, Steinhauser ML, Pizzimenti CL, Yang VK, Cai L, Wang M, *et al.*** Mammalian heart renewal by pre-existing cardiomyocytes. *Nature*. 2013; 493: 433–36.
29. **Beltrami AP, Barlucchi L, Torella D, Baker M, Limana F, Chimenti S, *et al.*** Adult Cardiac Stem Cells Are Multipotent and Support Myocardial Regeneration. *Cell*. 2003; 114: 763–76.
30. **Dawn B, Stein AB, Urbanek K, Rota M, Whang B, Rastaldo R, *et al.*** Cardiac stem cells delivered intravascularly traverse the vessel barrier, regenerate infarcted myocardium, and improve cardiac function. *Proceedings of the National Academy of Sciences of the United States of America*. 2005; 102: 3766–71.
31. **Cai C-L, Liang X, Shi Y, Chu P-H, Pfaff SL, Chen J, *et al.*** Isl1 Identifies a Cardiac Progenitor Population that Proliferates Prior to Differentiation and Contributes a Majority of Cells to the Heart. *Developmental cell*. 2003; 5: 877–89.
32. **Laugwitz K-L, Moretti A, Lam J, Gruber P, Chen Y, Woodard S, *et al.*** Postnatal isl1+ cardioblasts enter fully differentiated cardiomyocyte lineages. *Nature*. 2005; 433: 647–53.
33. **Oh H, Bradfute SB, Gallardo TD, Nakamura T, Gaussin V, Mishina Y, *et al.*** Cardiac progenitor cells from adult myocardium: homing, differentiation, and fusion after

infarction. *Proceedings of the National Academy of Sciences of the United States of America*. 2003; 100: 12313–18.

34. **Martin CM, Meeson AP, Robertson SM, Hawke TJ, Richardson JA, Bates S, *et al.*** Persistent expression of the ATP-binding cassette transporter, Abcg2, identifies cardiac SP cells in the developing and adult heart. *Developmental biology*. 2004; 265: 262–75.
35. **Minami E, Laflamme MA, Saffitz JE, Murry CE**. Extracardiac progenitor cells repopulate most major cell types in the transplanted human heart. *Circulation*. 2005; 112: 2951–58.
36. **Quaini F, Urbanek K, Beltrami AP, Finato N, Beltrami CA, Nadal-Ginard B, *et al.*** Chimerism of the transplanted heart. *The New England journal of medicine*. 2002; 346: 5–15.
37. **Hocht-Zeisberg E, Kahnert H, Guan K, Wulf G, Hemmerlein B, Schlott T, *et al.*** Cellular repopulation of myocardial infarction in patients with sex-mismatched heart transplantation. *European heart journal*. 2004; 25: 749–58.
38. **Deb A**. Bone Marrow-Derived Cardiomyocytes Are Present in Adult Human Heart: A Study of Gender-Mismatched Bone Marrow Transplantation Patients. *Circulation*. 2003; 107: 1247–49.
39. **Glaser R**. Smooth Muscle Cells, But Not Myocytes, of Host Origin in Transplanted Human Hearts. *Circulation*. 2002; 106: 17–19.
40. **Sahara M, Santoro F, Chien KR**. Programming and reprogramming a human heart cell. *The EMBO journal*. 2015; 34: 710–38.
41. **Vincent SD, Buckingham ME**. How to make a heart: the origin and regulation of cardiac progenitor cells. In: Organogenesis in Development. Current Topics in Developmental Biology: Elsevier; 2010. p. 1–41.
42. **Xin M, Olson EN, Bassel-Duby R**. Mending broken hearts: cardiac development as a basis for adult heart regeneration and repair. *Nature reviews. Molecular cell biology*. 2013; 14: 529–41.
43. **Paige SL, Plonowska K, Xu A, Wu SM**. Molecular regulation of cardiomyocyte differentiation. *Circulation research*. 2015; 116: 341–53.
44. **Marelli AJ, Mackie AS, Ionescu-Ittu R, Rahme E, Pilote L**. Congenital heart disease in the general population: changing prevalence and age distribution. *Circulation*. 2007; 115: 163–72.
45. **van der Linde D, Konings EE, Slager MA, Witsenburg M, Helbing WA, Takkenberg JJ, *et al.*** Birth prevalence of congenital heart disease worldwide: a systematic review and meta-analysis. *Journal of the American College of Cardiology*. 2011; 58: 2241–47.
46. **Chaix MA, Andelfinger G, Khairy P**. Genetic testing in congenital heart disease: A clinical approach. *World journal of cardiology*. 2016; 8: 180–91.
47. **Liu M, Zhao L, Yuan J**. Establishment of Relational Model of Congenital Heart Disease Markers and GO Functional Analysis of the Association between Its Serum Markers and Susceptibility Genes. *Computational and mathematical methods in medicine*. 2016; 2016: 9506829.

48. **Cowan, JR, Ware SM**. Genetics and genetic testing in congenital heart disease. *Clinics in perinatology*. 2015; 42: 373-93, ix.
49. **Zhu H**. Forkhead box transcription factors in embryonic heart development and congenital heart disease. *Life sciences*. 2016; 144: 194–201.
50. **Schott JJ, Benson DW, Basson CT, Pease W, Silberbach GM, Moak JP, *et al.*** Congenital heart disease caused by mutations in the transcription factor NKX2-5. *Science (New York, N.Y.)*. 1998; 281: 108–11.
51. **Benson DW, Silberbach GM, Kavanaugh-McHugh A, Cottrill C, Zhang Y, Riggs S, *et al.*** Mutations in the cardiac transcription factor NKX2.5 affect diverse cardiac developmental pathways. *The Journal of clinical investigation*. 1999; 104: 1567–73.
52. **McElhinney DB, Geiger E, Blinder J, Woodrow Benson D, Goldmuntz E**. NKX2.5 mutations in patients with congenital heart disease. *Journal of the American College of Cardiology*. 2003; 42: 1650–55.
53. **Elliott DA, Kirk EP, Yeoh T, Chandar S, McKenzie F, Taylor P, *et al.*** Cardiac homeobox gene NKX2-5 mutations and congenital heart disease. *Journal of the American College of Cardiology*. 2003; 41: 2072–76.
54. **Gioli-Pereira L, Pereira AC, Mesquita SM, Xavier-Neto J, Lopes AA, Krieger JE**. NKX2.5 mutations in patients with non-syndromic congenital heart disease. *International journal of cardiology*. 2010; 138: 261–65.
55. **Balci MM, Akdemir R**. NKX2.5 mutations and congenital heart disease: is it a marker of cardiac anomalies? *International journal of cardiology*. 2011; 147: e44-5.
56. **Ouyang P, Saarel E, Bai Y, Luo C, Lv Q, Xu Y, *et al.*** A de novo mutation in NKX2.5 associated with atrial septal defects, ventricular noncompaction, syncope and sudden death. *Clinica chimica acta; international journal of clinical chemistry*. 2011; 412: 170–75.
57. **Salazar M, Consoli F, Villegas V, Caicedo V, Maddaloni V, Daniele P, *et al.*** Search of somatic GATA4 and NKX2.5 gene mutations in sporadic septal heart defects. *European journal of medical genetics*. 2011; 54: 306–09.
58. **Ashraf H, Pradhan L, Chang EI, Terada R, Ryan NJ, Le Briggs, *et al.*** A mouse model of human congenital heart disease: high incidence of diverse cardiac anomalies and ventricular noncompaction produced by heterozygous Nkx2-5 homeodomain missense mutation. *Circulation. Cardiovascular genetics*. 2014; 7: 423–33.
59. **Xie X, Shi X, Xun X, Rao L**. Associations of NKX2-5 Genetic Polymorphisms with the Risk of Congenital Heart Disease: A Meta-analysis. *Pediatric cardiology*. 2016.
60. **Garg V, Kathiriya IS, Barnes R, Schluterman MK, King IN, Butler CA, *et al.*** GATA4 mutations cause human congenital heart defects and reveal an interaction with TBX5. *Nature*. 2003; 424: 443–47.
61. **Rajagopal SK, Ma Q, Obler D, Shen J, Manichaikul A, Tomita-Mitchell A, *et al.*** Spectrum of heart disease associated with murine and human GATA4 mutation. *Journal of molecular and cellular cardiology*. 2007; 43: 677–85.

62. **Zhang W, Li X, Shen A, Jiao W, Guan X, Li Z**. GATA4 mutations in 486 Chinese patients with congenital heart disease. *European journal of medical genetics*. 2008; 51: 527–35.
63. **Chen Y, Mao J, Sun Y, Zhang Q, Cheng HB, Yan WH*, et al.*** A novel mutation of GATA4 in a familial atrial septal defect. *Clinica chimica acta; international journal of clinical chemistry*. 2010; 411: 1741–45.
64. **Garcia-Martinez V, Schoenwolf GC**. Primitive-streak origin of the cardiovascular system in avian embryos. *Developmental biology*. 1993; 159: 706–19.
65. **Turner DA, Rue P, Mackenzie JP, Davies E, Martinez AA**. Brachyury cooperates with Wnt/beta-catenin signalling to elicit primitive-streak-like behaviour in differentiating mouse embryonic stem cells. *BMC biology*. 2014; 12: 63.
66. **Tam PP, Parameswaran M, Kinder SJ, Weinberger RP**. The allocation of epiblast cells to the embryonic heart and other mesodermal lineages: the role of ingression and tissue movement during gastrulation. *Development (Cambridge, England)*. 1997; 124: 1631–42.
67. **Saga Y**. Mesp1 Expression Is the Earliest Sign of Cardiovascular Development. *Trends in Cardiovascular Medicine*. 2000; 10: 345–52.
68. **David R, Brenner C, Stieber J, Schwarz F, Brunner S, Vollmer M*, et al.*** MesP1 drives vertebrate cardiovascular differentiation through Dkk-1-mediated blockade of Wnt-signalling. *Nat. Cell Biol.* 2008; 10: 338–45.
69. **David R, Jarsch VB, Schwarz F, Nathan P, Gegg M, Lickert H*, et al.*** Induction of MesP1 by Brachyury(T) generates the common multipotent cardiovascular stem cell. *Cardiovasc. Res.* 2011; 92: 115–22.
70. **Liang Q, Xu C, Chen X, Li X, Lu C, Zhou P*, et al.*** The roles of Mesp family proteins: functional diversity and redundancy in differentiation of pluripotent stem cells and mammalian mesodermal development. *Protein & cell*. 2015; 6: 553–61.
71. **Bondue A, Lapouge G, Paulissen C, Semeraro C, Iacovino M, Kyba M*, et al.*** Mesp1 acts as a master regulator of multipotent cardiovascular progenitor specification. *Cell stem cell*. 2008; 3: 69–84.
72. **Bondue A, Tannler S, Chiapparo G, Chabab S, Ramialison M, Paulissen C*, et al.*** Defining the earliest step of cardiovascular progenitor specification during embryonic stem cell differentiation. *The Journal of cell biology*. 2011; 192: 751–65.
73. **Kattman SJ, Huber TL, Keller GM**. Multipotent flk-1+ cardiovascular progenitor cells give rise to the cardiomyocyte, endothelial, and vascular smooth muscle lineages. *Developmental cell*. 2006; 11: 723–32.
74. **Liang X, Wang G, Lin L, Lowe J, Zhang Q, Bu L*, et al.*** HCN4 dynamically marks the first heart field and conduction system precursors. *Circulation research*. 2013; 113: 399–407.
75. **Stevens SM, Pu WT**. HCN4 charges up the first heart field. *Circulation research*. 2013; 113: 350–51.
76. **Brade T, Pane LS, Moretti A, Chien KR, Laugwitz K-L**. Embryonic heart progenitors and cardiogenesis. *Cold Spring Harbor perspectives in medicine*. 2013; 3: a013847.

77. **Später D, Abramczuk MK, Buac K, Zangi L, Stachel MW, Clarke J*, et al.*** A HCN4+ cardiomyogenic progenitor derived from the first heart field and human pluripotent stem cells. *Nature cell biology*. 2013; 15: 1098–106.
78. **Wu SM, Fujiwara Y, Cibulsky SM, Clapham DE, Lien CL, Schultheiss TM*, et al.*** Developmental origin of a bipotential myocardial and smooth muscle cell precursor in the mammalian heart. *Cell*. 2006; 127: 1137–50.
79. **Moorman AF, Christoffels VM, Anderson RH, van den Hoff MJ**. The heart-forming fields: one or multiple? *Philosophical transactions of the Royal Society of London. Series B, Biological sciences*. 2007; 362: 1257–65.
80. **Sizarov A, Ya J, Boer BA** de**, Lamers WH, Christoffels VM, Moorman AF**. Formation of the building plan of the human heart: morphogenesis, growth, and differentiation. *Circulation*. 2011; 123: 1125–35.
81. **George V, Colombo S, Targoff KL**. An early requirement for nkx2.5 ensures the first and second heart field ventricular identity and cardiac function into adulthood. *Developmental biology*. 2015; 400: 10–22.
82. **Buckingham M, Meilhac S, Zaffran S**. Building the mammalian heart from two sources of myocardial cells. *Nature reviews. Genetics*. 2005; 6: 826–35.
83. **Dyer LA, Kirby ML**. The role of secondary heart field in cardiac development. *Dev. Biol.* 2009; 336: 137–44.
84. **Rochais F, Mesbah K, Kelly RG**. Signaling pathways controlling second heart field development. *Circulation research*. 2009; 104: 933–42.
85. **Musunuru K, Domian IJ, Chien KR**. Stem cell models of cardiac development and disease. *Annu. Rev. Cell Dev. Biol.* 2010; 26: 667–87.
86. **Pandur P, Sirbu IO, Kühl SJ, Philipp M, Kühl M**. Islet1-expressing cardiac progenitor cells: a comparison across species. *Dev. Genes Evol.* 2013; 223: 117–29.
87. **Moretti A, Caron L, Nakano A, Lam JT, Bernshausen A, Chen Y*, et al.*** Multipotent embryonic isl1+ progenitor cells lead to cardiac, smooth muscle, and endothelial cell diversification. *Cell*. 2006; 127: 1151–65.
88. **Sun Y, Liang X, Najafi N, Cass M, Lin L, Cai CL*, et al.*** Islet 1 is expressed in distinct cardiovascular lineages, including pacemaker and coronary vascular cells. *Developmental biology*. 2007; 304: 286–96.
89. **Misfeldt AM, Boyle SC, Tompkins KL, Bautch VL, Labosky PA, Baldwin HS**. Endocardial cells are a distinct endothelial lineage derived from Flk1+ multipotent cardiovascular progenitors. *Developmental biology*. 2009; 333: 78–89.
90. **Bressan M, Liu G, Mikawa T**. Early mesodermal cues assign avian cardiac pacemaker fate potential in a tertiary heart field. *Science (New York, N.Y.)*. 2013; 340: 744–48.
91. **Schlueter J, Brand T**. Epicardial progenitor cells in cardiac development and regeneration. *Journal of cardiovascular translational research*. 2012; 5: 641–53.
92. **Katz TC, Singh MK, Degenhardt K, Rivera-Feliciano J, Johnson RL, Epstein JA*, et al.*** Distinct compartments of the proepicardial organ give rise to coronary vascular endothelial cells. *Developmental cell*. 2012; 22: 639–50.

93. **Zhou B, Ma Q, Rajagopal S, Wu SM, Domian I, Rivera-Feliciano J, *et al.*** Epicardial progenitors contribute to the cardiomyocyte lineage in the developing heart. *Nature*. 2008; 454: 109–13.
94. **Schultheiss TM, Burch JB, Lassar AB**. A role for bone morphogenetic proteins in the induction of cardiac myogenesis. *Genes & development*. 1997; 11: 451–62.
95. **Andrée B, Duprez D, Vorbusch B, Arnold H-H, Brand T**. BMP-2 induces ectopic expression of cardiac lineage markers and interferes with somite formation in chicken embryos. *Mechanisms of Development*. 1998; 70: 119–31.
96. **Schlange T, Andrée B, Arnold H-H, Brand T**. BMP2 is required for early heart development during a distinct time period. *Mechanisms of Development*. 2000; 91: 259–70.
97. **Lin HY, Lee DC, Wang HD, Chi YH, Im Chiu**. Activation of FGF1B Promoter and FGF1 Are Involved in Cardiogenesis Through the Signaling of PKC, but Not MAPK. *Stem cells and development*. 2015; 24: 2853–63.
98. **Samuel LJ, Latinkic BV**. Early activation of FGF and nodal pathways mediates cardiac specification independently of Wnt/beta-catenin signaling. *PloS one*. 2009; 4: e7650.
99. **Watanabe Y, Zaffran S, Kuroiwa A, Higuchi H, Ogura T, Harvey RP, *et al.*** Fibroblast growth factor 10 gene regulation in the second heart field by Tbx1, Nkx2-5, and Islet1 reveals a genetic switch for down-regulation in the myocardium. *Proceedings of the National Academy of Sciences of the United States of America*. 2012; 109: 18273–80.
100. **Pandur P, Lasche M, Eisenberg LM, Kuhl M**. Wnt-11 activation of a non-canonical Wnt signalling pathway is required for cardiogenesis. *Nature*. 2002; 418: 636–41.
101. **Ahmad SM, Bhattacharyya P, Jeffries N, Gisselbrecht SS, Am Michelson**. Two Forkhead transcription factors regulate cardiac progenitor specification by controlling the expression of receptors of the fibroblast growth factor and Wnt signaling pathways. *Development (Cambridge, England)*. 2016; 143: 306–17.
102. **Martin J, Afouda BA, Hoppler S**. Wnt/beta-catenin signalling regulates cardiomyogenesis via GATA transcription factors. *Journal of anatomy*. 2010; 216: 92–107.
103. **Nakamura T, Sano M, Songyang Z, Schneider MD**. A Wnt- and beta -catenin-dependent pathway for mammalian cardiac myogenesis. *Proceedings of the National Academy of Sciences of the United States of America*. 2003; 100: 5834–39.
104. **Kwon C, Arnold J, Hsiao EC, Taketo MM, Conklin BR, Srivastava D**. Canonical Wnt signaling is a positive regulator of mammalian cardiac progenitors. *Proceedings of the National Academy of Sciences of the United States of America*. 2007; 104: 10894–99.
105. **Clowes C, Boylan MG, La Ridge, Barnes E, Wright JA, Hentges KE**. The functional diversity of essential genes required for mammalian cardiac development. *Genesis (New York, N.Y. : 2000)*. 2014; 52: 713–37.
106. **Pradhan L, Gopal S, Li S, Ashur S, Suryanarayanan S, Kasahara H, *et al.*** Intermolecular Interactions of Cardiac Transcription Factors NKX2.5 and TBX5. *Biochemistry*. 2016; 55: 1702–10.
107. **Olson EN**. Gene regulatory networks in the evolution and development of the heart. *Science*. 2006; 313: 1922–27.

108. **Sylva M, van den Hoff MJ, Moorman AF**. Development of the human heart. *American journal of medical genetics. Part A*. 2014; 164A: 1347–71.
109. **Bodmer R**. The gene tinman is required for specification of the heart and visceral muscles in Drosophila. *Development (Cambridge, England)*. 1993; 118: 719–29.
110. **Azpiazu N, Frasch M**. tinman and bagpipe: two homeo box genes that determine cell fates in the dorsal mesoderm of Drosophila. *Genes & development*. 1993; 7: 1325–40.
111. **Sorrentino RP, Gajewski KM, Schulz RA**. GATA factors in Drosophila heart and blood cell development. *Seminars in cell & developmental biology*. 2005; 16: 107–16.
112. **Chen JN, Fishman MC**. Zebrafish tinman homolog demarcates the heart field and initiates myocardial differentiation. *Development (Cambridge, England)*. 1996; 122: 3809–16.
113. **Cleaver OB, Patterson KD, Krieg PA**. Overexpression of the tinman-related genes XNkx-2.5 and XNkx-2.3 in Xenopus embryos results in myocardial hyperplasia. *Development (Cambridge, England)*. 1996; 122: 3549–56.
114. **Reiter JF, Alexander J, Rodaway A, Yelon D, Patient R, Holder N, *et al.*** Gata5 is required for the development of the heart and endoderm in zebrafish. *Genes & development*. 1999; 13: 2983–95.
115. **Latinkić BV, Kotecha S, Mohun TJ**. Induction of cardiomyocytes by GATA4 in Xenopus ectodermal explants. *Development (Cambridge, England)*. 2003; 130: 3865–76.
116. **Hausburg F, David R**. Cell Programming for Future Regenerative Medicine. In: Steinhoff G, editor. Regenerative Medicine - from Protocol to Patient: 2. Stem Cell Science and Technology. 3rd ed. Cham, s.l.: Springer International Publishing; 2016. p. 389–424.
117. **Hausburg F, Jung JJ, Hoch M, Wolfien M, Yavari A, Rimmbach C, *et al.*** (Re-)programming of subtype specific cardiomyocytes. *Advanced drug delivery reviews*. 2017.
118. **Hausburg F, Jung JJ, David R**. Specific Cell (Re-)Programming: Approaches and Perspectives. *Advances in biochemical engineering/biotechnology*. 2017.
119. **Evans MJ, Kaufman MH**. Establishment in culture of pluripotential cells from mouse embryos. *Nature*. 1981; 292: 154–56.
120. **Martin GR**. Isolation of a pluripotent cell line from early mouse embryos cultured in medium conditioned by teratocarcinoma stem cells. *Proceedings of the National Academy of Sciences of the United States of America*. 1981; 78: 7634–38.
121. **Thomson JA**. Embryonic Stem Cell Lines Derived from Human Blastocysts. *Science*. 1998; 282: 1145–47.
122. **Smith AG**. Embryo-derived stem cells: of mice and men. *Annual review of cell and developmental biology*. 2001; 17: 435–62.
123. **Chen Y, Lai D**. Pluripotent states of human embryonic stem cells. *Cellular reprogramming*. 2015; 17: 1–6.
124. **Shiraki N, Ogaki S, Kume S**. Profiling of embryonic stem cell differentiation. *The review of diabetic studies : RDS*. 2014; 11: 102–14.
125. **Ginis I, Luo Y, Miura T, Thies S, Brandenberger R, Gerecht-Nir S, *et al.*** Differences between human and mouse embryonic stem cells. *Developmental biology*. 2004; 269: 360–80.

126. **Beck S, Lee B-K, Kim J**. Multi-layered global gene regulation in mouse embryonic stem cells. *Cellular and molecular life sciences : CMLS*. 2015; 72: 199–216.
127. **Molofsky AV, Pardal R, Morrison SJ**. Diverse mechanisms regulate stem cell self-renewal. *Current opinion in cell biology*. 2004; 16: 700–07.
128. **Odorico JS, Kaufman DS, Thomson JA**. Multilineage differentiation from human embryonic stem cell lines. *Stem cells (Dayton, Ohio)*. 2001; 19: 193–204.
129. **Draper JS, Fox V**. Human embryonic stem cells: multilineage differentiation and mechanisms of self-renewal. *Archives of medical research*. 2003; 34: 558–64.
130. **Nussbaum J, Minami E, Laflamme MA, Virag, Jitka A I, Ware CB, Masino A, *et al.*** Transplantation of undifferentiated murine embryonic stem cells in the heart: teratoma formation and immune response. *FASEB journal : official publication of the Federation of American Societies for Experimental Biology*. 2007; 21: 1345–57.
131. **Swijnenburg R-J, Sheikh AY, Robbins RC**. Comment on \"Transplantation of undifferentiated murine embryonic stem cells in the heart: teratoma formation and immune response\". *FASEB journal : official publication of the Federation of American Societies for Experimental Biology*. 2007; 21: 1290; author reply 1291.
132. **Swijnenburg R-J, Schrepfer S, Govaert JA, Cao F, Ransohoff K, Sheikh AY, *et al.*** Immunosuppressive therapy mitigates immunological rejection of human embryonic stem cell xenografts. *Proceedings of the National Academy of Sciences of the United States of America*. 2008; 105: 12991–96.
133. **Morgani SM, Brickman JM**. LIF supports primitive endoderm expansion during pre-implantation development. *Development (Cambridge, England)*. 2015; 142: 3488–99.
134. **Ohtsuka S, Nakai-Futatsugi Y, Niwa H**. LIF signal in mouse embryonic stem cells. *JAK-STAT*. 2015; 4: e1086520.
135. **Matsuda T, Nakamura T, Nakao K, Arai T, Katsuki M, Heike T, *et al.*** STAT3 activation is sufficient to maintain an undifferentiated state of mouse embryonic stem cells. *The EMBO journal*. 1999; 18: 4261–69.
136. **Niwa H, Burdon T, Chambers I, Smith A**. Self-renewal of pluripotent embryonic stem cells is mediated via activation of STAT3. *Genes & development*. 1998; 12: 2048–60.
137. **Burdon T, Stracey C, Chambers I, Nichols J, Smith A**. Suppression of SHP-2 and ERK signalling promotes self-renewal of mouse embryonic stem cells. *Developmental biology*. 1999; 210: 30–43.
138. **Park Y-G, Lee S-E, Kim E-Y, Hyun H, Shin M-Y, Son Y-J, *et al.*** Effects of Feeder Cell Types on Culture of Mouse Embryonic Stem Cell In Vitro. *Development & reproduction*. 2015; 19: 119–26.
139. **Amano K, Furuno T, Nakanishi M**. Conditioned medium from feeder STO cells increases the attachment of mouse embryonic stem cells. *Biological & pharmaceutical bulletin*. 2006; 29: 1747–50.
140. **Wobus AM, Wallukat G, Hescheler J**. Pluripotent mouse embryonic stem cells are able to differentiate into cardiomyocytes expressing chronotropic responses to adrenergic and cholinergic agents and Ca2+ channel blockers. *Differentiation*. 1991; 48: 173–82.

141. **Pacheco-Leyva I, Matias AC, Oliveira DV, Santos JMA, Nascimento R, Guerreiro E, *et al.*** CITED2 Cooperates with ISL1 and Promotes Cardiac Differentiation of Mouse Embryonic Stem Cells. *Stem cell reports*. 2016; 7: 1037–49.
142. **Kotoku T, Kosaka K, Nishio M, Ishida Y, Kawaichi M, Matsuda E**. CIBZ Regulates Mesodermal and Cardiac Differentiation of by Suppressing T and Mesp1 Expression in Mouse Embryonic Stem Cells. *Scientific reports*. 2016; 6: 34188.
143. **Rabiee F, Forouzanfar M, Ghazvini Zadegan F, Tanhaei S, Ghaedi K, Motovali Bashi M, *et al.*** Induced expression of Fndc5 significantly increased cardiomyocyte differentiation rate of mouse embryonic stem cells. *Gene*. 2014; 551: 127–37.
144. **Dorn T, Goedel A, Lam JT, Haas J, Tian Q, Herrmann F, *et al.*** Direct nkx2-5 transcriptional repression of isl1 controls cardiomyocyte subtype identity. *Stem cells (Dayton, Ohio)*. 2015; 33: 1113–29.
145. **Engels MC, Rajarajan K, Feistritzer R, Sharma A, Nielsen UB, Schalij MJ, *et al.*** Insulin-like growth factor promotes cardiac lineage induction in vitro by selective expansion of early mesoderm. *Stem cells (Dayton, Ohio)*. 2014; 32: 1493–502.
146. **Fynes K, Tostoes R, Ruban L, Weil B, Mason C, Veraitch FS**. The differential effects of 2% oxygen preconditioning on the subsequent differentiation of mouse and human pluripotent stem cells. *Stem cells and development*. 2014; 23: 1910–22.
147. **Kokkinopoulos I, Ishida H, Saba R, Coppen S, Suzuki K, Yashiro K**. Cardiomyocyte differentiation from mouse embryonic stem cells using a simple and defined protocol. *Developmental dynamics : an official publication of the American Association of Anatomists*. 2016; 245: 157–65.
148. **Ding H, Xu X, Qin X, Yang C, Feng Q**. Resveratrol promotes differentiation of mouse embryonic stem cells to cardiomyocytes. *Cardiovascular therapeutics*. 2016.
149. **Ivanyuk D, Budash G, Zheng Y, Gaspar JA, Chaudhari U, Fatima A, *et al.*** Ascorbic Acid-Induced Cardiac Differentiation of Murine Pluripotent Stem Cells: Transcriptional Profiling and Effect of a Small Molecule Synergist of Wnt/beta-Catenin Signaling Pathway. *Cellular physiology and biochemistry : international journal of experimental cellular physiology, biochemistry, and pharmacology*. 2015; 36: 810–30.
150. **Ionta V, Liang W, Kim EH, Rafie R, Giacomello A, Marban E, *et al.*** SHOX2 overexpression favors differentiation of embryonic stem cells into cardiac pacemaker cells, improving biological pacing ability. *Stem cell reports*. 2015; 4: 129–42.
151. **David R, Stieber J, Fischer E, Brunner S, Brenner C, Pfeiler S, *et al.*** Forward programming of pluripotent stem cells towards distinct cardiovascular cell types. *Cardiovasc. Res.* 2009; 84: 263–72.
152. **Chong, James J H, Yang X, Don CW, Minami E, Liu Y-W, Weyers JJ, *et al.*** Human embryonic-stem-cell-derived cardiomyocytes regenerate non-human primate hearts. *Nature*. 2014; 510: 273–77.
153. **Jung JJ, Husse B, Rimmbach C, Krebs S, Stieber J, Steinhoff G, *et al.*** Programming and isolation of highly pure physiologically and pharmacologically functional sinus-nodal bodies from pluripotent stem cells. *Stem cell reports*. 2014; 2: 592–605.

154. **Rimmbach C, Jung JJ, David R**. Generation of murine cardiac pacemaker cell aggregates based on ES-cell-programming in combination with Myh6-promoter-selection. *Journal of visualized experiments : JoVE*. 2015: e52465.
155. **Klug MG, Soonpaa MH, Koh GY, Field LJ**. Genetically selected cardiomyocytes from differentiating embronic stem cells form stable intracardiac grafts. *The Journal of clinical investigation*. 1996; 98: 216–24.
156. **Takahashi K, Yamanaka S**. Induction of pluripotent stem cells from mouse embryonic and adult fibroblast cultures by defined factors. *Cell*. 2006; 126: 663–76.
157. **Takahashi K, Tanabe K, Ohnuki M, Narita M, Ichisaka T, Tomoda K, *et al.*** Induction of pluripotent stem cells from adult human fibroblasts by defined factors. *Cell*. 2007; 131: 861–72.
158. **Yu J, Vodyanik MA, Smuga-Otto K, Antosiewicz-Bourget J, Frane JL, Tian S, *et al.*** Induced pluripotent stem cell lines derived from human somatic cells. *Science (New York, N.Y.)*. 2007; 318: 1917–20.
159. **Zhou W, Freed CR**. Adenoviral gene delivery can reprogram human fibroblasts to induced pluripotent stem cells. *Stem cells (Dayton, Ohio)*. 2009; 27: 2667–74.
160. **Kim D, Kim C-H, Moon J-I, Chung Y-G, Chang M-Y, Han B-S, *et al.*** Generation of human induced pluripotent stem cells by direct delivery of reprogramming proteins. *Cell stem cell*. 2009; 4: 472–76.
161. **Zhou H, Wu S, Joo JY, Zhu S, Han DW, Lin T, *et al.*** Generation of induced pluripotent stem cells using recombinant proteins. *Cell stem cell*. 2009; 4: 381–84.
162. **Warren L, Manos PD, Ahfeldt T, Loh Y-H, Li H, Lau F, *et al.*** Highly efficient reprogramming to pluripotency and directed differentiation of human cells with synthetic modified mRNA. *Cell Stem Cell*. 2010; 7: 618–30.
163. **Liu J, Verma PJ**. Synthetic mRNA Reprogramming of Human Fibroblast Cells. *Methods in molecular biology (Clifton, N.J.)*. 2015; 1330: 17–28.
164. **Preskey D, Allison TF, Jones M, Mamchaoui K, Unger C**. Synthetically modified mRNA for efficient and fast human iPS cell generation and direct transdifferentiation to myoblasts. *Biochemical and biophysical research communications*. 2016; 473: 743–51.
165. **Mandal PK, Rossi DJ**. Reprogramming human fibroblasts to pluripotency using modified mRNA. *Nat Protoc*. 2013; 8: 568–82.
166. **Yakubov E, Rechavi G, Rozenblatt S, Givol D**. Reprogramming of human fibroblasts to pluripotent stem cells using mRNA of four transcription factors. *Biochem. Biophys. Res. Commun.* 2010; 394: 189–93.
167. **Miyoshi N, Ishii H, Nagano H, Haraguchi N, Dewi DL, Kano Y, *et al.*** Reprogramming of mouse and human cells to pluripotency using mature microRNAs. *Cell stem cell*. 2011; 8: 633–38.
168. **Hou P, Li Y, Zhang X, Liu C, Guan J, Li H, *et al.*** Pluripotent stem cells induced from mouse somatic cells by small-molecule compounds. *Science (New York, N.Y.)*. 2013; 341: 651–54.

169. **Xiao X, Li N, Zhang D, Yang B, Guo H, Li Y**. Generation of Induced Pluripotent Stem Cells with Substitutes for Yamanaka's Four Transcription Factors. *Cellular reprogramming*. 2016; 18: 281–97.
170. **Mah N, Wang Y, Liao M-C, Prigione A, Jozefczuk J, Lichtner B, *et al.*** Molecular insights into reprogramming-initiation events mediated by the OSKM gene regulatory network. *PloS one*. 2011; 6: e24351.
171. **Polo JM, Anderssen E, Walsh RM, Schwarz BA, Nefzger CM, Lim SM, *et al.*** A molecular roadmap of reprogramming somatic cells into iPS cells. *Cell*. 2012; 151: 1617–32.
172. **Benevento M, Tonge PD, Puri MC, Hussein, Samer M I, Cloonan N, Wood DL, *et al.*** Proteome adaptation in cell reprogramming proceeds via distinct transcriptional networks. *Nature communications*. 2014; 5: 5613.
173. **Clancy JL, Patel HR, Hussein, Samer M I, Tonge PD, Cloonan N, Corso AJ, *et al.*** Small RNA changes en route to distinct cellular states of induced pluripotency. *Nature communications*. 2014; 5: 5522.
174. **Hussein, Samer M I, Puri MC, Tonge PD, Benevento M, Corso AJ, Clancy JL, *et al.*** Genome-wide characterization of the routes to pluripotency. *Nature*. 2014; 516: 198–206.
175. **Lee D-S, Shin J-Y, Tonge PD, Puri MC, Lee S, Park H, *et al.*** An epigenomic roadmap to induced pluripotency reveals DNA methylation as a reprogramming modulator. *Nature communications*. 2014; 5: 5619.
176. **Tonge PD, Corso AJ, Monetti C, Hussein, Samer M I, Puri MC, Michael IP, *et al.*** Divergent reprogramming routes lead to alternative stem-cell states. *Nature*. 2014; 516: 192–97.
177. **Hikabe O, Hamazaki N, Nagamatsu G, Obata Y, Hirao Y, Hamada N, *et al.*** Reconstitution in vitro of the entire cycle of the mouse female germ line. *Nature*. 2016.
178. **Bhattacharya S, Burridge PW, Kropp EM, Chuppa SL, Kwok W-M, Wu JC, *et al.*** High efficiency differentiation of human pluripotent stem cells to cardiomyocytes and characterization by flow cytometry. *Journal of visualized experiments : JoVE*. 2014: 52010.
179. **Fuerstenau-Sharp M, Zimmermann ME, Stark K, Jentsch N, Klingenstein M, Drzymalski M, *et al.*** Generation of highly purified human cardiomyocytes from peripheral blood mononuclear cell-derived induced pluripotent stem cells. *PloS one*. 2015; 10: e0126596.
180. **Pei F, Jiang J, Bai S, Cao H, Tian L, Zhao Y, *et al.*** Chemical-defined and albumin-free generation of human atrial and ventricular myocytes from human pluripotent stem cells. *Stem cell research*. 2017; 19: 94–103.
181. **Zhang J, Wilson GF, Soerens AG, Koonce CH, Yu J, Palecek SP, *et al.*** Functional cardiomyocytes derived from human induced pluripotent stem cells. *Circulation research*. 2009; 104: e30-41.
182. **Zwi L, Caspi O, Arbel G, Huber I, Gepstein A, Park I-H, *et al.*** Cardiomyocyte differentiation of human induced pluripotent stem cells. *Circulation*. 2009; 120: 1513–23.

183. **Bedada FB, Wheelwright M, Metzger JM**. Maturation status of sarcomere structure and function in human iPSC-derived cardiac myocytes. *Biochimica et biophysica acta*. 2016; 1863: 1829–38.
184. **Mummery C**. Induced pluripotent stem cells--a cautionary note. *The New England journal of medicine*. 2011; 364: 2160–62.
185. **Yamashita T, Kawai H, Tian F, Ohta Y, Abe K**. Tumorigenic development of induced pluripotent stem cells in ischemic mouse brain. *Cell transplantation*. 2011; 20: 883–91.
186. **Rosen MR, Myerburg RJ, Francis DP, Cole GD, Marbán E**. Translating stem cell research to cardiac disease therapies: pitfalls and prospects for improvement. *Journal of the American College of Cardiology*. 2014; 64: 922–37.
187. **Pavo N, Charwat S, Nyolczas N, Jakab A, Murlasits Z, Bergler-Klein J, *et al.*** Cell therapy for human ischemic heart diseases: critical review and summary of the clinical experiences. *Journal of molecular and cellular cardiology*. 2014; 75: 12–24.
188. **Matar AA, Chong JJ**. Stem cell therapy for cardiac dysfunction. *SpringerPlus*. 2014; 3: 440.
189. **Wang X, Zhang J, Zhang F, Li J, Li Y, Tan Z, *et al.*** The Clinical Status of Stem Cell Therapy for Ischemic Cardiomyopathy. *Stem cells international*. 2015; 2015: 135023.
190. **Wang D, Gao G**. State-of-the-art human gene therapy: part I. Gene delivery technologies. *Discovery medicine*. 2014; 18: 67–77.
191. **Sart S, Ma T, Li Y**. Preconditioning stem cells for in vivo delivery. *BioResearch open access*. 2014; 3: 137–49.
192. **Noort WA, Feye D,** Van Den Akker, F**, Stecher D,** Chamuleau, S A J**,** Sluijter, J P G**, *et al.*** Mesenchymal stromal cells to treat cardiovascular disease: strategies to improve survival and therapeutic results, Vol 52; 2010.
193. **Yang W, Zheng H, Wang Y, Lian F, Hu Z, Xue S**. Nesprin-1 has key roles in the process of mesenchymal stem cell differentiation into cardiomyocyte-like cells in vivo and in vitro. *Molecular medicine reports*. 2015; 11: 133–42.
194. **Li P, Zhang L**. Exogenous Nkx2.5- or GATA-4-transfected rabbit bone marrow mesenchymal stem cells and myocardial cell co-culture on the treatment of myocardial infarction in rabbits. *Molecular medicine reports*. 2015; 12: 2607–21.
195. **Li J, Zhu K, Wang Y, Zheng J, Guo C, Lai H, *et al.*** Combination of IGF1 gene manipulation and 5AZA treatment promotes differentiation of mesenchymal stem cells into cardiomyocytelike cells. *Molecular medicine reports*. 2015; 11: 815–20.
196. **Mohanty S, Bose S, Jain KG, Bhargava B, Airan B**. TGFβ1 contributes to cardiomyogenic-like differentiation of human bone marrow mesenchymal stem cells. *Int. J. Cardiol.* 2013; 163: 93–99.
197. **Feng Y, Yang P, Luo S, Zhang Z, Li H, Zhu P, *et al.*** Shox2 influences mesenchymal stem cell fate in a co-culture model in vitro. *Molecular medicine reports*. 2016; 14: 637–42.
198. **Huang F, Tang L, Fang Z-f, Hu X-q, Pan J-y, Zhou S-h**. miR-1-mediated induction of cardiogenesis in mesenchymal stem cells via downregulation of Hes-1. *BioMed research international*. 2013; 2013: 216286.

199. **Yu Z, Zou Y, Fan J, Li C, Ma L**. Notch1 is associated with the differentiation of human bone marrowderived mesenchymal stem cells to cardiomyocytes. *Molecular medicine reports*. 2016; 14: 5065–71.
200. **Hou J, Long H, Zhou C, Zheng S, Wu H, Guo T*, et al.*** Long noncoding RNA Braveheart promotes cardiogenic differentiation of mesenchymal stem cells in vitro. *Stem cell research & therapy*. 2017; 8: 4.
201. **Carvalho PH, Daibert APF, Monteiro BS, Okano BS, Carvalho JL, Cunha, Daise Nunes Queiroz da*, et al.*** Diferenciação de células-tronco mesenquimais derivadas do tecido adiposo em cardiomiócitos. *Arq. Bras. Cardiol.* 2013; 100: 82–89.
202. **Wystrychowski W, Patlolla B, Zhuge Y, Neofytou E, Robbins RC, Beygui RE**. Multipotency and cardiomyogenic potential of human adipose-derived stem cells from epicardium, pericardium, and omentum. *Stem cell research & therapy*. 2016; 7: 84.
203. **Gwak S-J, Bhang SH, Yang HS, Kim S-S, Lee D-H, Lee S-H*, et al.*** In vitro cardiomyogenic differentiation of adipose-derived stromal cells using transforming growth factor-beta1. *Cell biochemistry and function*. 2009; 27: 148–54.
204. **Nagata H, Ii M, Kohbayashi E, Hoshiga M, Hanafusa T, Asahi M**. Cardiac Adipose-Derived Stem Cells Exhibit High Differentiation Potential to Cardiovascular Cells in C57BL/6 Mice. *Stem cells translational medicine*. 2016; 5: 141–51.
205. **Choi YS, Dusting GJ, Stubbs S, Arunothayaraj S, Han XL, Collas P*, et al.*** Differentiation of human adipose-derived stem cells into beating cardiomyocytes. *Journal of cellular and molecular medicine*. 2010; 14: 878–89.
206. **Takahashi T, Nagai T, Kanda M, Liu M-L, Kondo N, Naito AT*, et al.*** Regeneration of the Cardiac Conduction System by Adipose Tissue-Derived Stem Cells. *Circulation journal : official journal of the Japanese Circulation Society*. 2015; 79: 2703–12.
207. **Sung I-Y, Son H-N, Ullah I, Bharti D, Park J-M, Cho Y-C*, et al.*** Cardiomyogenic Differentiation of Human Dental Follicle-derived Stem Cells by Suberoylanilide Hydroxamic Acid and Their In Vivo Homing Property. *International journal of medical sciences*. 2016; 13: 841–52.
208. **Zhang Y, Sivakumaran P, Newcomb AE, Hernandez D, Harris N, Khanabdali R*, et al.*** Cardiac Repair With a Novel Population of Mesenchymal Stem Cells Resident in the Human Heart. *Stem cells (Dayton, Ohio)*. 2015; 33: 3100–13.
209. **Orlandi A, Pagani F, Avitabile D, Bonanno G, Scambia G, Vigna E*, et al.*** Functional properties of cells obtained from human cord blood CD34+ stem cells and mouse cardiac myocytes in coculture. *American journal of physiology. Heart and circulatory physiology*. 2008; 294: H1541-9.
210. **Lopez-Ruiz E, Peran M, Picon-Ruiz M, Garcia MA, Carrillo E, Jimenez-Navarro M*, et al.*** Cardiomyogenic differentiation potential of human endothelial progenitor cells isolated from patients with myocardial infarction. *Cytotherapy*. 2014; 16: 1229–37.
211. **Chen G, Yue A, Yu H, Ruan Z, Yin Y, Wang R*, et al.*** Mesenchymal Stem Cells and Mononuclear Cells From Cord Blood: Cotransplantation Provides a Better Effect in Treating Myocardial Infarction. *Stem cells translational medicine*. 2016; 5: 350–57.

212. **Avitabile D, Crespi A, Brioschi C, Parente V, Toietta G, Devanna P*, et al.*** Human cord blood CD34+ progenitor cells acquire functional cardiac properties through a cell fusion process. *American journal of physiology. Heart and circulatory physiology*. 2011; 300: H1875-84.
213. **Freeman BT, Kouris NA, Ogle BM**. Tracking fusion of human mesenchymal stem cells after transplantation to the heart. *Stem cells translational medicine*. 2015; 4: 685–94.
214. **Davis RL, Weintraub H, Lassar AB**. Expression of a Single Transfected cDNA Converts Fibroblasts to Myoblasts. *Cell Press*. 1987; 51: 987–1000.
215. **Smith DK, Zhang C-L**. Regeneration through Reprogramming Adult Cell Identity in Vivo. *The American journal of pathology*. 2015.
216. **Xu J, Du Y, Deng H**. Direct lineage reprogramming: strategies, mechanisms, and applications. *Cell stem cell*. 2015; 16: 119–34.
217. **Chen S-l, Fang W-w, Ye F, Liu Y-H, Qian J, Shan S-j, *et al.*** Effect on left ventricular function of intracoronary transplantation of autologous bone marrow mesenchymal stem cell in patients with acute myocardial infarction. *The American journal of cardiology*. 2004; 94: 92–95.
218. **Ong S-G, Lee WH, Kodo K, Wu JC**. MicroRNA-mediated regulation of differentiation and trans-differentiation in stem cells. *Advanced drug delivery reviews*. 2015; 88: 3–15.
219. **Budniatzky I, Gepstein L**. Concise review: reprogramming strategies for cardiovascular regenerative medicine: from induced pluripotent stem cells to direct reprogramming. *Stem Cells Transl Med*. 2014; 3: 448–57.
220. **Blum HE**. Advances in individualized and regenerative medicine. *Advances in medical sciences*. 2014; 59: 7–12.
221. **Gao Y, Chu M, Hong J, Shang J, Di Xu**. Hypoxia induces cardiac fibroblast proliferation and phenotypic switch: a role for caveolae and caveolin-1/PTEN mediated pathway. *Journal of thoracic disease*. 2014; 6: 1458–68.
222. **Moore-Morris T, Cattaneo P, Puceat M, Evans SM**. Origins of cardiac fibroblasts. *Journal of molecular and cellular cardiology*. 2016; 91: 1–5.
223. **Ieda M, Fu J-D, Delgado-Olguin P, Vedantham V, Hayashi Y, Bruneau BG*, et al.*** Direct reprogramming of fibroblasts into functional cardiomyocytes by defined factors. *Cell*. 2010; 142: 375–86.
224. **Chen JX, Krane M, Deutsch M-A, Wang L, Rav-Acha M, Gregoire S*, et al.*** Inefficient reprogramming of fibroblasts into cardiomyocytes using Gata4, Mef2c, and Tbx5. *Circ. Res.* 2012; 111: 50–55.
225. **Qian L, Huang Y, Spencer CI, Foley A, Vedantham V, Liu L*, et al.*** In vivo reprogramming of murine cardiac fibroblasts into induced cardiomyocytes. *Nature*. 2012; 485: 593–98.
226. **Inagawa K, Miyamoto K, Yamakawa H, Muraoka N, Sadahiro T, Umei T*, et al.*** Induction of cardiomyocyte-like cells in infarct hearts by gene transfer of Gata4, Mef2c, and Tbx5. *Circ. Res.* 2012; 111: 1147–56.

227. **Qian L, Berry EC, Fu J-D, Ieda M, Srivastava D**. Reprogramming of mouse fibroblasts into cardiomyocyte-like cells in vitro. *Nature protocols*. 2013; 8: 1204–15.
228. **Srivastava D**. Making or breaking the heart: from lineage determination to morphogenesis. *Cell*. 2006; 126: 1037–48.
229. **Zhao R, Watt AJ, Battle MA, Li J, Bondow BJ, Duncan SA**. Loss of both GATA4 and GATA6 blocks cardiac myocyte differentiation and results in acardia in mice. *Developmental biology*. 2008; 317: 614–19.
230. **Herrmann F, Groß A, Zhou D, Kestler HA, Kühl M**. A boolean model of the cardiac gene regulatory network determining first and second heart field identity. *PLoS ONE*. 2012; 7: e46798.
231. **Bruneau BG, Nemer G, Schmitt JP, Charron F, Robitaille L, Caron S, *et al.*** A Murine Model of Holt-Oram Syndrome Defines Roles of the T-Box Transcription Factor Tbx5 in Cardiogenesis and Disease. *Cell*. 2001; 106: 709–21.
232. **Ghosh TK, Song FF, Packham EA, Buxton S, Robinson TE, Ronksley J, *et al.*** Physical interaction between TBX5 and MEF2C is required for early heart development. *Molecular and cellular biology*. 2009; 29: 2205–18.
233. **Maitra M, Schluterman MK, Nichols HA, Richardson JA, Lo CW, Srivastava D, *et al.*** Interaction of Gata4 and Gata6 with Tbx5 is critical for normal cardiac development. *Developmental biology*. 2009; 326: 368–77.
234. **Wang L, Liu Z, Yin C, Asfour H, Chen O, Li Y, *et al.*** Stoichiometry of Gata4, Mef2c, and Tbx5 influences the efficiency and quality of induced cardiac myocyte reprogramming. *Circulation research*. 2015; 116: 237–44.
235. **Song K, Nam Y-J, Luo X, Qi X, Tan W, Huang GN, *et al.*** Heart repair by reprogramming non-myocytes with cardiac transcription factors. *Nature*. 2012; 485: 599–604.
236. **Palazzolo G, Quattrocelli M, Toelen J, Dominici R, Anastasia L, Tettamenti G, *et al.*** Cardiac Niche Influences the Direct Reprogramming of Canine Fibroblasts into Cardiomyocyte-Like Cells. *Stem cells international*. 2016; 2016: 4969430.
237. **Zhou H, Dickson ME, Kim MS, Bassel-Duby R, Olson EN**. Akt1/protein kinase B enhances transcriptional reprogramming of fibroblasts to functional cardiomyocytes. *Proceedings of the National Academy of Sciences of the United States of America*. 2015; 112: 11864–69.
238. **Islas JF, Liu Y, Weng K-C, Robertson MJ, Zhang S, Prejusa A, *et al.*** Transcription factors ETS2 and MESP1 transdifferentiate human dermal fibroblasts into cardiac progenitors. *Proc. Natl. Acad. Sci. U.S.A.* 2012; 109: 13016–21.
239. **Wang H, Cao N, Spencer CI, Nie B, Ma T, Xu T, *et al.*** Small molecules enable cardiac reprogramming of mouse fibroblasts with a single factor, Oct4. *Cell reports*. 2014; 6: 951–60.
240. **Zhao Y, Londono P, Cao Y, Sharpe EJ, Proenza C, O'Rourke R, *et al.*** High-efficiency reprogramming of fibroblasts into cardiomyocytes requires suppression of pro-fibrotic signalling. *Nature communications*. 2015; 6: 8243.

241. **Douglas KL**. Toward development of artificial viruses for gene therapy: a comparative evaluation of viral and non-viral transfection. *Biotechnology progress*. 2008; 24: 871–83.
242. **Yin H, Kanasty RL, Eltoukhy AA, Vegas AJ, Dorkin JR, Anderson DG**. Non-viral vectors for gene-based therapy. *Nature reviews. Genetics*. 2014; 15: 541–55.
243. **Nowakowski A, Andrzejewska A, Janowski M, Walczak P, Lukomska B**. Genetic engineering of stem cells for enhanced therapy. *Acta neurobiologiae experimentalis*. 2013; 73: 1–18.
244. **Sahin U, Kariko K, Tureci O**. mRNA-based therapeutics--developing a new class of drugs. *Nature reviews. Drug discovery*. 2014; 13: 759–80.
245. **Youn H, Chung J-K**. Modified mRNA as an alternative to plasmid DNA (pDNA) for transcript replacement and vaccination therapy. *Expert opinion on biological therapy*. 2015; 15: 1337–48.
246. **David R, Joos TO, Dreyer C**. Anteroposterior patterning and organogenesis of Xenopus laevis require a correct dose of germ cell nuclear factor (xGCNF). *Mechanisms of Development*. 1998; 79: 137–52.
247. **Kriegmair, Maximilian C M, Frenz S, Dusl M, Franz W-M, David R, Rupp, Ralph A W**. Cardiac differentiation in Xenopus is initiated by mespa. *Cardiovasc. Res.* 2013; 97: 454–63.
248. **Wolff JA, Malone RW, Williams P, Chong W, Acsadi G, Jani A, *et al.*** Direct gene transfer into mouse muscle in vivo. *Science*. 1990; 247: 1465–68.
249. **Wu X, Brewer G**. The regulation of mRNA stability in mammalian cells: 2.0. *Gene*. 2012; 500: 10–21.
250. **Grudzien-Nogalska E, Kowalska J, Su W, Kuhn AN, Slepenkov SV, Darzynkiewicz E, *et al.*** Synthetic mRNAs with superior translation and stability properties. *Methods in molecular biology (Clifton, N.J.)*. 2013; 969: 55–72.
251. **Gilboa E, Vieweg J**. Cancer immunotherapy with mRNA-transfected dendritic cells. *Immunol. Rev.* 2004; 199: 251–63.
252. **Pascolo S**. Vaccination with messenger RNA (mRNA). *Handb Exp Pharmacol*. 2008: 221–35.
253. **Van Craenenbroeck, Amaryllis H, Smits, Evelien L J, Anguille S, Van de Velde, Ann, Stein B, Braeckman T, *et al.*** Induction of Cytomegalovirus-Specific T Cell Responses in Healthy Volunteers and Allogeneic Stem Cell Recipients Using Vaccination With Messenger RNA-Transfected Dendritic Cells. *Transplantation*. 2014.
254. **Phua, Kyle K L, Nair SK, Leong KW**. Messenger RNA (mRNA) nanoparticle tumour vaccination. *Nanoscale*. 2014; 6: 7715–29.
255. **Pollard C, Koker S** de**, Saelens X, Vanham G, Grooten J**. Challenges and advances towards the rational design of mRNA vaccines. *Trends Mol Med*. 2013; 19: 705–13.
256. **Kormann, Michael S D, Hasenpusch G, Aneja MK, Nica G, Flemmer AW, Herber-Jonat S, *et al.*** Expression of therapeutic proteins after delivery of chemically modified mRNA in mice. *Nat. Biotechnol.* 2011; 29: 154–57.

257. **Karikó K, Muramatsu H, Keller JM, Weissman D**. Increased erythropoiesis in mice injected with submicrogram quantities of pseudouridine-containing mRNA encoding erythropoietin. *Mol. Ther.* 2012; 20: 948–53.
258. **D A Melton, P A Krieg, M R Rebagliati, T Maniatis, K Zinn, and M R Green**. Efficient in vitro synthesis of biologically active RNA and RNA hybridization probes from plasmids containing a bacteriophage SP6 promoter. *Nucleic Acids Res.* 1984: 7035–56.
259. **P Davanloo, A H Rosenberg, J J Dunn, and F W Studier**. Cloning and expression of the gene for bacteriophage T7 RNA polymerase. *Proc. Natl. Acad. Sci. U.S.A.* 1984: 2035–39.
260. **Zohra FT, Chowdhury EH, Tada S, Hoshiba T, Akaike T**. Effective delivery with enhanced translational activity synergistically accelerates mRNA-based transfection. *Biochem. Biophys. Res. Commun.* 2007; 358: 373–78.
261. **Gingras AC, Raught B, Sonenberg N**. eIF4 initiation factors: effectors of mRNA recruitment to ribosomes and regulators of translation. *Annual review of biochemistry*. 1999; 68: 913–63.
262. **Izaurralde E, Lewis J, McGuigan C, Jankowska M, Darzynkiewicz E, Mattaj IW**. A nuclear cap binding protein complex involved in pre-mRNA splicing. *Cell*. 1994; 78: 657–68.
263. **Coutts M, Krowczynska A, Brawerman G**. Protection of mRNA against nucleases in cytoplasmic extracts of mouse sarcoma ascites cells. *Biochimica et Biophysica Acta (BBA) - Gene Structure and Expression*. 1993; 1173: 49–56.
264. **Ziemniak M, Kowalska J, Lukaszewicz M, Zuberek J, Wnek K, Darzynkiewicz E*, et al.*** Phosphate-modified analogues of m(7)GTP and m(7)Gppppm(7)G-Synthesis and biochemical properties. *Bioorganic & medicinal chemistry*. 2015; 23: 5369–81.
265. **Byszewska M, Smietanski M, Purta E, Bujnicki JM**. RNA methyltransferases involved in 5' cap biosynthesis. *RNA biology*. 2014; 11: 1597–607.
266. **Mathonnet G, Fabian MR, Svitkin YV, Parsyan A, Huck L, Murata T, *et al.*** MicroRNA inhibition of translation initiation in vitro by targeting the cap-binding complex eIF4F. *Science (New York, N.Y.)*. 2007; 317: 1764–67.
267. **Zdanowicz A, Thermann R, Kowalska J, Jemielity J, Duncan K, Preiss T, *et al.*** Drosophila miR2 primarily targets the m7GpppN cap structure for translational repression. *Molecular cell*. 2009; 35: 881–88.
268. **Kozak M**. An analysis of 5'-noncoding sequences from 699 vertebrate messenger RNAs. *Nucleic acids research*. 1987; 15: 8125–48.
269. **Nakagawa S, Niimura Y, Gojobori T, Tanaka H, Miura K-i**. Diversity of preferred nucleotide sequences around the translation initiation codon in eukaryote genomes. *Nucleic acids research*. 2008; 36: 861–71.
270. **Polychronakos C**. Gene expression as a quantitative trait: what about translation? *Journal of medical genetics*. 2012; 49: 554–57.
271. **Karikó K, Buckstein M, Ni H, Weissman D**. Suppression of RNA recognition by Toll-like receptors: the impact of nucleoside modification and the evolutionary origin of RNA. *Immunity*. 2005; 23: 165–75.

272. **Karikó K, Muramatsu H, Welsh FA, Ludwig J, Kato H, Akira S, *et al.*** Incorporation of pseudouridine into mRNA yields superior nonimmunogenic vector with increased translational capacity and biological stability. *Mol. Ther.* 2008; 16: 1833–40.
273. **Davis DR**. Stabilization of RNA stacking by pseudouridine. *Nucleic Acids Res.* 1995: 5020–26.
274. **Nallagatla SR, Bevilacqua PC**. Nucleoside modifications modulate activation of the protein kinase PKR in an RNA structure-specific manner. *RNA*. 2008; 14: 1201–13.
275. **Hornung V, Ellegast J, Kim S, Brzózka K, Jung A, Kato H, *et al.*** 5'-Triphosphate RNA is the ligand for RIG-I. *Science*. 2006; 314: 994–97.
276. **Hausburg F, Naß S, Voronina N, Skorska A, Müller P, Steinhoff G, *et al.*** Defining optimized properties of modified mRNA to enhance virus- and DNA- independent protein expression in adult stem cells and fibroblasts. *Cellular physiology and biochemistry : international journal of experimental cellular physiology, biochemistry, and pharmacology*. 2015; 35: 1360–71.
277. **Li B, Luo X, Dong Y**. Effects of Chemically Modified Messenger RNA on Protein Expression. *Bioconjugate chemistry*. 2016; 27: 849–53.
278. **Eberhardt W, Doller A, Akool E-S, Pfeilschifter J**. Modulation of mRNA stability as a novel therapeutic approach. *Pharmacology & therapeutics*. 2007; 114: 56–73.
279. **Espel E**. The role of the AU-rich elements of mRNAs in controlling translation. *Seminars in cell & developmental biology*. 2005; 16: 59–67.
280. **Su W, Slevin MK, Marzluff WF, Rhoads RE**. Synthetic mRNA with Superior Properties that Mimics the Intracellular Fates of Natural Histone mRNA. *Methods in molecular biology (Clifton, N.J.)*. 2016; 1428: 93–114.
281. **Peng J, Murray EL, Schoenberg DR**. In vivo and in vitro analysis of poly(A) length effects on mRNA translation. *Methods in molecular biology (Clifton, N.J.)*. 2008; 419: 215–30.
282. **Chang H, Lim J, Ha M, Kim VN**. TAIL-seq: genome-wide determination of poly(A) tail length and 3' end modifications. *Molecular cell*. 2014; 53: 1044–52.
283. **Gallie DR**. The cap and poly(A) tail function synergistically to regulate mRNA translational efficiency. *Genes & development*. 1991; 5: 2108–16.
284. **Karikó K, Muramatsu H, Ludwig J, Weissman D**. Generating the optimal mRNA for therapy: HPLC purification eliminates immune activation and improves translation of nucleoside-modified, protein-encoding mRNA. *Nucleic Acids Res.* 2011; 39: e142.
285. **Weide B, Pascolo S, Scheel B, Derhovanessian E, Pflugfelder A, Eigentler TK, *et al.*** Direct injection of protamine-protected mRNA: results of a phase 1/2 vaccination trial in metastatic melanoma patients. *Journal of immunotherapy (Hagerstown, Md. : 1997)*. 2009; 32: 498–507.
286. **Rittig SM, Haentschel M, Weimer KJ, Heine A, Muller MR, Brugger W, *et al.*** Intradermal vaccinations with RNA coding for TAA generate CD8+ and CD4+ immune responses and induce clinical benefit in vaccinated patients. *Molecular therapy : the journal of the American Society of Gene Therapy*. 2011; 19: 990–99.

287. **Zangi L, Lui KO, Gise A** von**, Ma Q, Ebina W, Ptaszek LM*, et al.*** Modified mRNA directs the fate of heart progenitor cells and induces vascular regeneration after myocardial infarction. *Nat. Biotechnol.* 2013; 31: 898–907.
288. **Huang C-L, Leblond A-L, Turner EC, Kumar AH, Martin K, Whelan D*, et al.*** Synthetic chemically modified mrna-based delivery of cytoprotective factor promotes early cardiomyocyte survival post-acute myocardial infarction. *Molecular pharmaceutics*. 2015; 12: 991–96.
289. **Turnbull IC, Eltoukhy AA, Fish KM, Nonnenmacher M, Ishikawa K, Chen J, *et al.*** Myocardial Delivery of Lipidoid Nanoparticle Carrying modRNA Induces Rapid and Transient Expression. *Molecular therapy : the journal of the American Society of Gene Therapy*. 2016; 24: 66–75.
290. **Porrello ER**. microRNAs in cardiac development and regeneration. *Clinical science (London, England : 1979)*. 2013; 125: 151–66.
291. **Liu N, Olson EN**. MicroRNA regulatory networks in cardiovascular development. *Developmental cell*. 2010; 18: 510–25.
292. **Kamps JA, Krenning G**. Micromanaging cardiac regeneration: Targeted delivery of microRNAs for cardiac repair and regeneration. *World journal of cardiology*. 2016; 8: 163–79.
293. **Chitwood DH, Timmermans MCP**. Target mimics modulate miRNAs. *Nature genetics*. 2007; 39: 935–36.
294. **Behm-Ansmant I, Rehwinkel J, Izaurralde E**. MicroRNAs silence gene expression by repressing protein expression and/or by promoting mRNA decay. *Cold Spring Harbor symposia on quantitative biology*. 2006; 71: 523–30.
295. **Grimson A, Farh KK-H, Johnston WK, Garrett-Engele P, Lim LP, Bartel DP**. MicroRNA targeting specificity in mammals: determinants beyond seed pairing. *Molecular cell*. 2007; 27: 91–105.
296. **Bartel DP**. MicroRNAs: genomics, biogenesis, mechanism, and function. *Cell*. 2004; 116: 281–97.
297. **Bartel DP**. MicroRNAs: target recognition and regulatory functions. *Cell*. 2009; 136: 215–33.
298. **Kozomara A, Griffiths-Jones S**. miRBase: annotating high confidence microRNAs using deep sequencing data. *Nucleic acids research*. 2014; 42: D68-73.
299. **Guo H, Ingolia NT, Weissman JS, Bartel DP**. Mammalian microRNAs predominantly act to decrease target mRNA levels. *Nature*. 2010; 466: 835–40.
300. **Hendrickson DG, Hogan DJ, McCullough HL, Myers JW, Herschlag D, Ferrell JE*, et al.*** Concordant regulation of translation and mRNA abundance for hundreds of targets of a human microRNA. *PLoS biology*. 2009; 7: e1000238.
301. **Baek D, Villen J, Shin C, Camargo FD, Gygi SP, Bartel DP**. The impact of microRNAs on protein output. *Nature*. 2008; 455: 64–71.

302. **Selbach M, Schwanhausser B, Thierfelder N, Fang Z, Khanin R, Rajewsky N**. Widespread changes in protein synthesis induced by microRNAs. *Nature*. 2008; 455: 58–63.
303. **Fu J-D, Rushing SN, Lieu DK, Chan CW, Kong C-W, Geng L*, et al.*** Distinct roles of microRNA-1 and -499 in ventricular specification and functional maturation of human embryonic stem cell-derived cardiomyocytes. *PloS one*. 2011; 6: e27417.
304. **Wilson KD, Hu S, Venkatasubrahmanyam S, Fu J-D, Sun N, Abilez OJ*, et al.*** Dynamic microRNA expression programs during cardiac differentiation of human embryonic stem cells: role for miR-499. *Circulation. Cardiovascular genetics*. 2010; 3: 426–35.
305. **Zhao Y, Samal E, Srivastava D**. Serum response factor regulates a muscle-specific microRNA that targets Hand2 during cardiogenesis. *Nature*. 2005; 436: 214–20.
306. **Liu N, Williams AH, Kim Y, McAnally J, Bezprozvannaya S, Sutherland LB*, et al.*** An intragenic MEF2-dependent enhancer directs muscle-specific expression of microRNAs 1 and 133. *Proceedings of the National Academy of Sciences of the United States of America*. 2007; 104: 20844–49.
307. **Qian L, Wythe JD, Liu J, Cartry J, Vogler G, Mohapatra B*, et al.*** Tinman/Nkx2-5 acts via miR-1 and upstream of Cdc42 to regulate heart function across species. *The Journal of cell biology*. 2011; 193: 1181–96.
308. **Ivey KN, Muth A, Arnold J, King FW, Yeh R-F, Fish JE*, et al.*** MicroRNA regulation of cell lineages in mouse and human embryonic stem cells. *Cell stem cell*. 2008; 2: 219–29.
309. **Kwon C, Han Z, Olson EN, Srivastava D**. MicroRNA1 influences cardiac differentiation in Drosophila and regulates Notch signaling. *Proceedings of the National Academy of Sciences of the United States of America*. 2005; 102: 18986–91.
310. **Sokol NS, Ambros V**. Mesodermally expressed Drosophila microRNA-1 is regulated by Twist and is required in muscles during larval growth. *Genes & development*. 2005; 19: 2343–54.
311. **Jayawardena TM, Egemnazarov B, Finch EA, Zhang L, Payne JA, Pandya K*, et al.*** MicroRNA-mediated in vitro and in vivo direct reprogramming of cardiac fibroblasts to cardiomyocytes. *Circ. Res.* 2012; 110: 1465–73.
312. **Jayawardena T, Mirotsou M, Dzau VJ**. Direct reprogramming of cardiac fibroblasts to cardiomyocytes using microRNAs. *Methods Mol. Biol.* 2014; 1150: 263–72.
313. **Sluijter, Joost P G, van Mil A, van Vliet P, Metz, Corina H G, Liu J, Doevendans PA*, et al.*** MicroRNA-1 and -499 regulate differentiation and proliferation in human-derived cardiomyocyte progenitor cells. *Arteriosclerosis, thrombosis, and vascular biology*. 2010; 30: 859–68.
314. **Hosoda T, Zheng H, Cabral-da-Silva M, Sanada F, Ide-Iwata N, Ogórek B*, et al.*** Human cardiac stem cell differentiation is regulated by a mircrine mechanism. *Circulation*. 2011; 123: 1287–96.
315. **Song C-L, Liu B, Wang J-P, Zhang B-L, Zhang J-C, Zhao L-Y*, et al.*** Anti-apoptotic effect of microRNA-30b in early phase of rat myocardial ischemia-reperfusion injury model. *Journal of cellular biochemistry*. 2015; 116: 2610–19.

316. **Yu B, Kim HW, Gong M, Wang J, Millard RW, Wang Y, *et al.*** Exosomes secreted from GATA-4 overexpressing mesenchymal stem cells serve as a reservoir of anti-apoptotic microRNAs for cardioprotection. *International journal of cardiology*. 2015; 182: 349–60.
317. **Wang H, Li J, Chi H, Zhang F, Zhu X, Cai J, *et al.*** MicroRNA-181c targets Bcl-2 and regulates mitochondrial morphology in myocardial cells. *Journal of cellular and molecular medicine*. 2015; 19: 2084–97.
318. **Song S, Seo H-H, Lee S-Y, Lee CY, Lee J, Yoo K-J, *et al.*** MicroRNA-17-mediated down-regulation of apoptotic protease activating factor 1 attenuates apoptosome formation and subsequent apoptosis of cardiomyocytes. *Biochemical and biophysical research communications*. 2015; 465: 299–304.
319. **Chen Z, Qi Y, Gao C**. Cardiac myocyte-protective effect of microRNA-22 during ischemia and reperfusion through disrupting the caveolin-3/eNOS signaling. *International journal of clinical and experimental pathology*. 2015; 8: 4614–26.
320. **Jakob P, Landmesser U**. Role of microRNAs in stem/progenitor cells and cardiovascular repair. *Cardiovascular Research*. 2012; 93: 614–22.
321. **Toldo S, Das A, Mezzaroma E, Chau VQ, Marchetti C, Durrant D, *et al.*** Induction of microRNA-21 with exogenous hydrogen sulfide attenuates myocardial ischemic and inflammatory injury in mice. *Circulation. Cardiovascular genetics*. 2014; 7: 311–20.
322. **Guo W, Liu H, Li L, Yang M, Du A**. Regulation of lovastatin on a key inflammation-related microRNA in myocardial cells. *Chinese medical journal*. 2014; 127: 2977–81.
323. **Ambros V**. The functions of animal microRNAs. *Nature*. 2004; 431: 350–55.
324. **Auerbach W, Dunmore JH, Fairchild-Huntress V, Fang Q, Auerbach AB, Huszar D, *et al.*** Establishment and chimera analysis of 129/SvEv- and C57BL/6-derived mouse embryonic stem cell lines. *BioTechniques*. 2000; 29: 1024-8, 1030, 1032.
325. **Gaebel R, Furlani D, Sorg H, Polchow B, Frank J, Bieback K, *et al.*** Cell origin of human mesenchymal stem cells determines a different healing performance in cardiac regeneration. *PLoS ONE*. 2011; 6: e15652.
326. **Sutherland DR, Anderson L, Keeney M, Nayar R, Chin-Yee I**. The ISHAGE guidelines for CD34+ cell determination by flow cytometry. International Society of Hematotherapy and Graft Engineering. *Journal of hematotherapy*. 1996; 5: 213–26.
327. **Voronina N, Lemcke H, Wiekhorst F, Kuhn J-P, Rimmbach C, Steinhoff G, *et al.*** Non-viral magnetic engineering of endothelial cells with microRNA and plasmid-DNA-An optimized targeting approach. *Nanomedicine : nanotechnology, biology, and medicine*. 2016.
328. **Müller P, Voronina N, Hausburg F, Lux CA, Wiekhorst F, Steinhoff G, *et al.*** Magnet-Bead Based MicroRNA Delivery System to Modify CD133+ Stem Cells. *Stem cells international*. 2016; 2016: 7152761.
329. **Almstatter I, Mykhaylyk O, Settles M, Altomonte J, Aichler M, Walch A, *et al.*** Characterization of magnetic viral complexes for targeted delivery in oncology. *Theranostics*. 2015; 5: 667–85.

330. **Poller WC, Lowa N, Wiekhorst F, Taupitz M, Wagner S, Moller K, *et al.*** Magnetic Particle Spectroscopy Reveals Dynamic Changes in the Magnetic Behavior of Very Small Superparamagnetic Iron Oxide Nanoparticles During Cellular Uptake and Enables Determination of Cell-Labeling Efficacy. *Journal of biomedical nanotechnology*. 2016; 12: 337–46.
331. **Seki A, Fishbein MC**. Predicting the development of cardiac allograft vasculopathy. *Cardiovascular pathology : the official journal of the Society for Cardiovascular Pathology*. 2014; 23: 253–60.
332. Eurotransplant International Foundation. Annual Report 2015. Leiden; 2015.
333. **Zhang L, Nomura-Kitabayashi A, Sultana N, Cai W, Cai X, Moon AM, *et al.*** Mesodermal Nkx2.5 is necessary and sufficient for early second heart field development. *Developmental biology*. 2014; 390: 68–79.
334. **Niwa H**. How is pluripotency determined and maintained? *Development (Cambridge, England)*. 2007; 134: 635–46.
335. **Bugorsky R, Perriard J-C, Vassalli G**. Genetic selection system allowing monitoring of myofibrillogenesis in living cardiomyocytes derived from mouse embryonic stem cells. *European journal of histochemistry : EJH*. 2008; 52: 1–10.
336. **Xu XQ, Zweigerdt R, Soo SY, Ngoh ZX, Tham SC, Wang ST, *et al.*** Highly enriched cardiomyocytes from human embryonic stem cells. *Cytotherapy*. 2008; 10: 376–89.
337. **Kita-Matsuo H, Barcova M, Prigozhina N, Salomonis N, Wei K, Jacot JG, *et al.*** Lentiviral vectors and protocols for creation of stable hESC lines for fluorescent tracking and drug resistance selection of cardiomyocytes. *PloS one*. 2009; 4: e5046.
338. **Mahdavi V, Chambers AP, Nadal-Ginard B**. Cardiac alpha- and beta-myosin heavy chain genes are organized in tandem. *Proceedings of the National Academy of Sciences of the United States of America*. 1984; 81: 2626–30.
339. **Nadal-Ginard B, Mahdavi V**. Expression of the cardiac ventricular alpha- and beta-myosin heavy chain genes is developmentally and hormonally regulated. *The Journal of biological chemistry*. 1984; 259: 6437–46.
340. **Mercadier JJ, Wisnewsky C, Bouveret P, Pantaloni C, D'Albis A, Schwartz K**. Species- and age-dependent changes in the relative amounts of cardiac myosin isoenzymes in mammals. *Developmental biology*. 1981; 84: 286–90.
341. **Mamidi R, Mallampalli SL, Wieczorek DF, Chandra M**. Identification of two new regions in the N-terminus of cardiac troponin T that have divergent effects on cardiac contractile function. *The Journal of physiology*. 2013; 591: 1217–34.
342. **Zot AS, Potter JD**. Structural aspects of troponin-tropomyosin regulation of skeletal muscle contraction. *Annual review of biophysics and biophysical chemistry*. 1987; 16: 535–59.
343. **Ford SJ, Chandra M**. The effects of slow skeletal troponin I expression in the murine myocardium are influenced by development-related shifts in myosin heavy chain isoform. *The Journal of physiology*. 2012; 590: 6047–63.

344. **Verheule S, Kaese S**. Connexin diversity in the heart: Insights from transgenic mouse models. *Front. Pharmacol.* 2013; 4.
345. **Takebe K, Oyamada Y**. Regulation of connexin expression by transcription factors and epigenetic mechanisms. *Biochimica et biophysica acta*. 2013; 1828: 118–33.
346. **Goodenough DA, Goliger JA, Paul DL**. Connexins, connexons, and intercellular communication. *Annual review of biochemistry*. 1996; 65: 475–502.
347. **Herve J-C, Bourmeyster N, Sarrouilhe D, Duffy HS**. Gap junctional complexes: from partners to functions. *Progress in biophysics and molecular biology*. 2007; 94: 29–65.
348. **Bruzzone R, White TW, Paul DL**. Connections with Connexins: The Molecular Basis of Direct Intercellular Signaling. *Eur J Biochem*. 1996; 238: 1–27.
349. **Harris AL**. Connexin channel permeability to cytoplasmic molecules. *Progress in biophysics and molecular biology*. 2007; 94: 120–43.
350. **Kasahara H, Wakimoto H, Liu M, Maguire CT, Converso KL, Shioi T*, et al.*** Progressive atrioventricular conduction defects and heart failure in mice expressing a mutant Csx/Nkx2.5 homeoprotein. *The Journal of clinical investigation*. 2001; 108: 189–201.
351. **Dupays L, Jarry-Guichard T, Mazurais D, Calmels T, Izumo S, Gros D*, et al.*** Dysregulation of connexins and inactivation of NFATc1 in the cardiovascular system of Nkx2-5 null mutants. *Journal of molecular and cellular cardiology*. 2005; 38: 787–98.
352. **Kasahara H, Ueyama T, Wakimoto H, Liu MK, Maguire CT, Converso KL*, et al.*** Nkx2.5 homeoprotein regulates expression of gap junction protein connexin 43 and sarcomere organization in postnatal cardiomyocytes. *Journal of molecular and cellular cardiology*. 2003; 35: 243–56.
353. **Teunissen BEJ, Jansen AT, van Amersfoorth, Shirley C M, O'Brien TX, Jongsma HJ, Bierhuizen MFA**. Analysis of the rat connexin 43 proximal promoter in neonatal cardiomyocytes. *Gene*. 2003; 322: 123–36.
354. **Bers DM**. Macromolecular complexes regulating cardiac ryanodine receptor function. *Journal of molecular and cellular cardiology*. 2004; 37: 417–29.
355. **Camors E, Valdivia HH**. CaMKII regulation of cardiac ryanodine receptors and inositol triphosphate receptors. *Frontiers in pharmacology*. 2014; 5: 101.
356. **Nenasheva TA, Neary M, Mashanov GI, Birdsall NJM, Breckenridge RA, Molloy JE**. Abundance, distribution, mobility and oligomeric state of M(2) muscarinic acetylcholine receptors in live cardiac muscle. *Journal of molecular and cellular cardiology*. 2013; 57: 129–36.
357. **Haga K, Kruse AC, Asada H, Yurugi-Kobayashi T, Shiroishi M, Zhang C*, et al.*** Structure of the human M2 muscarinic acetylcholine receptor bound to an antagonist. *Nature*. 2012; 482: 547–51.
358. **Petitprez S, Jespersen T, Pruvot E, Keller DI, Corbaz C, Schlapfer J*, et al.*** Analyses of a novel SCN5A mutation (C1850S): conduction vs. repolarization disorder hypotheses in the Brugada syndrome. *Cardiovascular Research*. 2008; 78: 494–504.

359. **Liu M, Yang K-C, Dudley SC, JR**. Cardiac Sodium Channel Mutations: Why so Many Phenotypes? *Current topics in membranes*. 2016; 78: 513–59.
360. **DeMarco KR, Clancy CE**. Cardiac Na Channels: Structure to Function. *Current topics in membranes*. 2016; 78: 287–311.
361. **Goldin AL**. Resurgence of sodium channel research. *Annual review of physiology*. 2001; 63: 871–94.
362. **Brette F, Orchard CH**. No apparent requirement for neuronal sodium channels in excitation-contraction coupling in rat ventricular myocytes. *Circulation research*. 2006; 98: 667–74.
363. **Haufe V, Camacho JA, Dumaine R, Gunther B, Bollensdorff C, Banchet GS** von***, et al.*** Expression pattern of neuronal and skeletal muscle voltage-gated Na+ channels in the developing mouse heart. *The Journal of physiology*. 2005; 564: 683–96.
364. **Malhotra JD, Chen C, Rivolta I, Abriel H, Malhotra R, Mattei LN, *et al.*** Characterization of Sodium Channel - and -Subunits in Rat and Mouse Cardiac Myocytes. *Circulation*. 2001; 103: 1303–10.
365. **Maier SKG, Westenbroek RE, McCormick KA, Curtis R, Scheuer T, Catterall WA**. Distinct subcellular localization of different sodium channel alpha and beta subunits in single ventricular myocytes from mouse heart. *Circulation*. 2004; 109: 1421–27.
366. **Maier SKG, Westenbroek RE, Schenkman KA, Feigl EO, Scheuer T, Catterall WA**. An unexpected role for brain-type sodium channels in coupling of cell surface depolarization to contraction in the heart. *Proceedings of the National Academy of Sciences of the United States of America*. 2002; 99: 4073–78.
367. **Lei M, Jones SA, Liu J, Lancaster MK, Fung SS-M, Dobrzynski H, *et al.*** Requirement of neuronal- and cardiac-type sodium channels for murine sinoatrial node pacemaking. *The Journal of physiology*. 2004; 559: 835–48.
368. **Duclohier H**. Neuronal sodium channels in ventricular heart cells are localized near T-tubules openings. *Biochemical and biophysical research communications*. 2005; 334: 1135–40.
369. **Torres NS, Larbig R, Rock A, Goldhaber JI, Bridge JHB**. Na+ currents are required for efficient excitation-contraction coupling in rabbit ventricular myocytes: a possible contribution of neuronal Na+ channels. *The Journal of physiology*. 2010; 588: 4249–60.
370. **Bodi I, Mikala G, Koch SE, Akhter SA, Schwartz A**. The L-type calcium channel in the heart: the beat goes on. *The Journal of clinical investigation*. 2005; 115: 3306–17.
371. **Leuranguer V, Mangoni ME, Nargeot J, Richard S**. Inhibition of T-type and L-type calcium channels by mibefradil: physiologic and pharmacologic bases of cardiovascular effects. *Journal of cardiovascular pharmacology*. 2001; 37: 649–61.
372. **Bergson P, Lipkind G, Lee SP, Duban M-E, Hanck DA**. Verapamil block of T-type calcium channels. *Molecular pharmacology*. 2011; 79: 411–19.
373. **Ono K, Iijima T**. Pathophysiological significance of T-type Ca2+ channels: properties and functional roles of T-type Ca2+ channels in cardiac pacemaking. *Journal of pharmacological sciences*. 2005; 99: 197–204.

374. **Ono K, Iijima T**. Cardiac T-type Ca(2+) channels in the heart. *Journal of molecular and cellular cardiology*. 2010; 48: 65–70.
375. **Martin RL, Lee JH, Cribbs LL, Perez-Reyes E, Hanck DA**. Mibefradil block of cloned T-type calcium channels. *The Journal of pharmacology and experimental therapeutics*. 2000; 295: 302–08.
376. **Clozel JP, Ertel EA, Ertel SI**. Discovery and main pharmacological properties of mibefradil (Ro 40-5967), the first selective T-type calcium channel blocker. *Journal of hypertension. Supplement : official journal of the International Society of Hypertension*. 1997; 15: S17-25.
377. **Avci-Adali M, Behring A, Keller T, Krajewski S, Schlensak C, Wendel HP**. Optimized conditions for successful transfection of human endothelial cells with in vitro synthesized and modified mRNA for induction of protein expression. *J Biol Eng*. 2014; 8: 8.
378. **Avci-Adali M, Behring A, Steinle H, Keller T, Krajeweski S, Schlensak C*, et al.*** In vitro synthesis of modified mRNA for induction of protein expression in human cells. *Journal of visualized experiments : JoVE*. 2014: e51943.
379. **Andries O, Mc Cafferty S, Smedt SC** de**, Weiss R, Sanders NN, Kitada T**. N(1)-methylpseudouridine-incorporated mRNA outperforms pseudouridine-incorporated mRNA by providing enhanced protein expression and reduced immunogenicity in mammalian cell lines and mice. *Journal of controlled release : official journal of the Controlled Release Society*. 2015; 217: 337–44.
380. **Schiaffino S, Reggiani C**. Myosin isoforms in mammalian skeletal muscle. *Journal of applied physiology (Bethesda, Md. : 1985)*. 1994; 77: 493–501.
381. **Stamm C, Kleine H-D, Choi Y-H, Dunkelmann S, Lauffs J-A, Lorenzen B*, et al.*** Intramyocardial delivery of CD133+ bone marrow cells and coronary artery bypass grafting for chronic ischemic heart disease: safety and efficacy studies. *The Journal of Thoracic and Cardiovascular Surgery*. 2007; 133: 717–25.
382. **Zhang X, Lian W, Lou W, Han S, Lu C, Zuo K*, et al.*** Transcatheter Arterial Infusion of Autologous CD133(+) Cells for Diabetic Peripheral Artery Disease. *Stem cells international*. 2016; 2016: 6925357.
383. **King A, Barton D, Beard HA, Than N, Moore J, Corbett C*, et al.*** REpeated AutoLogous Infusions of STem cells In Cirrhosis (REALISTIC): a multicentre, phase II, open-label, randomised controlled trial of repeated autologous infusions of granulocyte colony-stimulating factor (GCSF) mobilised CD133+ bone marrow stem cells in patients with cirrhosis. A study protocol for a randomised controlled trial. *BMJ open*. 2015; 5: e007700.
384. **Moore JK, Stutchfield BM, Forbes SJ**. Systematic review: the effects of autologous stem cell therapy for patients with liver disease. *Alimentary pharmacology & therapeutics*. 2014; 39: 673–85.
385. **Martinez HR, Molina-Lopez JF, Gonzalez-Garza MT, Moreno-Cuevas JE, Caro-Osorio E, Gil-Valadez A*, et al.*** Stem cell transplantation in amyotrophic lateral sclerosis

patients: methodological approach, safety, and feasibility. *Cell transplantation*. 2012; 21: 1899–907.

386. **Jimenez-Quevedo P, Gonzalez-Ferrer JJ, Sabate M, Garcia-Moll X, Delgado-Bolton R, Llorente L*, et al.*** Selected CD133(+) progenitor cells to promote angiogenesis in patients with refractory angina: final results of the PROGENITOR randomized trial. *Circulation research*. 2014; 115: 950–60.
387. **Raval AN, Schmuck EG, Tefera G, Leitzke C, Ark CV, Hei D*, et al.*** Bilateral administration of autologous CD133+ cells in ambulatory patients with refractory critical limb ischemia: lessons learned from a pilot randomized, double-blind, placebo-controlled trial. *Cytotherapy*. 2014; 16: 1720–32.
388. **Andreone P, Catani L, Margini C, Brodosi L, Lorenzini S, Sollazzo D*, et al.*** Reinfusion of highly purified CD133+ bone marrow-derived stem/progenitor cells in patients with end-stage liver disease: A phase I clinical trial. *Digestive and liver disease : official journal of the Italian Society of Gastroenterology and the Italian Association for the Study of the Liver*. 2015; 47: 1059–66.
389. **Arici V, Perotti C, Fabrizio C, Del Fante C, Ragni F, Alessandrino F*, et al.*** Autologous immuno magnetically selected CD133+ stem cells in the treatment of no-option critical limb ischemia: clinical and contrast enhanced ultrasound assessed results in eight patients. *Journal of translational medicine*. 2015; 13: 342.
390. **Zali A, Arab L, Ashrafi F, Mardpour S, Niknejhadi M, Hedayati-Asl AA*, et al.*** Intrathecal injection of CD133-positive enriched bone marrow progenitor cells in children with cerebral palsy: feasibility and safety. *Cytotherapy*. 2015; 17: 232–41.
391. **Al-Zoubi A, Jafar E, Jamous M, Al-Twal F, Al-Bakheet S, Zalloum M, *et al.*** Transplantation of purified autologous leukapheresis-derived CD34+ and CD133+ stem cells for patients with chronic spinal cord injuries: long-term evaluation of safety and efficacy. *Cell transplantation*. 2014; 23 Suppl 1: S25-34.
392. **Isidori A, Motta MR, Tani M, Terragna C, Zinzani P, Curti A*, et al.*** Positive selection and transplantation of autologous highly purified CD133(+) stem cells in resistant/relapsed chronic lymphocytic leukemia patients results in rapid hematopoietic reconstitution without an adequate leukemic cell purging. *Biology of blood and marrow transplantation : journal of the American Society for Blood and Marrow Transplantation*. 2007; 13: 1224–32.
393. **Nasseri BA, Ebell W, Dandel M, Kukucka M, Gebker R, Doltra A, *et al.*** Autologous CD133+ bone marrow cells and bypass grafting for regeneration of ischaemic myocardium: the Cardio133 trial. *European heart journal*. 2014; 35: 1263–74.
394. **Meregalli M, Farini A, Belicchi M, Torrente Y**. CD133(+) cells isolated from various sources and their role in future clinical perspectives. *Expert opinion on biological therapy*. 2010; 10: 1521–28.
395. **Lee S, Yoon Y-S**. Revisiting cardiovascular regeneration with bone marrow-derived angiogenic and vasculogenic cells. *British journal of pharmacology*. 2013; 169: 290–303.
396. **Beksac M, Preffer F**. Is it time to revisit our current hematopoietic progenitor cell quantification methods in the clinic? *Bone marrow transplantation*. 2012; 47: 1391–96.

397. **Barcelos LS, Duplaa C, Krankel N, Graiani G, Invernici G, Katare R, *et al.*** Human CD133+ progenitor cells promote the healing of diabetic ischemic ulcers by paracrine stimulation of angiogenesis and activation of Wnt signaling. *Circulation research*. 2009; 104: 1095–102.
398. **Gehling UM, Ergun S, Schumacher U, Wagener C, Pantel K, Otte M, *et al.*** In vitro differentiation of endothelial cells from AC133-positive progenitor cells. *Blood*. 2000; 95: 3106–12.
399. **Akita M, Tanaka K, Matsumoto S, Komatsu K, Fujita K**. Detection of the Hematopoietic Stem and Progenitor Cell Marker CD133 during Angiogenesis in Three-Dimensional Collagen Gel Culture. *Stem cells international*. 2013; 2013: 927403.
400. **Meng J, Chun S, Asfahani R, Lochmuller H, Muntoni F, Morgan J**. Human skeletal muscle-derived CD133(+) cells form functional satellite cells after intramuscular transplantation in immunodeficient host mice. *Molecular therapy : the journal of the American Society of Gene Therapy*. 2014; 22: 1008–17.
401. **Ohkawa S, Kamei N, Kamei G, Shi M, Adachi N, Deie M, *et al.*** Magnetic targeting of human peripheral blood CD133+ cells for skeletal muscle regeneration. *Tissue engineering. Part C, Methods*. 2013; 19: 631–41.
402. **Negroni E, Riederer I, Chaouch S, Belicchi M, Razini P, Di Santo J, *et al.*** In vivo myogenic potential of human CD133+ muscle-derived stem cells: a quantitative study. *Molecular therapy : the journal of the American Society of Gene Therapy*. 2009; 17: 1771–78.
403. **Shi M, Ishikawa M, Kamei N, Nakasa T, Adachi N, Deie M, *et al.*** Acceleration of skeletal muscle regeneration in a rat skeletal muscle injury model by local injection of human peripheral blood-derived CD133-positive cells. *Stem cells (Dayton, Ohio)*. 2009; 27: 949–60.
404. **Agbulut O, Vandervelde S, Al Attar N, Larghero J, Ghostine S, Leobon B, *et al.*** Comparison of human skeletal myoblasts and bone marrow-derived CD133+ progenitors for the repair of infarcted myocardium. *Journal of the American College of Cardiology*. 2004; 44: 458–63.
405. **Papapetrou EP, Zoumbos NC, Athanassiadou A**. Genetic modification of hematopoietic stem cells with nonviral systems: past progress and future prospects. *Gene therapy*. 2005; 12 Suppl 1: S118-30.
406. **Peng B, Chen Y, Leong KW**. MicroRNA delivery for regenerative medicine. *Advanced drug delivery reviews*. 2015; 88: 108–22.
407. **Delyagina E, Li W, Ma N, Steinhoff G**. Magnetic targeting strategies in gene delivery. *Nanomedicine (Lond)*. 2011; 6: 1593–604.
408. **Schade A, Delyagina E, Scharfenberg D, Skorska A, Lux C, David R, *et al.*** Innovative Strategy for MicroRNA Delivery in Human Mesenchymal Stem Cells via Magnetic Nanoparticles. *Int J Mol Sci*. 2013; 14: 10710–26.

409. **Schade A, Müller P, Delyagina E, Voronina N, Skorska A, Lux C*, et al.*** Magnetic Nanoparticle Based Nonviral MicroRNA Delivery into Freshly Isolated CD105(+) hMSCs. *Stem Cells Int*. 2014; 2014: 197154.
410. **Hobel S, Aigner A**. Polyethylenimines for siRNA and miRNA delivery in vivo. *Wiley interdisciplinary reviews. Nanomedicine and nanobiotechnology*. 2013; 5: 484–501.
411. **Cubillos-Ruiz JR, Sempere LF, Conejo-Garcia JR**. Good things come in small packages: Therapeutic anti-tumor immunity induced by microRNA nanoparticles. *Oncoimmunology*. 2012; 1: 968–70.
412. **Fujioka Y, Tanaka N, Nakanishi K, Kamei N, Nakamae T, Izumi B*, et al.*** Magnetic field-based delivery of human CD133(+) cells promotes functional recovery after rat spinal cord injury. *Spine*. 2012; 37: E768-77.
413. **Furlani EP, Xue X**. A model for predicting field-directed particle transport in the magnetofection process. *Pharmaceutical research*. 2012; 29: 1366–79.
414. **Fouriki A, Farrow N, Clements MA, Dobson J**. Evaluation of the magnetic field requirements for nanomagnetic gene transfection. *Nano reviews*. 2010; 1.
415. **Walasek MA, van Os R, Haan G** de. Hematopoietic stem cell expansion: challenges and opportunities. *Annals of the New York Academy of Sciences*. 2012; 1266: 138–50.
416. **Sauvageau G, Iscove NN, Humphries RK**. In vitro and in vivo expansion of hematopoietic stem cells. *Oncogene*. 2004; 23: 7223–32.
417. **Targoff KL, Colombo S, George V, Schell T, Kim SH, Solnica-Krezel L*, et al.*** Nkx genes are essential for maintenance of ventricular identity. *Development (Cambridge, England)*. 2013; 140: 4203–13.
418. **Lang C, Lehner S, Todica A, Boening G, Zacherl M, Franz W-M*, et al.*** In-vivo comparison of the acute retention of stem cell derivatives and fibroblasts after intramyocardial transplantation in the mouse model. *European journal of nuclear medicine and molecular imaging*. 2014; 41: 2325–36.
419. **Caveliers V, Keulenaer G** de**, Everaert H, van Riet I, van Camp G, Verheye S*, et al.*** In vivo visualization of 111In labeled CD133+ peripheral blood stem cells after intracoronary administration in patients with chronic ischemic heart disease. *The quarterly journal of nuclear medicine and molecular imaging : official publication of the Italian Association of Nuclear Medicine (AIMN) [and] the International Association of Radiopharmacology (IAR), [and] Section of the Society of...* 2007; 51: 61–66.

II. List of figures

III. List of tables

IV. List of abbreviations

abbreviations	Definition
α/βMHC	Alpha/beta myosin heavy chain
AV	atrioventricular
bp	Base pairs
BM	Bone marrow
Bry^+	Brachyury (T)
CABG	Coronary artery bypass graft
CHD	Congenital heart defect
CPC	Cardiac progenitor cell
CS	Conduction system
CVD	Cardiovascular diseases
cTnT	Cardiac Troponin T
DMEM	dulbecco's modified eagle medium
DNA	desoxyribonucleic acid
EB	embryoid body
(m)EF	(murine) embryonic fibroblast
EGFP	Enhanced green fluorescent protein
EMEM	eagle's minimal essential medium
(m/h)ESC	(murine/human) embryonic stem cell
FA	formaldehyde
FHF	First heart field
FITC	Fluorescein isothiocyanate
HSC	hematopoetic stem cells
IBM	Iscove's basal medium
iCM	Induced cardiomyocytes

IVT	*In vitro* transcription
LVEF	Left ventricular ejection fraction
MI	Myocard infarct
mmRNA	modified messengerRNA
MNC	Mononuclear cells
MPS	Magnetic particle spectroscopy
(h)MSC	(human) mesenchymal stem cell
Ψ	Pseudouridine-5'-triphosphate
qPCR	Quantitative real-time polymerase chain reaction
RNA	Ribonucleic acid
RT	Roomtemperature
SHF	Second heart field
TF	Transcription factor
THF	Tertiary heart field
5mC	5-methylcytidine-5'-triphosphate

V. Materials

Table 2: Antibodies and staining solutions

Antibody	Spezies	Conjugate	ID	company
anti-Cx43	rabbit, polyclonal		Sc9059	Santa Cruz Biotechnology, Inc., USA
anti-cTnnT	rabbit, polyconal		ab115134	Abcam, UK
anti-GFP	goat, polyclonal	FITC	ab6662	Abcam, UK
anti-MyHC (Myh6)	mouse, monoclonal		ab15	Abcam, UK
anti-Myosin (skeletal, slow) (Myh7)	mouse, monoclonal		M8421	Sigma-Aldrich GmbH, Germany
anti-Nkx2.5 (N-19)	goat, polyclonal		Sc8697	Santa Cruz Bio-technology, Inc., USA
anti-Oct4	rabbit, polyconal		ab19857	Abcam, UK
anti-sarcomeric α actinin	mouse, monoclonal		ab9465	Abcam, UK
anti-goat	donkey	Alexa Fluor® 568	A11036	Thermo Fisher Scientific Inc., USA
anti-mouse	goat	Alexa Fluor® 647	A21235	Thermo Fisher Scientific Inc., USA
anti-rabbit	donkey	Alexa Fluor® 488	A21206	Thermo Fisher Scientific Inc., USA
anti-rabbit	goat	Alexa Fluor® 568	A11011	Thermo Fisher Scientific Inc., USA
Atto 565				ATTO-TEC GmbH, Germany
Cy5™ dye				Molecular Probes, USA
FluoReporter® Oregon Green® 488				Molecular Probes, USA
Fluoroshield™ with DAPI				Sigma-Aldrich GmbH, Germany
Phalloidin		FITC		Enzo Life Science, Inc., USA
X-Rhod-1				Thermo Fisher Scientific Inc., USA

Table 3: Cell lines and primary cultures

Common name	description	Species	Company
BJ	foreskin fibroblasts	human, newborn	Stemgent, Cambridge, USA
COS7	kidney	monkey	ATCC, USA
C3H10T1/2	clone 8	murine, embryonic	ATCC, USA
SNL 76/7	STO cell line	murine, embryonic	Applied StemCell, Inc, USA
W4	mouse strain: 129/SvEV [324]	murine, embryonic	Taconic, Germantown, NY, USA
MSC	bone marrow	human, adult	sternal BM aspirates from donors, University Hospital Rostock, Germany*
CD133	bone marrow	human, adult	sternal BM aspirates from donors, University Hospital Rostock, Germany*

*approved by the ethical committee of the University of Rostock in 2010 and renewed in 2015 (registration number A 2010 23).

Table 4: Chemicals and reagents

products	company
Accutase® solution	Sigma-Aldrich GmbH, Germany
B18R Recombinant Protein	eBioscience, USA
β-mercaptoethanol	Sigma-Aldrich GmbH, Germany
Blasticidin (solution)	InvivoGen, USA
Cell Shield®	Minerva Biolabs GmbH, Germany
Cy5™ dye	Mirus Bio LLC, USA
Collagenase, Type: CLS IV (230 U/mg)	Biochrom AG, Germany
DMEM	Biochrom AG, Germany
EMEM	Biochrom AG, Germany
FBS	Pan Biotech GmbH, Germany
FBS superior	
FluoReporter® Oregon Green® 488	Molecular Probes, USA
Formaldehyde	Sigma-Aldrich GmbH, Germany
Gelatine (from cold water fish skin; 40-50% in H2O)	Sigma-Aldrich GmbH, Germany
glucose	MP Biomedicals, Germany
Herculase enhanced proof-reading DNA polymerase	Agilent Technologies, USA
horse serum	Life Technologies, USA
Hygromycin B Gold (solution)	InvivoGen, USA

leukemia inhibitory factor	Phoenix Europe GmbH, Germany
Mesenchymal Stem Cell Growth Medium; MSCGM™	Lonza, Walkersville, MD, USA
Near-IR LIVE/DEAD Fixable Dead Cell Stain Kit	Molecular Probes, USA
non-essential amino acids	Biochrom AG, Germany
PEI	Sigma-Aldrich GmbH, Germany
Penicillin/Streptomycin	PAA Laboratories GmbH, Germany
Pre-miR™ miRNA Precursor Molecules – Negative Control #1	Ambion, USA
pseudouridine-5'-triphosphate	TriLink Biotechnologies, USA
Puromycin (solution)	InvivoGen, USA
Saponin from quillaja bark; Sapogenin content ≥ 10%	Sigma-Aldrich GmbH, Germany
Streptavidin MagneSphere® Paramagnetic Particles	Promega Corporation, USA
TaqMan® Gene Expression Assays	Thermo Fisher Scientific Inc., USA
TaqMan® Universal PCR Master Mix	Thermo Fisher Scientific Inc., USA
UltraPure™ DNase/Rnase-Free Distilled Water	Thermo Fisher Scientific Inc., USA
3′-O-Me-m7G(ppp)G RNA cap structure analog	New England Biolabs, USA
5-methylcytidine-5'-triphosphate	TriLink Biotechnologies, USA

Table 5: Equipment

equipment	company
Axiovert 40 CFL	Carl Zeiss, Germany
BD FACS LSRII flow cytometer	BD Biosciences, Germany
ELYRA PS.1 LSM 780 confocal microscope	Carl Zeiss, Germany
MJ Mini™ thermal cycler	Bio-Rad Laboratories GmbH, Germany
NanoDrop 1000 Spectrophotometer	Thermo Fisher Scientific Inc., USA
StepOnePlus™ Real-Time PCR System	Applied Biosystems, Germany

Table 6: Flow cytometry antibodies

Antibody	Conjugate	company
Anti-CD34 (clone: AC136)	FITC	Miltenyi Biotec GmbH, Germany
anti-CD133/2 (clone: 293C3)	PE	Miltenyi Biotec GmbH, Germany
isotype control mouse IgG 2b	PE	Miltenyi Biotec GmbH, Germany
anti-	APC-H7	BD Biosciences, Germany

CD45 (clone: 2D1)	
7-AAD	BD Biosciences, Germany
Near-IR LIVE/DEAD Fixable Dead Cell Stain Kit	Molecular Probes, USA

Table 7: Kits

products	company
MACS CD133 MicroBeads, human	Miltenyi Biotec GmbH, Germany
GeneJET RNA Purification Kit	Thermo Fisher Scientific Inc., USA
jetPEI® DNA transfection reagent	Polyplus transfection®, USA
MEGAscript® SP6 Kit	Ambion, USA
MEGAscript® T7 Kit	Ambion, USA
NucleoSpin® RNA isolation kit	Macherey-Nagel, Germany
NucleoSpin® RNA isolation kit XS	Macherey-Nagel, Germany
peqGOLD Cycle-Pure Kit	peqlab, UK
RevertAid H Minus First Strand cDNA Synthesis Kit	Thermo Fisher Scientific Inc., USA

Table 8: Plasmids

Gene	Vector	company
αMHC-puromycin cassette	pGK-hygro	[155]
EGFP	pCS2+	
MyoD	pCS2+	
hNkx2.5	pEF-DEST51	Imagenes, Germany

Table 9: Primer PCR

Gene	Vector	Primer	Sequence	Size	Company
EGFP/ MyoD	pCS2+	pCS2SP6up20	5'-GTCGGAGCAAGCTTGATTAGG-3'	21 bp	
		pCS2pAlo152	5'-T100GTCTGGATCTACGTAATACG-3'		
Nkx2.5	pEF-DEST51				

Table 10: Software

Software	company
Adobe Photoshop CS6	Adobe Systems, USA
Adobe Illustrator CS6	Adobe Systems, USA
BD FACSDiva Software 6.1.2	BD Biosciences, Germany
CorelDraw Graphics Suite X5	Corel Corporation, USA
GraphPad Prism	GraphPad Software Inc., USA
ImageJ 1.48	NIH, USA
NanoDrop ND-1000 V3.7.1	NanoDrop products, USA
OriginPro 2016	OriginLab Corporation, USA
SigmaPlot 13.0	Systat Software GmbH, Germany
StepOne™ Software Version 2	Applied Biosystems, Germany
ZEN2011 software	Carl Zeiss, Germany

Table 11: TaqMan® Gene Expression Assays

Gene	Name	Species	Amplicon Length	Fluoro phore	Assay-ID
cTnnT2	Cardiac muscle troponin T	mouse	110	FAM	Mm01290256_m1
Fut4	3-fucosyl-N-acetyl-lactosamine, CD15 (Ssea1)	mouse	67	FAM	Mm00487448_s1
Gja1	Gap juction protein, alpha 1 (Cx43)	mouse	65	FAM	Mm00439105_m1
Gja3	Gap juction protein, alpha 3 (Cx46)	mouse	120	FAM	Mm01319074_m1
Hcn4	Potassium/sodium hyperpolarization-activated cyclic nucleotide-gate channel 4	mouse	70	FAM	Mm01176086_m1
Hprt	Hypoxanthine-guanine phosphoribosyltransferase	mouse	65	FAM	Mm00446968_m1
Isl1	Insulin gene enhancer protein	mouse	65	FAM	Mm00517585_m1
MesP1	Mesoderm posterior 1 homolog	mouse		FAM	Mm00801883_m1
Myh6	Myosin heavy chain, α isoform	mouse	67	FAM	Mm00440359_m1
Myh7	Myosin heavy chain, β isoform	mouse		FAM	
Myl2	Myosin regulatory light chain 2/	mouse	90	FAM	Mm00440384_m1

	ventricular/cardiac muscle isoform				
Nanog	Homeobox protein	mouse		FAM	Mm02019550_s1
Nkx2.5	Homeobox protein	mouse	56	FAM	Mm01309813_s1
Nkx2.5	Homeobox protein	human	64	FAM	Hs00231763_m1
Polr2a	DNA-directed RNA polymerase II subunit RPB1	mouse	85	FAM	Mm00839493_m1
Pou5f1	Octamer-binding transcription factor 4 (Oct4)	mouse		FAM	
Tbx3	T-box transcription factor 3	mouse	65	FAM	Mm01195726_m1
Tbx5	T-box transcription factor 5	mouse	94	FAM	Mm01195728_m1

All qPCR TaqMan® Gene Expression Assays were purchased from Thermo Fisher Scientific Inc., USA

VI. Supplementary figures

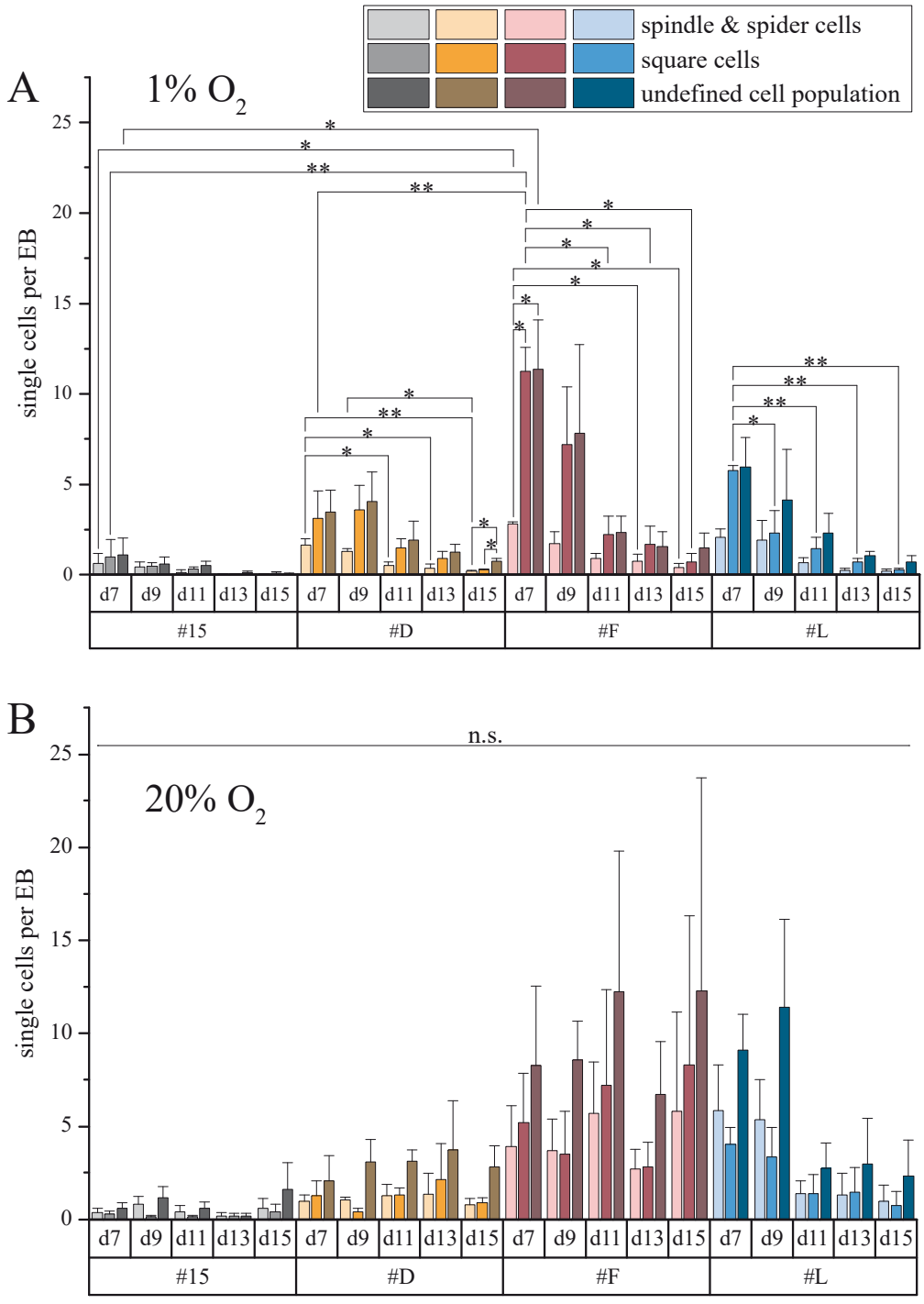

Figure 33: Quantitative determination of the optimal time point of antibiotic selection - single cell analysis

Quantitative analysis of antibiotic selection during cardiogenic differentiation of W4 αMHC clones – single cell analysis by cell morphology (spindle & spider cells: light colour, square cells: normal colour and an undefined cell population: dark colour). Enumerated single cells per EB under (A) 1 % O_2 and (B) 20 % O_2 oxygen conditions.

Values are presented as mean ± SEM; n=3; statistic was performed as multiple comparison of mean (ANOVA), *p ≤ 0.05, **p ≤ 0.01, ***p ≤ 0.001.

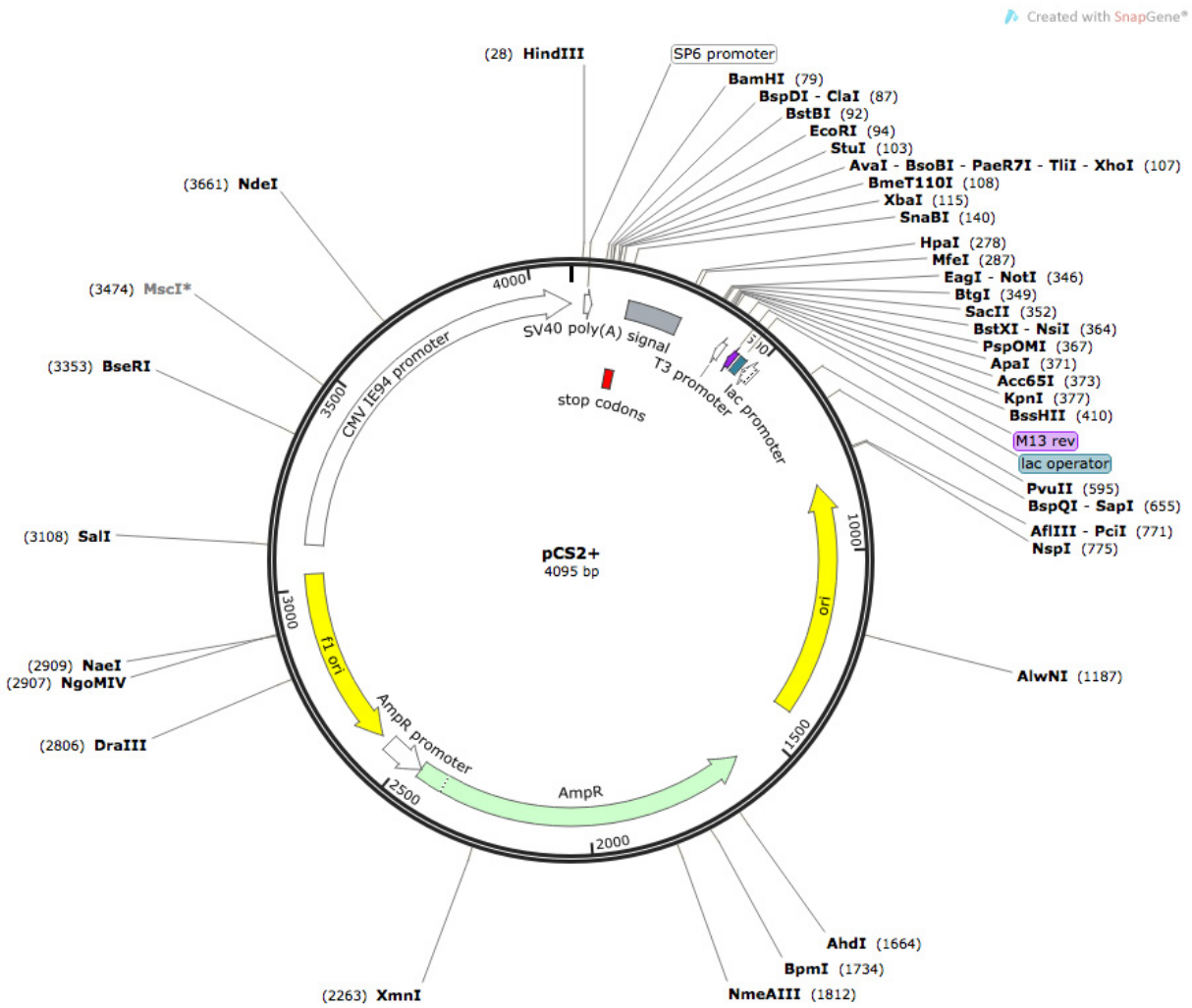

Figure 34: pCS2+ expression vector map (snapgene.com I.M.A.G.E. Consortium)

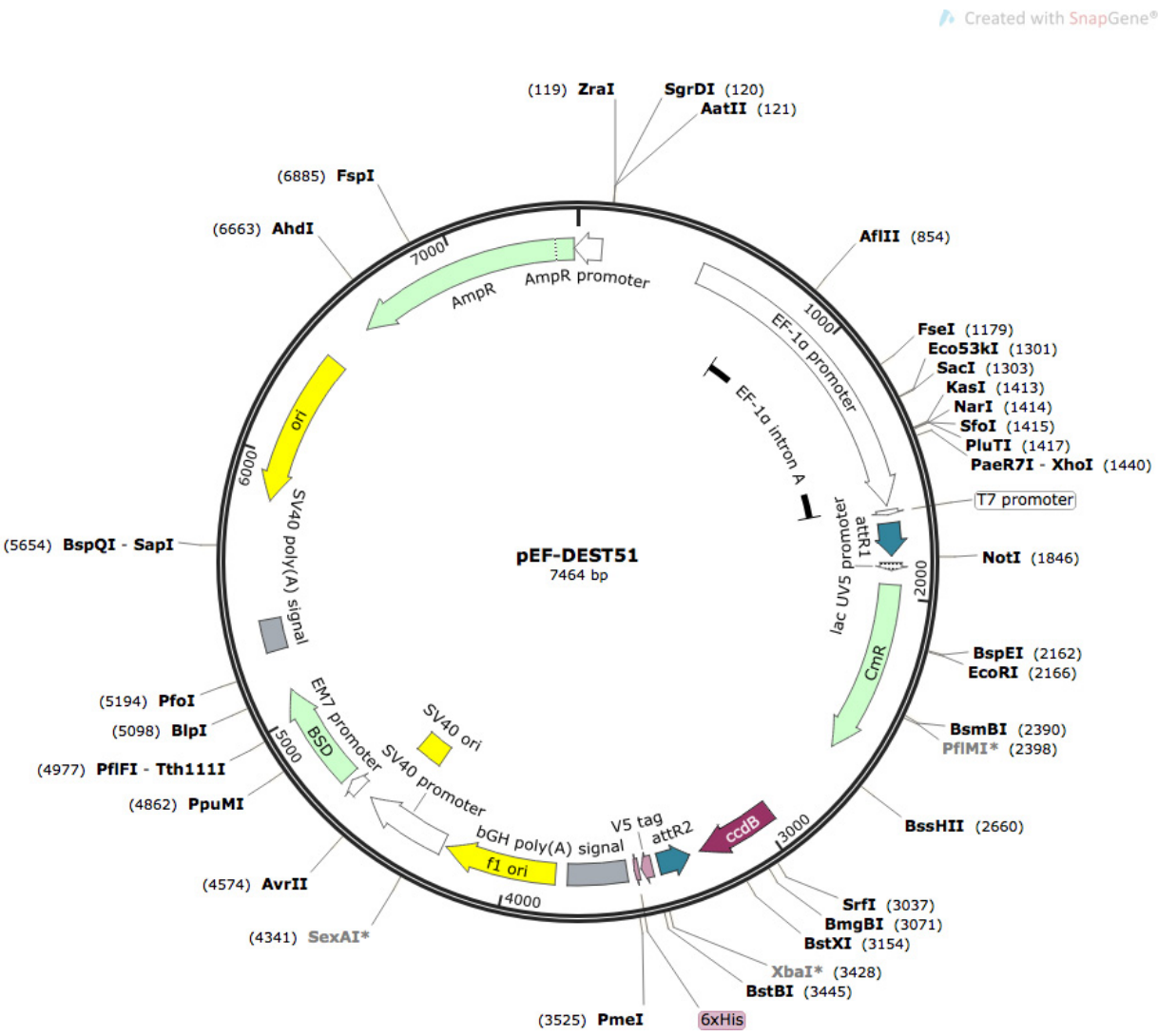

Figure 35: pEF-DEST51 expression vector map (snapgene.com I.M.A.G.E. Consortium)

VII. Wissenschaftlicher Lebenslauf

2013-2017 **Mitglied im strukturierten Promotionsstudiengang "Molekulare Mechanismen Regenerativer Prozesse"**, *Graduierten Akademie Universität Rostock*, Universitätsmedizin Rostock

2012-2017 **Promotion**, *Universitätsmedizin Rostock, Referenz- und Translationszentrum für kardiale Stammzelltherapie*, „Optimierung stammzellbasierter Ansätze für die kardiale Regeneration" (*Optimisation of Stem Cell based Approaches towards cardiac Regeneration*)

2006–2012 **Biologiestudium**, *Universität Rostock, Institut für Biowissenschaften*